Surficial Geology, Stratigraphy, and Placer Deposits of the Ruby Range, Yukon Territory

by

Derek Cronmiller

B.Sc., University of Victoria, 2011

Thesis Submitted in Partial Fulfillment of the
Requirements for the Degree of
Master of Science

in the
Department of Earth Science
Faculty of Science

SIMON FRASER UNIVERSITY
Summer 2019

Approval

Name:	**Derek Cronmiller**
Degree:	**Master of Science**
Title:	**Surficial Geology, Stratigraphy, and Placer Deposits of the Ruby Range, Yukon Territory**
Examining Committee:	**Chair:** Gwenn Flowers Professor
	Brent Ward Senior Supervisor
	Professor Simon Fraser University
	Jeffrey Bond Supervisor Surficial Geologist Yukon Geological Survey
	Matthew Leybourne Supervisor Associate Professor Queens University
	Brian Menounos External Examiner Professor, Canada Research Chair in Glacier Change Department of Geography University of Northern British Columbia
Date Defended/Approved:	June 7th, 2019

Abstract

The Quaternary history of the central Ruby Range, southwest Yukon, was studied through 1:50,000 scale surficial mapping and stratigraphic analysis. Stratigraphy in Gladstone Creek provides evidence for at least two glaciations of the Cordilleran Ice Sheet's (CIS) St. Elias lobe, during marine oxygen isotope stages 2 and 4. Significant ice was produced from cirques and ice caps within the Ruby Range, that likely contributed to the CIS incursion within Gladstone Creek. Advances from Ruby Range cirques appear to have preceded CIS advances and are preferentially preserved in the stratigraphy due to lower base-levels associated with their advance. Stratigraphic units are constrained by tephrochronology, luminescence, and radiocarbon dating. ^{10}Be dating on erratics suggests alpine glacier readvances occurred in Raft and Rockslide creeks at 13.7 ± 0.9 ka, significantly later than the last glacial maximum of the CIS (17.2 ± 0.9 ka). Placer deposits in Gladstone Creek have been reworked by repeated cycles of glaciation resulting in complex stratigraphic distributions, generally occurring on bedrock and false bedrock surfaces. Gold appears to be sourced from both epithermal mineralization in Kluane schist, as well as gold-rich porphyry mineralization in the Ruby Range batholith.

Keywords: Quaternary stratigraphy, surficial geology, glacial limits, dating, placer, sedimentology

Dedication

To family.

Acknowledgements

First and foremost, thanks to my supervisors Brent Ward and Jeff Bond for the time and energy they have invested in me and this project. It is hard to properly express my gratitude for them on this page, I hope their mentorship is adequately reflected in all my future work. Matthew Leybourne and Daniel Layton-Matthews provided support for geochemical aspects of this thesis. Megan Simao is thanked for providing competent field assistance during a particularly rainy field season. Michel Lamothe, Laurence Forget Brisson, John Gosse, Alice Telka, and Britta Jensen provided age constraints and valuable insight into their methods. Grant Zazula is thanked for providing photos, data, and insight on the horse bones collected in Gladstone Creek. Kristen Kennedy and Derek Turner are thanked for taking their time to share the knowledge of the surrounding regions. Thanks to Al Dendys and his crew at TIC Exploration for their hospitality, local knowledge, and enthusiasm for digging a little deeper. Gioachino Roberti is thanked for being a good friend and labmate, always willing to help. Richard Guthrie is owed a debt of gratitude for his years of mentorship and constant nudging towards grad school. Finally, my deepest thanks to my wife Justine for her patience and unwavering support.

Funding for this project was provided by the Yukon Geological Survey and CANNOR's Strategic Investments in Northern Economic Development. The project area is located within the traditional territories of the Kluane and Champagne Aishihik First Nations.

Table of Contents

List of Tables

List of Figures

List of Acronyms

3D	Three dimensional
CIS	Cordilleran Ice Sheet
DEM	Digital elevation model
GIS	Geographic information system
GPS	Global positioning system
IRSL	Infrared-stimulated luminescence
LA-ICPMS	Laser ablation inductively coupled plasma mass spectrometry
LIA	Little Ice Age
MIS	Marine-oxygen isotope stage
NTS	National topographic system
SEM	Scanning electron microscope
TCN	Terrestrial cosmogenic nuclide
UAV	Unmanned aerial vehicle
YGS	Yukon Geological Survey

Chapter 1. Introduction

1.1. Thesis organization

This is a modified paper format thesis consisting of five chapters; thus, there is some repetition of information between chapters. Chapter 1 (this chapter) introduces the project and study area. Chapter 2 reviews previous regional and local surficial geology and glacial limits mapping and presents new surficial geology mapping for the Gladstone Creek and Kluane Lake area (NTS 115G7/8) published as Cronmiller et al., 2018 (Appendix A). Chapter 2 serves as supplemental information for description and interpretation of the mapping. Chapter 3 reviews regional stratigraphy in southwest Yukon and presents new data from stratigraphic sections on Gladstone and Raft creeks as well as select sites throughout the study area. This stratigraphic data is synthesized with the results of Chapter 2 to provide further insight into the Quaternary history of the Ruby Range and southwest Yukon. Chapter 4 examines placer geology within Gladstone Creek and the implications of gold grain geochemistry and morphology for local mineralization. This chapter was published in Yukon Exploration and Geology, 2018 (Cronmiller et al., 2019). Chapter 5 summarizes the main findings of this thesis and suggests next steps for furthering our understanding of the Quaternary geology of the Ruby Range and southwest Yukon.

1.2. Background

The Ruby Range, located on the east side of Kluane Lake in southwest Yukon, has been affected by multiple glaciations throughout the Quaternary (2.588 Ma to present) (Figure 1.1). The timing and extent of these glaciations is the subject of recent revision, with the penultimate glaciation being locally constrained to marine-oxygen isotope stage (MIS) 4 (Ward et al., 2007) rather than the MIS 6 age for much of central Yukon (Ward et al., 2008). The study area of this thesis is near the northeastern all-time limit of the St. Elias lobe of the Cordilleran Ice Sheet (CIS). Interactions between the CIS and local alpine glaciers are poorly understood. Understanding the extent, timing, and style of glaciations within the region is critical to understanding the distribution of surficial materials throughout the region and the evolution of the many economic placer deposits in the river valleys.

Mineral exploration in the area currently relies on outdated, low-resolution surficial geology and glacial limits mapping to validate their soil and stream geochemical data sets.

This project aims to increase our understanding of the timing, extent, and style of glaciations within the study area and determine how these glaciations have impacted the distribution of surficial sediments and evolution of placer deposits in the Ruby Range.

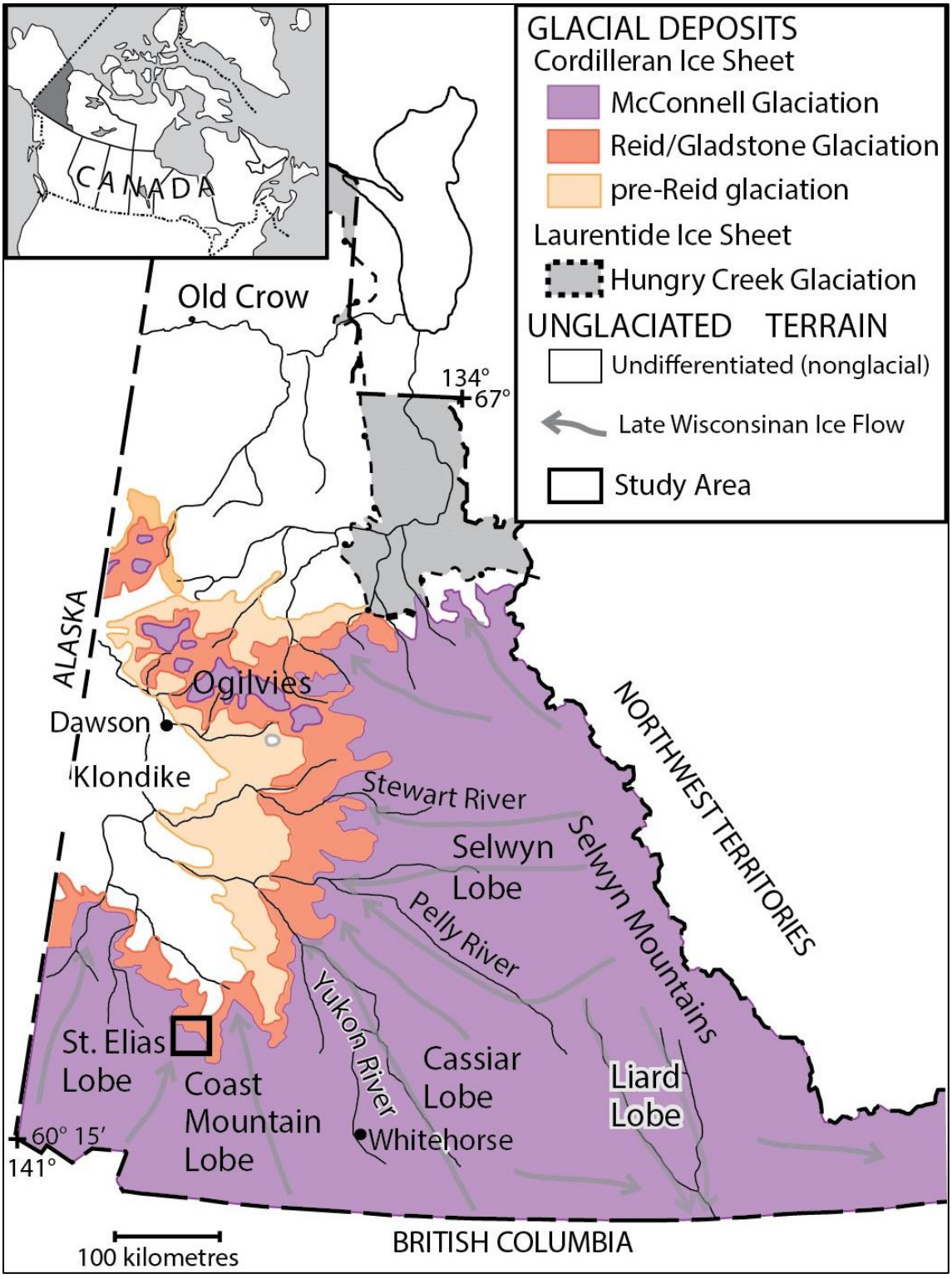

Figure 1.1 Study area boundary overlain on a map of Yukon glacial limits. The study area is located on the southeast margin of the St. Elias lobe, which coalesced with the Coast Mountain lobe during earlier glaciations. In SW Yukon, Gladstone (MIS 4) limits are thought to be approximately the same extent as Reid (MIS 6) limits. Glacial limits are modified from Duk-Rodkin, 1999.

1.2.1. **Physiography**

The Ruby Range comprises the majority of the study area (Figure 1.2). The northeast corner of the study area overlaps with the west margin of the Nisling Range. These mountain ranges were formed by dissection of the Klondike Plateau during uplift in the Late Miocene or Pliocene (Tempelman-Kluit, 1980). The rolling plateau surfaces in the east of the study area represent partial dissection of the initial lower relief surfaces, whereas the rugged peaks in the centre and west of the study represent complete dissection of this surface (Figure 1.3, cf. Tempelman-Kluit, 1980). The highest point in the area is Ruby Peak, at 2360 m asl; the lowest point is Kluane Lake, at 780 m asl. Deep U-shaped valleys, with truncated spurs, separate the peaks of the Ruby Range and Nisling Range. Well-developed cirques exist at high elevations on cold aspects. North-draining valleys tend to be broader and deeper than south-draining valleys due to the relative effectiveness of alpine glacier erosion compared to fluvial erosion (cf. Montgomery, 2002). Modern glaciation is limited to rare rock glaciers in high cirques. Trunk valleys are commonly filled with thick sediments. Steeper slopes and high elevation surfaces are commonly covered with thin colluvium, weathered bedrock, and traces of till.

The study area is drained by two major westward-flowing creeks, Gladstone Creek and Raft Creek. These creeks flow into Kluane Lake, then into the Kluane, Donjek, White, and Yukon rivers, and ultimately into the Bering Sea. The east margin of the study area is drained by Talbot, Albert and Isaac creeks. Talbot Creek flows northwest into the Talbot arm of Kluane Lake. Albert and Isaac creeks flow east into the Aishihik Basin, which drains into the Aishihik River, then into the Dezadeash and Alsek rivers, and ultimately into the Gulf of Alaska.

Kluane Lake, located in the Shakwak Trench, forms the western margin of the study area. Kluane Lake is the largest lake in Yukon. The lake is bounded by the Duke River fan at the north end of the lake, and Kaskawulsh Glacier's valley train deposits in the Slim's River valley at the south end of the lake. The water level of Kluane Lake controls base-level for Gladstone and Raft creeks. Water levels of Kluane Lake have fluctuated by tens of metres (Brahney et al., 2008) over the Holocene in response to aggradation and incisions of the Duke River fan at the north end of the lake, and sedimentation from the Kaskawulsh Glacier (Bostock, 1969). Water contributions from the Kaskawulsh Glacier, which vary with glacial advance and retreat (Brahney et al., 2008; Shugar et al., 2017),

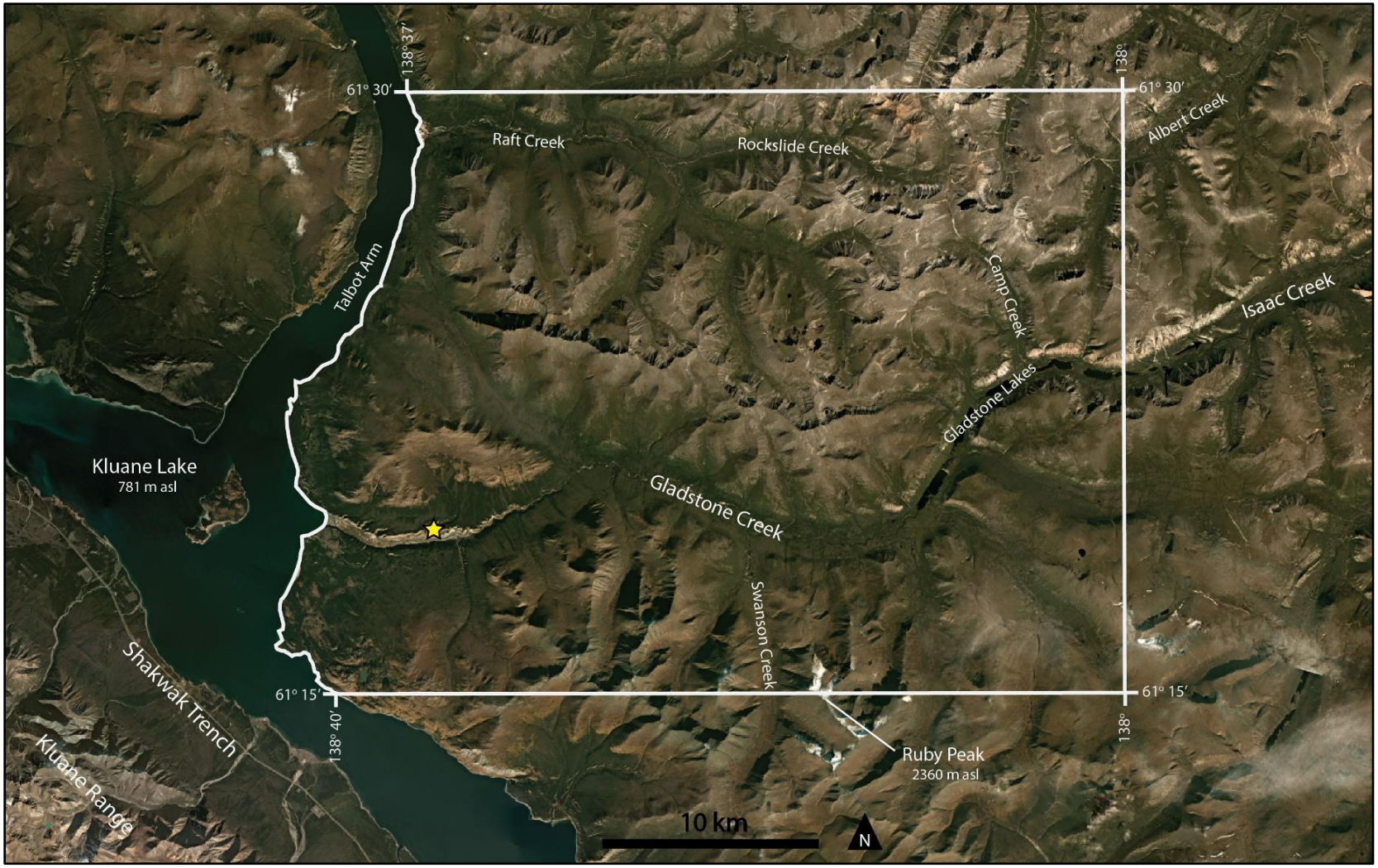

Figure 1.2 Study area and surficial geology mapping boundary, with key physiographic features labeled. The location of TIC Exploration's placer mine is indicated by the star. Base image is a 3-month (July-Sept, 2017) mosaic of Planetscope, Rapideye, and Skysat satellite imagery from Planet.

also control Kluane Lake levels. Clague et al. (2006), suggested that Kluane Lake was more than 30 m lower than its current level for much of the Holocene until the Little Ice Age (LIA) advance of the Kaskawulsh Glacier at approximately 1650 AD. When lake levels were at their lowest, it is likely that water flowed south through the Slims valley and out to the Pacific Ocean via the Kaskawulsh and Alsek rivers. The LIA advance of the Kaskawulsh Glacier caused a drainage reversal so that Kluane Lake and its tributaries now drain north through the Kluane River (Brahney et al., 2008). It is possible that the recent retreat of the Kaskawulsh Glacier will eventually cause Kluane Lake to drain into the Kaskawush watershed again, lowering lake levels once more (Shugar et al., 2017). Prior to the McConnell Glaciation, it is unknown whether Kluane Lake would have existed.

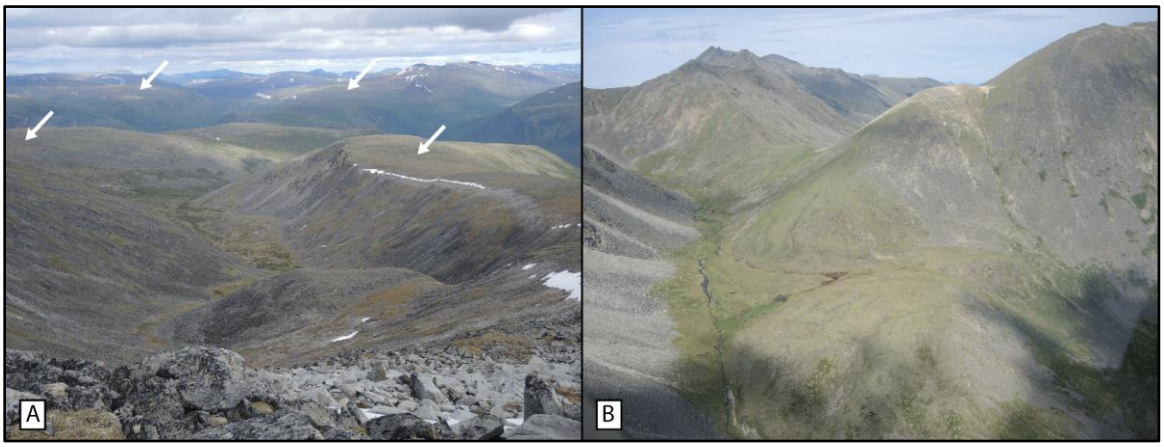

Figure 1.3 Topography of the Ruby Range A. The remnant surface (arrows) of uplifted Klondike Plateau in the southeastern portion of the study area is moderately dissected. B. Rugged terrain characteristic of the more heavily dissected plateau in the central and western portions of the study area. The original plateau surface is not readily distinguishable.

The Shakwak Trench is a graben feature formed by normal faulting along the Denali fault during the Pliocene (Tempelman-Kluit, 1980). Work by Turner et al. (2016) analyzing tilted glaciolacustrine sediments found that uplift of the St. Elias Mountains, forming the west side of the Shakwak Trench, has continued through the Pleistocene at rates of up to 1.9 mm a^{-1}.

1.2.2. **Climate and Ecology**

The Ruby Range's eponymous ecoregion is one of the driest in Yukon, receiving only 250-300 mm of precipitation each year, the majority of which falls as snow (Smith et al., 2004). The aridity of the region is attributed to the rain shadow effect of the nearby St.

Elias Mountains. Mean annual temperature in the Ruby Ranges varies from -3° to -7° C, with January temperatures averaging in the -30° Cs and July temperatures averaging approximately 10° C. Colder temperatures generally occur in the western and higher elevation portions of the study area (Smith et al., 2004). As a result, the study area is underlain by extensive discontinuous permafrost in valley bottoms and on south-facing slopes, and continuous permafrost at higher elevations and on north-facing slopes (Bonnaventure et al., 2012; Figure 1.4).

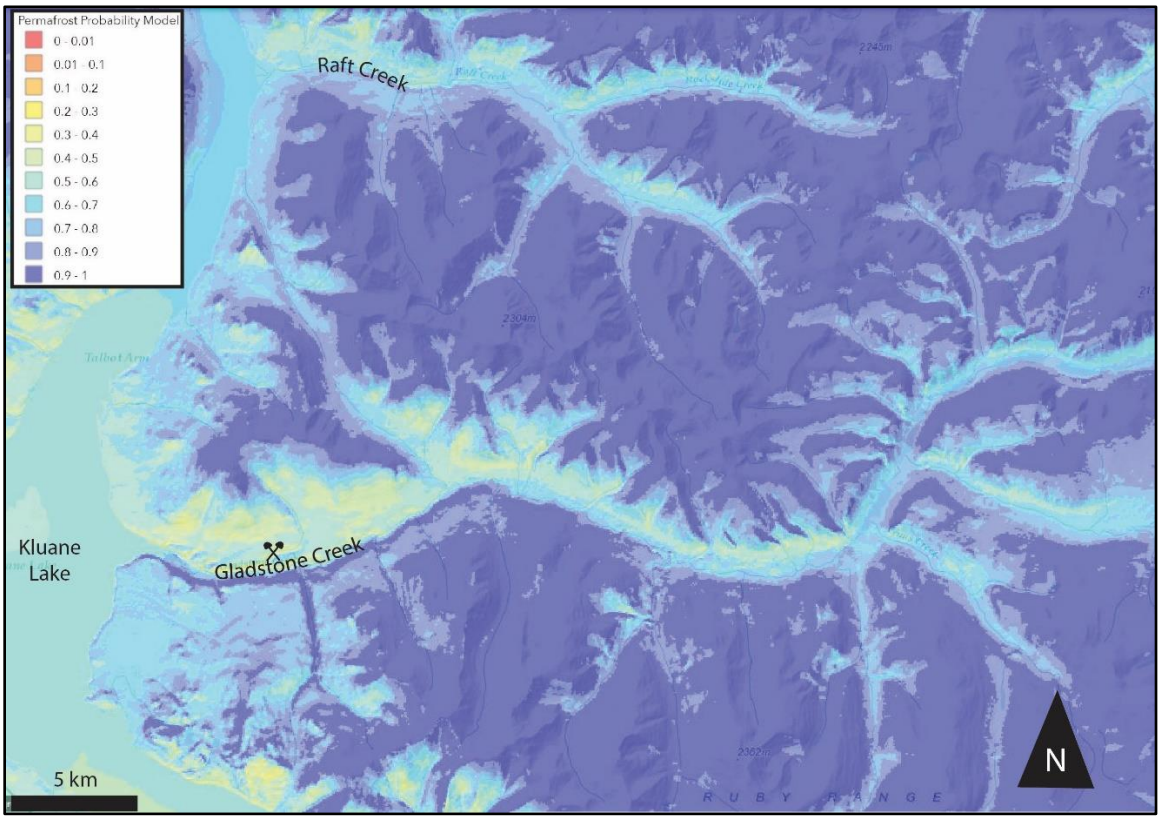

Figure 1.4 The probability of permafrost in the study area as modelled by Bonnaventure et al. (2012). The location of TIC Exploration's placer mine on Gladstone Creek is indicated by crossed shovels symbol.

The high elevations and cold temperatures result in approximately 60% of the Ruby Ranges ecoregion being covered by alpine tundra and barren rocklands (Smith et al., 2004). The flanks and valley bottoms of Gladstone Creek and lower Raft Creek are host to coniferous boreal forest and rare lakes and wetland areas, making up the remaining 40% of landcover (Smith et al., 2004)

1.2.3. **Bedrock Geology**

Bedrock in the study area consists of Kluane schist, Ruby Range batholith, gneiss, and small exposures of the Doghead assemblage (Figure 1.5; Israel et al., 2011A, B). Valley bottoms are covered with thick Quaternary sediments. Mineralization potential exists in both Kluane schist and the Ruby Range batholith and is discussed further in Chapter 5.

The Ruby Range batholith underlies most of the northwest portions of the study area, including all of Raft and Rockslide creeks, upper Gladstone Creek and upper Albert Creek. The Ruby Range batholith comprises quartz-diorite, tonalite, and granodiorite, with minor diorite, gabbro, and granite (Israel et al. 2011A). Primary phases of emplacement occurred in the Paleocene, between 64-57 Ma (Israel et al. 2011B).

Kluane schist underlies the southwest portion of the study area and comprises fine-grained, quartz-muscovite and quartz-biotite schist. Accretion of the Kluane schist occurred in the Late Cretaceous, between 95 and 82 Ma (Israel et al. 2011A).

Gneiss of unknown origin is located between the Kluane schist and Ruby Range batholith (Israel et al. 2011A). This gneiss is suspected to be either a gneissic/migmatitic equivalent of the Kluane schist, or basement rock to the Yukon Tanana terrane (Israel et al. 2011A). Field traverses in Raft Creek found gneissic bedrock within areas mapped as Ruby Range batholith.

The late Triassic Doghead assemblage is contained within the Kluane schist as small slivers of serpentinite schist with olivine and talc (Murphy et al., 2009; Israel et al. 2011A). These slivers are remnants of oceanic crust that was accreted along with the Kluane schist.

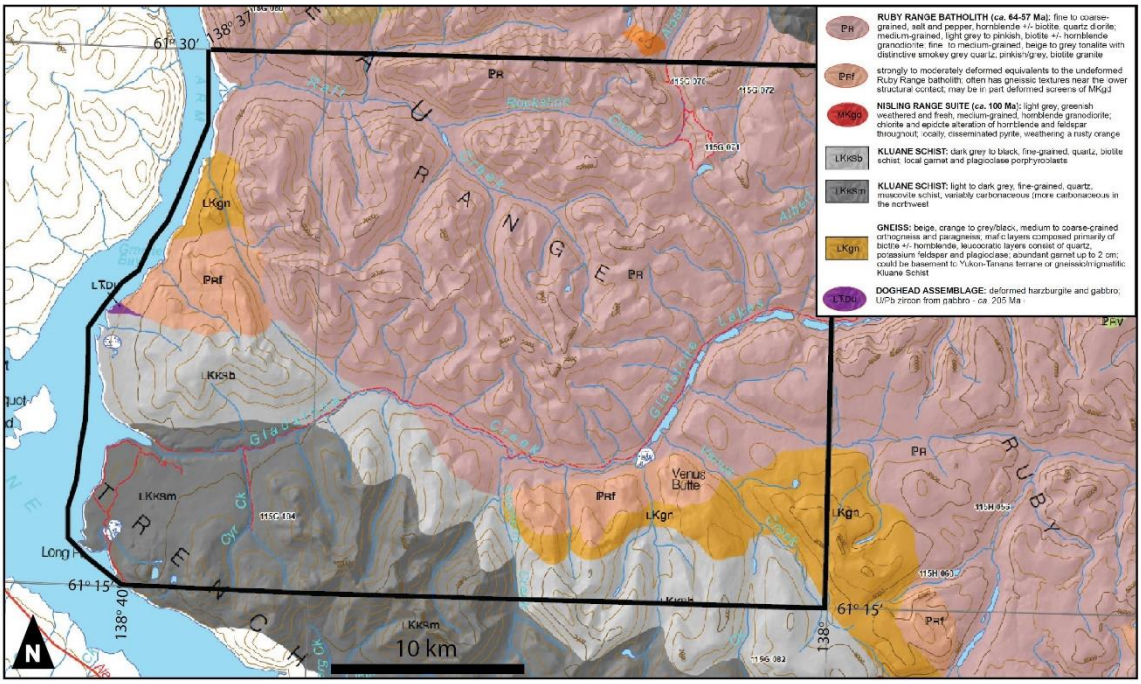

Figure 1.5 Bedrock geology of the study area. The Ruby Range batholith dominates the northeast and central study area. The south and western portions of the study area are underlain by Kluane schist, gneiss, and minor outcrops of the Doghead assemblage. Modified from Israel et al. (2011B).

1.3. Thesis Objectives

The objective of this thesis is to answer the following questions:

- What is the distribution of surficial sediments in the central Ruby Range?
- What is the glacial history of the study area?
- What is the extent and timing of mid- to late-Pleistocene CIS glaciation in the Ruby Range, and can glacial surfaces and landforms that are MIS 4 or older be differentiated using desktop and field mapping techniques?
- How does the distribution and character of gold vary throughout the stratigraphy of Gladstone Creek, how have economic placer gold concentrations evolved, and is it possible to determine the origin of the placer gold based on gold grain morphology, geochemistry, and stratigraphic position?

These questions were answered by completing the following:

- 1:50,000 scale surficial geology and glacial limits mapping for the study area,
- Stratigraphic logging and analysis of sediments within Gladstone and Raft creeks,
- Dating and correlating surficial materials and stratigraphic units using ^{10}Be, tephrochronology, radiocarbon, and infrared stimulated luminescence methods, and
- Sampling and analysing the stratigraphic distribution, morphology, and geochemistry of placer gold in Gladstone Creek.

1.4. Methods

1.4.1. Surficial Geology

Surficial mapping was completed using desktop mapping and field traverses. Desktop mapping was completed using DAT/EM Summit Evolution 3D heads-up mapping software running alongside ESRI ArcMap geographic information system (GIS) software. Summit allows for 3D visualization of aerial photographs, whereas digitization is captured in ArcMap. The aerial photographs used were a combination of 1:50,000 scale black and white images from 1988 and 1:20,000 scale colour images from 2012. Hard copies of the black and white photographs were used for field mapping and navigation. Hillshade models derived from a 2 m resolution version of the Arctic DEM (Porter et al., 2018) were used to aid interpretation.

Field mapping was completed in June through August 2017. Field traverses were conducted by truck in the southwestern-most portion of the study area with road access, around Cyr and Gladstone creeks. Field traverses were helicopter assisted in the remainder of the study area. Fly-camps were established at locations where multiple traverses could be made covering surfaces and geomorphic features requiring field confirmation. Fly-camps were occupied from 2-5 days, and traverses were made on foot from the camps each day. Two additional one-day trips were made to collect boulder

samples for cosmogenic nuclide dating. These trips occurred in September 2017, and July 2018.

Field stations were marked with handheld GPS and notes were made at all locations of significance. Field notes included: terrain symbols based on the BC Terrain Classification System (Howes and Kenk, 1997), estimated age of the surface, presence of erratics, surficial processes, bedrock lithology, slope and slope position, elevation, aspect, and soil pit profiles as appropriate. Field sketches and miscellaneous notes were made as deemed necessary. Photographs of field sites were taken using handheld cameras and a camera-equipped unmanned aerial vehicle (UAV).

Dating Methods

Terrestrial cosmogenic nuclide dating (^{10}Be)

Terrestrial cosmogenic nuclide (TCN) dating utilizes the constant bombardment of high energy cosmic radiation to determine the ages of surface features based on the concentration of accumulated rare cosmogenic nuclides present in a sample (Cockburn and Summerfield, 2004). Protons comprise most of the radiation responsible for the generation of TCNs (Gosse and Phillips, 2001). By knowing the production rate of the specific nuclide (^{10}Be, ^{36}Cl, etc.), the measured concentration allows calculation of the age.^{10}Be, used in this study, is produced through spallation of oxygen and nitrogen.

Rock chip samples were taken from 16 boulders in or adjacent to the study area for TCN dating at the Terrestrial Cosmogenic Nuclide Facility at Dalhousie University. Results from five of these samples are reported here, the remaining samples are pending further lab analysis. Samples were extracted from the surface of boulders using a gas-powered rock saw and a hammer and chisel (Figure 1.7). Latitude, longitude, and elevation are recorded to determine site specific ^{10}Be production rates. Measurements of boulder dimensions and skyline profiles were collected for the calculation of edge effects and topographic shielding, respectively. Boulders were selected based on their size (larger is better), height (taller is better), shape (flatter top better), and weathering (less is better). Larger boulders have a decreased chance of edge effects and inheritance, yielding an erroneously older age. Taller boulders have a lower chance of having been exhumed from the surrounding surficial materials and are less likely to be affected by seasonal snow cover. Boulders should be located on stable landforms to reduce the chance of

exhumation, or other movements that may yield ages younger than the landform (Putkonen et al., 2003; Heyman et al., 2011; Figure 1.6). For example, a boulder located just behind a moraine may be preferable to one located on the moraine ridge itself, as a steeper landform is more prone to erosion and mass movement.

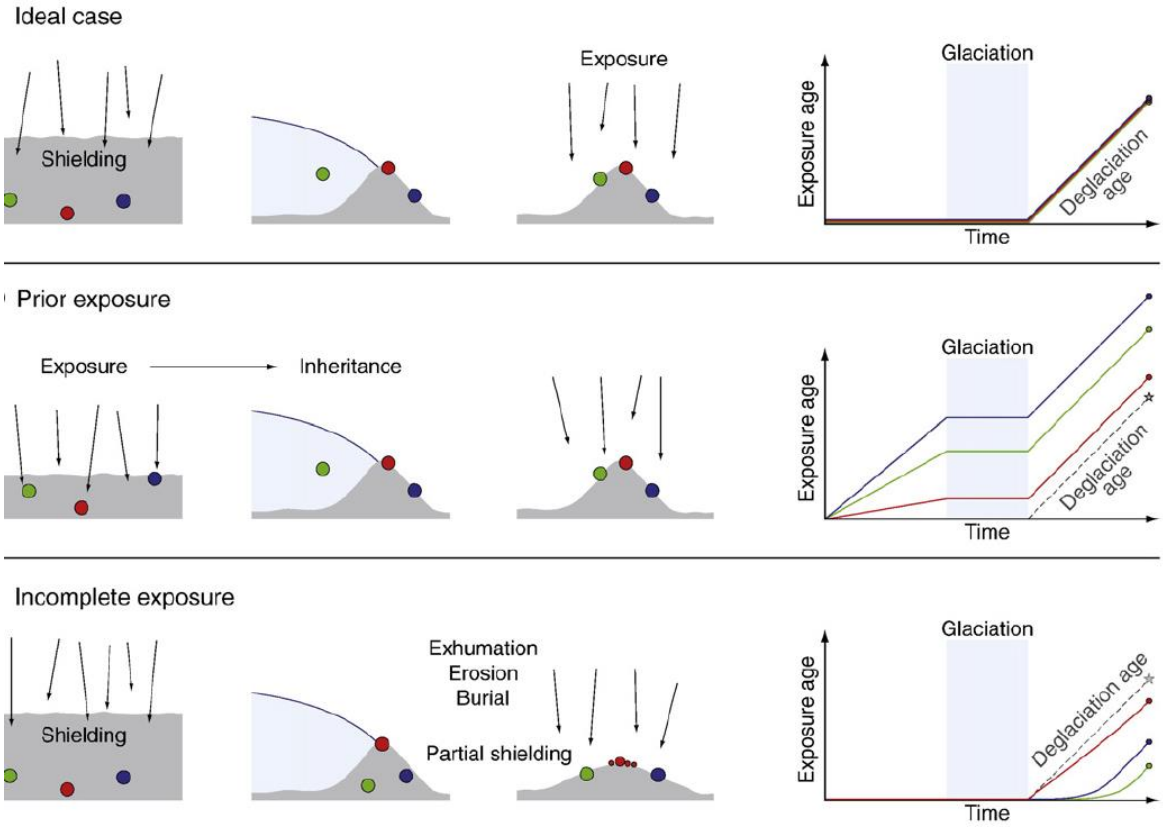

Figure 1.6 The effects of three exposure and burial histories on calculated exposure ages (modified from Heyman et al., 2011). The ideal case has no inheritance in the samples prior to glaciation and has not been exhumed post-deposition.

Figure 1.7 Removing rock chip sample (RS-03) from erratic on a moraine ridge in upper Rockslide Creek using a hammer and chisel.

1.4.2. **Stratigraphy**

Gladstone and Raft creeks have thick packages of sediment exposed in their lower reaches. The stratigraphy exposed in these sections makes up a significant component of this project. Stratigraphic sections were logged at 19 sites on Gladstone Creek, two sites on Cyr Creek (a tributary to Gladstone), five sites on Raft Creek, and one site on Camp Creek. The locations of sections on Raft, Gladstone, and Cyr creeks are shown in Figure 3.2 and Figure 3.20.

In the field, photographs of sections and individual stratigraphic units were collected using digital cameras, and a UAV. Hand tools were used for minor excavation and cleaning of sections where clean natural exposures or mining cuts were not present. Position and distance measurements were taken using a hand-held Garmin GPS, stadia rods, and a laser rangefinder.

Stratigraphic sections were divided into discrete units based on relative age and depositional environment. Unit descriptions include: a unit number, descriptive name, unit

thickness, description of lower contact, clast sizes and lithologies, matrix texture, clast and matrix proportions, sorting and rounding of particles, primary and secondary sedimentary structures, cohesion and consolidation, and fossil and organic content. Sediment descriptions use the Wentworth terms for grade and classification (Wentworth, 1922). The orientation of clast a-axes were measured in diamicton units to help determine their genesis (till vs colluvium) based on their fabric (Hicock et al., 1996). Fabric analyses generally aimed for a minimum of 25 clasts, although occasionally fewer were collected due to time constraints and the scarcity of suitable clasts. Clast fabrics were plotted on equal-area, lower-hemisphere Schmidt stereonets using *Stereonet* software. This software was used to calculate the principal eigenvector, representing the mean down-plunge orientation of clasts. Stratigraphic logs were produced from field notes using *Adobe Illustrator*. Heights recorded on stratigraphic sections use the local elevation of Gladstone Creek as their base level.

Dating Methods

Radiocarbon and macrofossils

Radiocarbon (^{14}C) dating was used where organic material was found in stratigraphic units lacking chronological constraint. Bone and plant and insect macrofossil samples were collected when found in section to determine paleoenvironmental conditions associated with the units in which they were found. Bone samples were sent to Dr Grant Zazula with Yukon Government for processing and identification. Plant and insect macrofossil samples were sent to Paleotec Services in Ottawa for identification and isolation of carbon samples for dating.

Samples of bone obtained from GLD-01 were prepared by Dr Grant Zazula and sent for dating at Keck Carbon Cycle Laboratory at the University of California and A.E. Lalonde AMS Laboratory at the University of Ottawa. Insect macrofossils obtained from GLD-205 were also dated at the Keck Carbon Cycle Laboratory.

Infrared stimulated luminescence

Infrared stimulated luminescence (IRSL) utilizes the emission of electrons from quartz and feldspar under optical or thermal stimulation to determine the amount of time the sampled sediment has been buried. Radioactive elements in surrounding sediments, such a U, Th, and K, and cosmogenic radiation excite electrons which are trapped in the

crystalline structures of quartz and feldspar (Figure 1.8). When samples are stimulated in the lab using infrared light, the release of elections is measured and can be used to determine the time of burial. The burial age of a sample is determined by the equation:

Age (k) = Equivalent dose (Gy) / Annual Dose (Gy / ka)

IRSL samples were taken from several locations in sections where the sediment was likely to have been exposed to light sufficient to release electrons contained within traps in potassium feldspars prior to burial. This is most common with windblown-subaerial and clear-water subaqueous deposition of fine materials (silt and sand). The IRSL samples were collected in PVC and copper pipes driven into the sediment with a mallet. IRSL samples were sent to the LUX Laboratory at Université du Québec à Montréal for processing. Laboratory analysis used a Freiberg Instrument Lexsyg Smart Luminescence System equipped with a ^{90}Sr beta irradiator and a Canberra gamma spectrometer. Analysis generally followed procedures for IRSL dating on potassium feldspar as outlined in Duller, 2008. A single aliquot regenerative protocol modified using a low preheat protocol according to Forget Brisson et al. (submitted) was used to determine the equivalent dose. The annual dose was calculated using gamma spectrometry and analysis of water content. Variation in water content of the samples over time is likely due to their complex burial histories resulting in changes in groundwater conditions. This temporal variability in water content may introduce error into the age calculations (Duller, 2008).

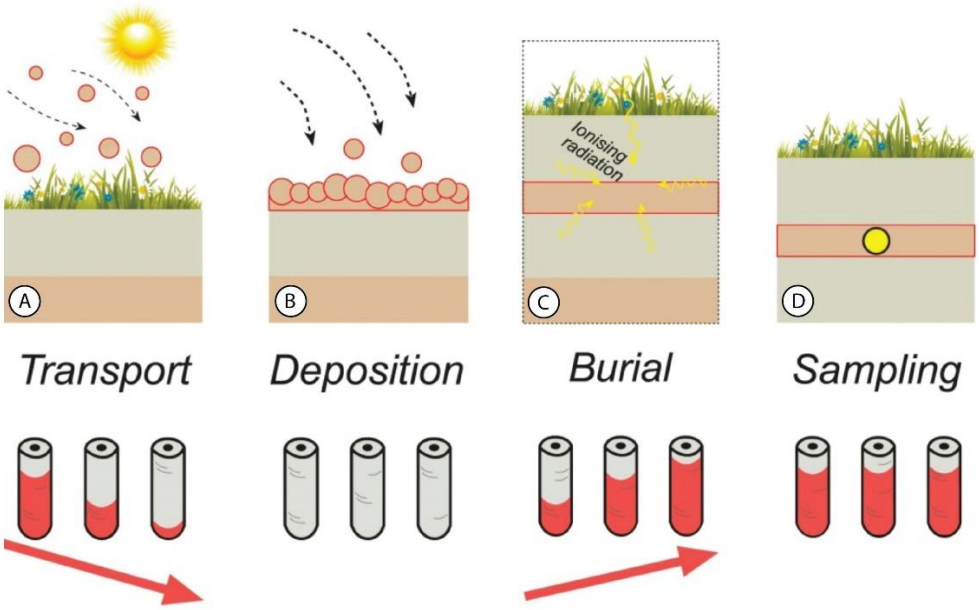

Figure 1.8 Example of how electron traps are reset during transport, accumulate electrons due to radiation during burial, and then are measured at the lab by exposure in infrared light causing their emission. Modified from Duller, 2008.

Figure 1.9 Collecting an IRSL sample from GLD-01 for luminescence dating. The tube is hammered into the sediment with a mallet then excavated from its surroundings. The sample tube is then sealed to prevent loss of sample and exposure to light.

Tephrochronology

Tephras are deposits of volcanic ash. Numerous beds of tephra are present throughout Yukon from eruptions originating in the Wrangell Mountains and the Aleutian arc-Alaska Peninsula (Westgate et al., 2001). These distal tephra beds are widespread and can be used to correlate stratigraphy across the region. Tephra samples were collected from sections in plastic sample bags, then sieved on a shaker to isolate the fraction finer than 125 µm. The fine fractions of samples were sent to Dr Britta Jensen at the University of Alberta for chemical analysis and comparison of major chemical composition to a database of known tephra samples.

1.4.3. **Gold Grain Analysis**

The granule and finer fraction of sediment located within the cobble gravel framework of streambeds is a site of heavy mineral accumulation (*cf.* Day and Fletcher, 1991) and was targeted for gold grain sample collection. Gold grains were sampled from gravels from two sites on Gladstone Creek, and one site on Cyr Creek. Attempts were made to obtain samples from Raft Creek by panning at multiple locations. Considerable amounts of black sand (magnetite) were recovered; however, no gold was found.

The heavy minerals were isolated from the sieved material using gold pans, portable sluices, and TIC Exploration's sluice box. Gold then was extracted from these heavy mineral concentrates. Gold grain samples were sent to Dr Daniel Layton-Matthews at Queens University for scanning electron microscope (SEM) imaging and chemical analysis using laser ablation induced coupled plasma mass spectrometry (LA-ICPMS). The objectives of these analyses are to determine transport distance using gold grain morphology, style of gold mineralization using chemical composition, and the number of sources based on variance within the gold samples. Gold grain morphology was analyzed using *SPIP* scanning probe image processing software.

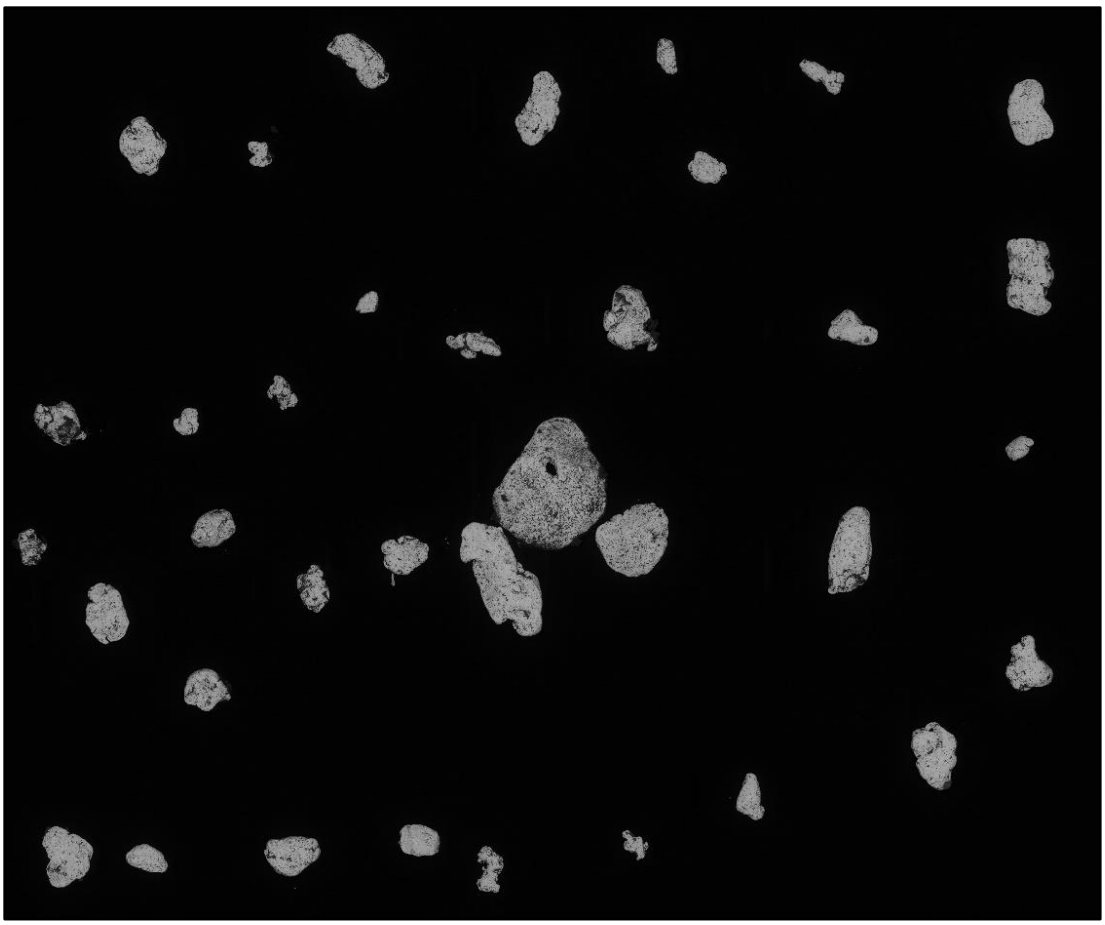

Figure 1.10 Backscattered electron image of grains from sample GLD207-G1, generated using a scanning electron microscope. The backscatter images are used for morphological characterization in SPIP software.

Chapter 2. Surficial Geology of the Ruby Range

2.1. Introduction

This chapter accompanies surficial geology mapping for the Gladstone Creek map sheet and part of Kluane Lake map sheet, which was published by the Yukon Geological Survey (Cronmiller et al., 2018; Appendix A). The chapter reviews previous work resolving the history of the northern margin of the Cordilleran Ice Sheet, and then focuses on mapping and dating glacial limits in southwest Yukon. The remainder of the chapter provides descriptions and examples of the surficial materials, landforms and processes with the study area. The newly-mapped glacial limits are discussed and compared to previous mapping. Finally, challenges associated with the mapping are discussed.

2.1.1. Regional Quaternary History

During the Pleistocene, the Cordilleran Ice Sheet (CIS) covered much of Yukon Territory, as well as the entirety of British Columbia and portions of Alaska during repeated glaciations. In Yukon, the CIS was formed by coalescing lobes flowing from ice divides located in the St. Elias, Coast, Cassiar, Pelly, and Selwyn mountains (Jackson et al., 1991). These lobes flowed mostly independent of each other from different source areas and were strongly controlled by topography (Jackson et al., 1991).

The effects of glaciation on the Yukon landscape were first published by G.M. Dawson, and R.G. McConnell (Dawson, 1889). The earliest in-depth work on understanding the glacial history of the CIS in Yukon was completed by Bostock (1966), who identified and mapped glacial surfaces of varying ages in central Yukon and separated them into four glaciations: Nansen, Klaza, Reid, and McConnell. The first attempt at mapping glacial surfaces using the chronology proposed by Bostock (1966) throughout Yukon, was Hughes et al. (1969), who produced maps of glacial limits and ice flow directions. Hughes et. al. (1969) identified surfaces as pre-Reid, Reid, or McConnell, based on relative preservation of glacial landform morphology. They found that each subsequent glaciation was less extensive. The variable extent of the glaciations may be the result of moisture availability, as glacial growth in Yukon is thought to be precipitation limited (Ward et al., 2007). Glacial limits were later re-mapped for all of Yukon Territory at

1:1,000,000 by Duk-Rodkin (1999), using the same pre-Reid, Reid and McConnell nomenclature used by Hughes et al. (1969).

The term “pre-Reid” was applied to surfaces older than penultimate (Reid) due to the difficulty in differentiating between the earlier glaciations. This composite Pre-Reid surface is characterized by subdued surface morphology with poorly preserved glacial features (Hughes et al. 1969). Bostock (1966) found no ice-marginal moraines while mapping pre-Reid surfaces. Pedological studies by Smith et al. (1986) reported a well-developed paleosol, the Wounded Moose, on pre-Reid and unglaciated surfaces. Many attempts have been made to date pre-Reid glaciation using paleomagnetism (Jackson et al., 1996; Froese et al., 2000), tephra-chronology (Westgate et al., 2001), and terrestrial cosmogenic nuclide (TCN) dating (Hidy et al., 2013). The pre-Reid is now thought to consist of 10 or more glaciations (Barendregt et al. 2010). The earliest of these glaciations dates to the late Pliocene at 2.64 +0.20/-0.18 Ma (Hidy et al., 2013) and fits with the preferred late Gauss Chron interpretation of earlier paleomagnetic work (Froese et al., 2000).

The penultimate glacial limit in much of Yukon was reached by the Reid Glaciation (Bostock 1966). The Reid Glaciation was defined by Bostock (1966) based on its greater extent than the McConnell, and the relative preservation of glacial landforms and sediments compared to the degraded forms of the pre-Reid and the distinctly younger McConnell. The Reid Glaciation was first considered to be MIS 4 (Wisconsinan) (Bostock, 1966). Later, a MIS 6 (Illinoain) age was proposed by Foscolos et al. (1977) based on the presence of a paleosol, now known as the Diversion Creek paleosol (Smith et al. 1986), which appeared to have developed during an interglacial period. A minimum age of MIS 8 was proposed by Westgate et al. (2001), based on the presence of Sheep Creep tephra, then thought to be 190 ka (Berger et al., 1996), on top of Reid deposits. A MIS 8 age seemed to be confirmed with Reid outwash above 330 ka basalt at Fort Selkirk (Huscroft et al., 2004). However, it was then discovered that there were more than one Sheep Creek tephra with similar compositions. The tephra on Reid deposits, Sheep Creek Klondike, is 80 ka, which allows an age from MIS 8 through cooler stages in MIS 5. A MIS 6 age was finally confirmed by the discovery of Old Crow tephra overlying Reid deglacial sediments (Ward et al., 2008) and infrared-stimulated luminescence (IRSL) dating of glaciofluvial sands bracketing Reid till (Demuro et al., 2012). The advance and retreat glaciofluvial sands date to 158 ± 18 ka and 132 ± 18 ka, respectively (Demuro et al., 2012).

The penultimate glacial limit in Yukon may be diachronous in age. In southwest Yukon TCN ages on deglacial boulders indicate a MIS 4 age (Ward et al., 2007). This is similar to TCN ages from alpine moraines in parts of Alaska (Briner et al. 2005). In southwest Yukon along the White River, section analysis combined with tephrochronology indicates that MIS 6 glaciation was only 4 km more extensive than MIS 4 (Turner et al., 2013). Thus, the penultimate glaciation occurred in MIS 4 (Figure 2.1) and was nearly as extensive as MIS 6 in southwest Yukon, and possibly more extensive in some locations.

The most recent glaciation, the McConnell, was the least extensive of the known glaciations in Yukon. McConnell surfaces are readily distinguished by its relatively well-preserved morphology (Hughes, 1969). The age of the McConnell Glaciation has long been constrained as MIS 2 (Late Wisconsinan) by radiocarbon ages underlying McConnell deposits (Matthews et al., 1990; Jackson and Harington, 1991). Ice began to accumulate in source areas in mountainous regions around 29 ka, with the lobe coalescing to form a contiguous ice sheet sometime after 24 ka (Jackson et al. 1991). The St. Elias lobe of the McConnell CIS reached its maximum extent between 17.7 ± 0.9 and 16.7 ± 0.8 ka (Bond and Lipovsky, 2009C).

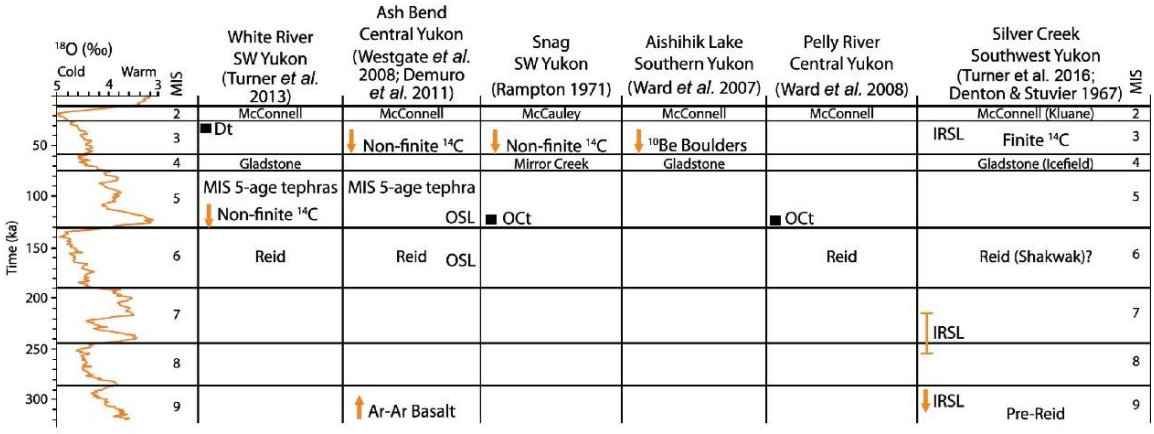

Figure 2.1 Constraints on ages of middle to late Pleistocene glaciations in Yukon. Modified from Turner et al., 2016. OCt – Old Crow tepha, Dt – Dawson tephra

2.1.2. **Glaciation of southwest Yukon**

Recent work by Ward et al. (2007) and Turner (2013) found the penultimate glaciation of the St. Elias lobe occurred in MIS 4, in contrast to the MIS 6 age penultimate Reid Glaciation in central Yukon. Stroeven et al. (2014) suggest the penultimate limit of

the Coast Mountain lobe may also be MIS 4 in age. This glaciation is known as the Gladstone (Ward et al., 2007) and correlates to MIS 4 glaciation found in southern Alaska (Brinner et al. 2005, Brinner and Kaufman, 2008) and the Icefield glaciation in Silver Creek (Denton and Stuiver, 1967; Turner et al., 2016). Mapping by Hughes et al. (1969), Hughes (1990), Bond et al. (2008), and Bond and Lipovsky (2009B) found no evidence of the extensive pre-Reid glaciation produced by the St. Elias lobe as was mapped by Duk-Rodkin (1999). Turner et al. (2013, 2016), spent considerable time looking at stratigraphy in White River and Silver Creek north and south of Kluane Lake, respectively. Turner et al. (2016) found evidence of pre-Reid glaciation in Silver Creek, indicating that although glacial advances did occur, they were likely less extensive than the late Pleistocene Reid, Gladstone and McConnell glaciations. Turner et al. (2013), found evidence of MIS 4 glaciation in stratigraphy and distinguished the Gladstone limit coming within 4 km of the Reid limit along White River. Further mapping in southwest Yukon may find areas where Gladstone limits extend beyond Reid.

The sections examined on Silver Creek by Turner et al. (2016) are located 30 km south of the study area. The stratigraphy in Silver Creek records at least five distinct advances from the St. Elias mountains correlating to MIS 2, 4, 6, and two older glaciations which occurred sometime before ca. 320 ka. These older glaciations are the only stratigraphic evidence supporting pre-Reid advances of the St. Elias lobe. Peat beds between MIS 4 and MIS 2 till units date to MIS 3 and indicate this area, which is closer to St. Elias source areas than the Ruby Range, was ice free. This suggests that ice extents in MIS 3 were similar to the present day. It is suspected that during MIS 3, CIS glaciation was confined to cirques in mountainous regions (Clark et al., 1993).

The stratigraphy in White River contains a record of glaciations correlating to MIS 2, 4, and 6 (Turner et al., 2013). The glacial limits found nearby these sections are separated by tens to a few hundred metres along lateral margins and only become separated by up to 4 km near the terminus of the former glaciers.

Stratigraphy in Gladstone Creek was previously examined (Madsen, 2001) as part of an honours thesis at the University of Victoria. Madsen identified deposits from at least two glaciations with interglacial deposits between. She found placer gold in the lowest four stratigraphic units she examined. The highest concentrations of gold were in low-level terrace gravels; suggesting MIS 2 glaciofluvial and Holocene fluvial processes have

reworked and re-concentrated the valley-fill deposits. This work was completed before the Gladstone Glaciation was identified (Ward et al., 2007), so the lithostratigraphic model proposed by Madsen (2001) requires re-interpretation.

Glacial limits within the study area were previously mapped as part of coarser scale (1:250,000 to 1:100,000) studies by Muller (1967), Hughes et al. (1969), and Duk-Rodkin (1999). Surficial geology was previously mapped for the western margin of the study area (NTS 105G/07) at 1:100,000 (Rampton, 1978). These previous mapping efforts warrant updating at a finer scale, given the progress made in understanding the glacial history of Yukon.

2.2. Surficial Mapping

A 1:50,000 scale map of surficial geology and glacial limits was produced for the study area (Appendix A, Cronmiller et al., 2018). This map covers national topographic system (NTS) map sheet 115G/08 and part of 115G/07. Surficial geology was previously mapped at 1:100,000 scale for 115G/07 as part of a larger mapping project (Rampton, 1978).

Surficial units are delineated in accordance with Yukon Geological Survey's adapted version of the BC Terrain Classification System (Howes and Kenk, 1997). This system divides an area into a continuous mosaic of polygons based on the genesis of the surficial materials, their texture, the landforms associated with their deposition or erosion, and geomorphic processes acting on the unit. Polygons are defined on the basis of internal variation being less than the variation between polygons (Figure 2.2). The texture, surficial material, surface expression, age, and geomorphic processes within the map area are described in the following sections. Ages are only assigned to glaciogenic materials using (M) McConnell, (G) Gladstone, and (R) Reid.

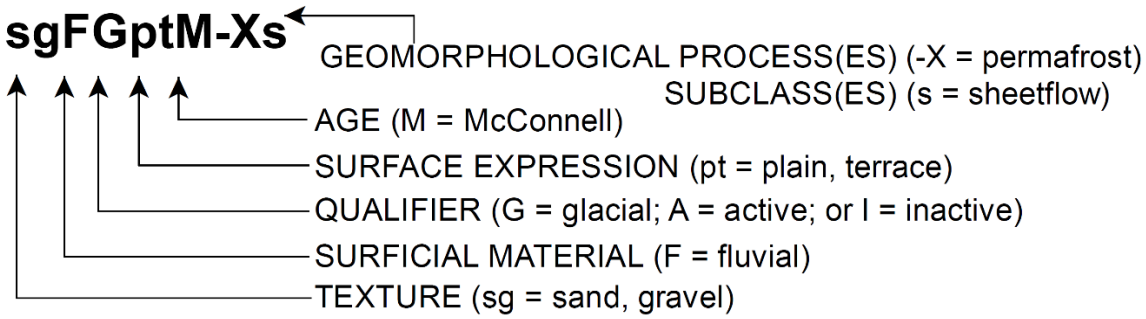

Figure 2.2 Example terrain symbol used to describe map polygons.

2.2.1. **Surficial Materials**

This section provides descriptions of the surficial materials used to define polygons (Cronmiller et al., 2018; Appendix A); the map codes for the material and associated landforms are given in parentheses following the material type.

Organic (O; v, b)

Organic material is the accumulations of plant remains (Figure 2.3). Organics are mapped where accumulations are thicker than 1 m. These accumulations occur most commonly in areas with a shallow water table due to poor drainage. Poor drainage is typical of low angle slopes with shallow permafrost tables, commonly overlying fine-grained materials such as distal glaciolacustrine or basal till, or on floodplains. Thin veneers (< 1 m) of organics are nearly ubiquitous in valley bottoms within the study area but are generally unmapped. Surface expressions include blankets (b) and veneers (v).

Figure 2.3 Organic materials and associated landforms in the Gladstone Map area. A. Fibric to mesic organic material from soil pit at the location shown in B. B. Organic blankets around a small lake. This surface may be seasonally inundated. C. Organic accumulations above a shallow permafrost table. D. Stunted forest growing on organic materials overlying shallow permafrost in Raft Creek valley.

Eolian (E; v, r)

Eolian is material transported and deposited by wind (Figure 2.4). During the last glacial cycle, silt and fine sand transported by katabatic winds was deposited over the entire study area. This loess is present as thin veneers on stable sites. Most of the map area has undergone significant colluviation and cryoturbation that has mixed the loess into underlying surficial materials. In addition, loess is generally a thin surface layer, making differentiation as a discrete map unit difficult. Where undisturbed by post-depositional processes, deposits are massive to weakly stratified. Eolian materials are only mapped in

one polygon with active dune formation at Gladstone Lakes. Surface expressions include veneers and ridges (r). Eolian material is common in described sections. Disseminated organics are common within eolian sediments.

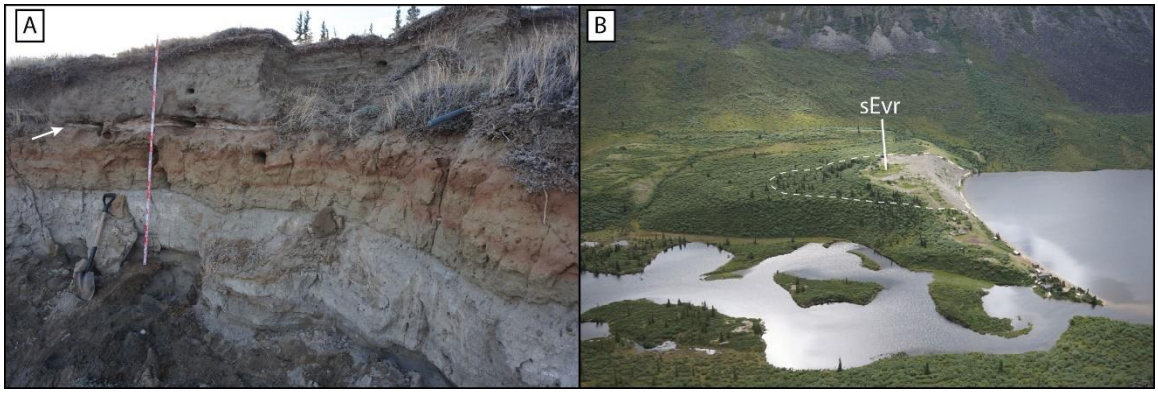

Figure 2.4 Eolian sediment and landforms in the Gladstone map area. A) Thick loess accumulations on the east shore of Kluane Lake. Distinct stratification may be the result of climatic shifts. White river tephra (see arrow) separates an oxidized paleosol (Holocene) from more recent accumulations, possibly related to the Little Ice Age readvance of the Kaskawulsh Glacier or fluctuations of Kluane Lake levels. B) Active dune building on a glaciofluvial terrace adjacent to Gladstone Lakes.

Colluvium (C; b, v, c, f)

Colluvium is sediment transported and deposited directly by mass-wasting processes (Figure 2.5). These processes include solifluction, landslides, and snow avalanches. The composition of colluvium is dependent on the material it is sourced from and the distance it has travelled from its source. Colluvium derived from slow mass movement (e.g., solifluction) of morainal deposits typically closely reflects the original textures of the till. Colluvium generated by rockfall will typically be coarse, angular, and well-drained. Colluvium is the most spatially extensive material in the map area (Appendix A). The majority of colluvium in the study area is generated through cryoturbation and solifluction of weathered bedrock and till. Colluvium typically occurs as veneers (v), blankets (b), cones (c), and fans (f). Deposits are typically poorly-sorted to diamictic.

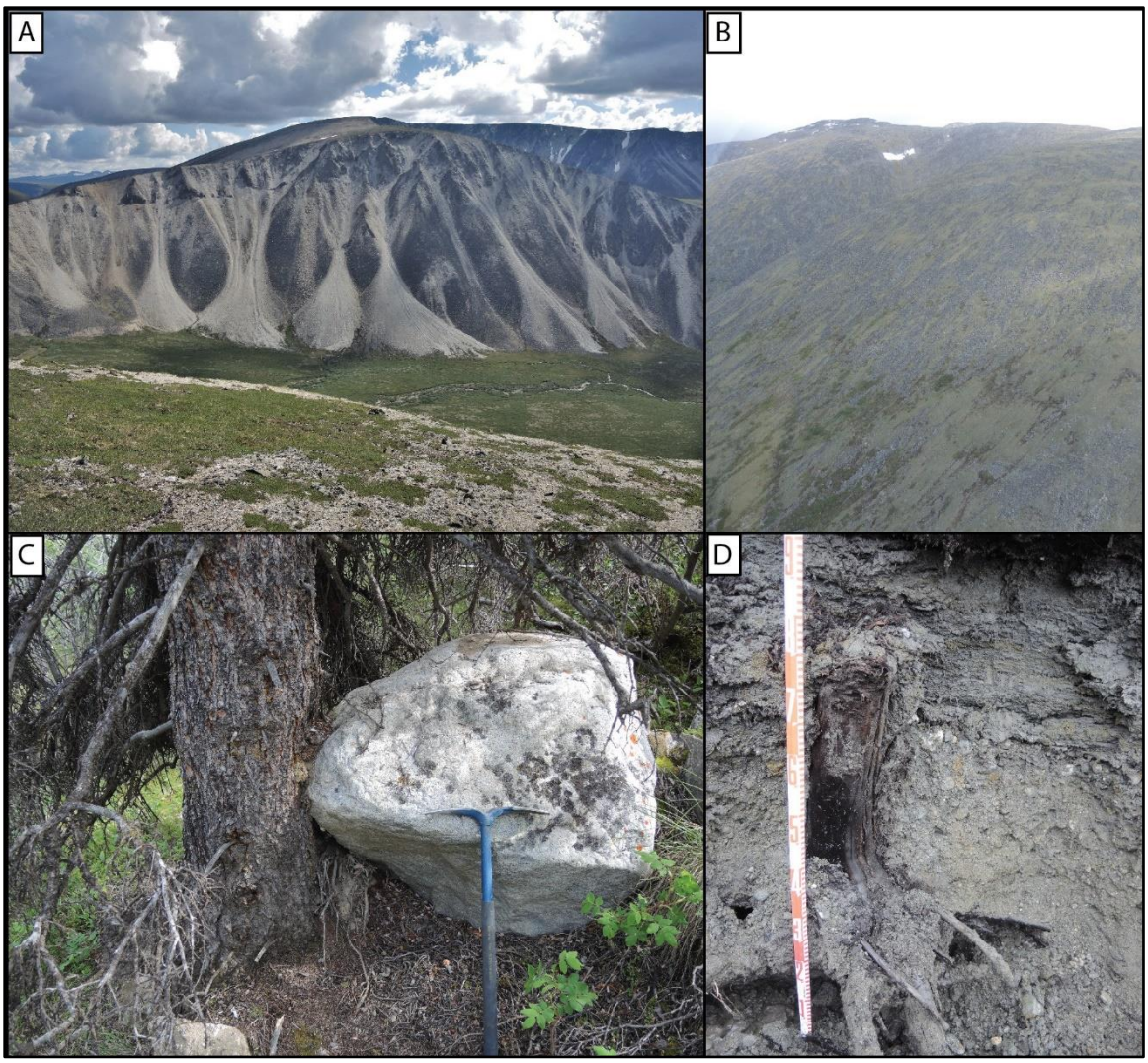

Figure 2.5 Colluvial sediment and landforms in the Gladstone map area. A) Colluvial cones and veneers developed by rockfall from steep rock slopes of cirque headwalls in upper Rockslide Creek. Because cirques in the study area are typically north facing rockfall is more common on north aspects. B) Slope creep is ubiquitous on high elevation slopes in the map area. C) A recent rockfall impacted and damaged a tree in upper Gladstone Creek. D) Mixed colluvial apron sediments in lower Gladstone Creek containing woody debris and massive ice. This apron formed through repeated events, likely resultant from active layer detachments initiation on the overhead slopes as permafrost in the area slowly degrades.

Volcanic (V)

Volcanic materials are restricted to deposits of ash from volcanic eruptions (Figure 2.6). White River tephra is present throughout the map area in thin deposits ranging from approximately 1-25 cm thick. Because White River tephra is typically very thin in the map

area, it is not mapped as a surficial unit despite its near ubiquity. Other tephras were only observed in section also in non-mappable quantities.

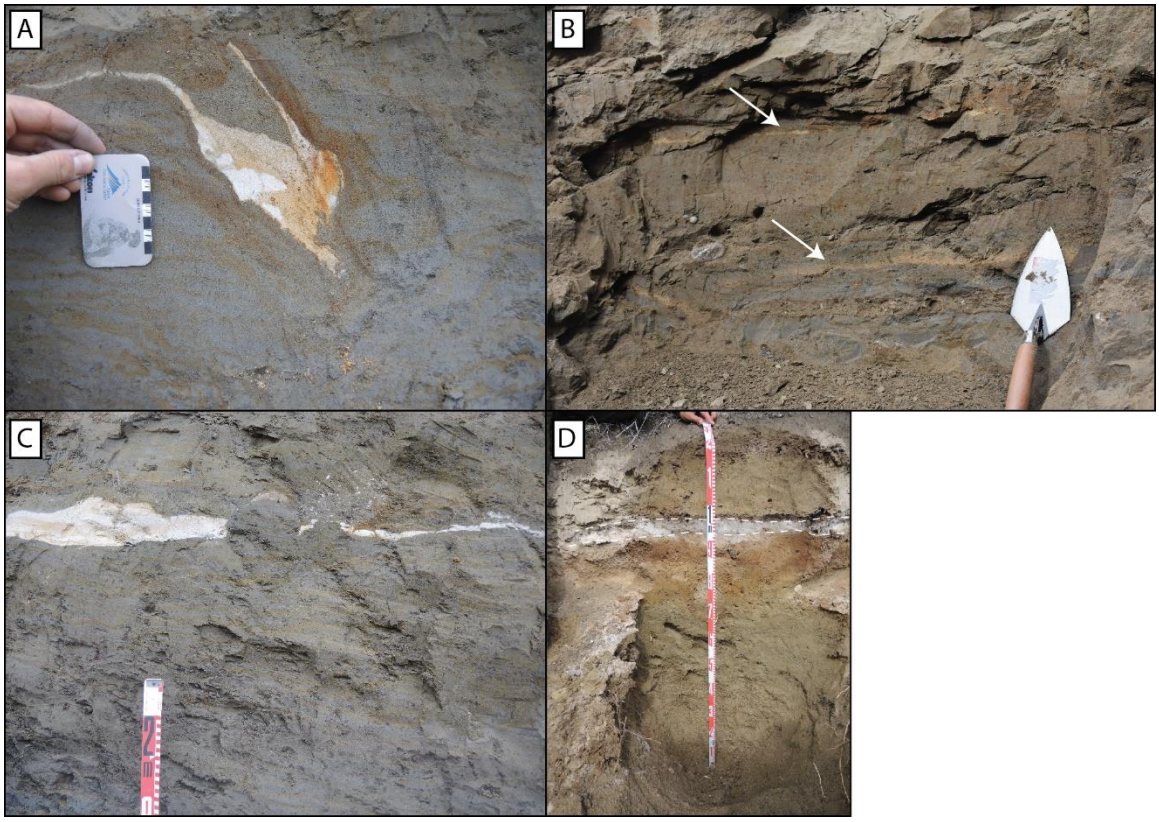

Figure 2.6 Volcanic sediments in the Gladstone map area. A) Deformed Dawson tephra from GLD-205. B) Two unknown tephra beds from GLD-01 (arrows). C) Bioturbated Dawson tephra from GLD-205. D) White River tephra from lower Raft Creek buried by loess.

Weathered Bedrock (D; v)

Weathered bedrock in the map area is primarily derived through in situ mechanical weathering by periglacial processes (Figure 2.7). The generation of weathered bedrock is slow and ongoing. Mappable accumulations of weathered bedrock are generally indicative of old surfaces and commonly occur near or beyond the all-time limit of glaciation. Blocky fields of weathered bedrock generated by periglacial processes are commonly referred to as “felsenmeer” (Figure 2.7A). Felsenmeer slopes rarely display fabrics indicating that motion occurs on these surfaces through periglacial activity, more than downslope movement (White, 1976). Rare saprolitic bedrock exists near faults. Landforms such as cryoplanation terraces (Figure 2.7B) and tors (Figure 2.10B) occur in association with

weathered bedrock. Cryoplanation terraces form very slowly by complex mass wasting processes in periglacial environments and generally indicate an area is unglaciated (Reger and Pewe, 1976). Granitic bedrock tends to weather spheroidally, creating clasts that resemble erratics. Deposit textures range from muddy sand (grus) to blocks.

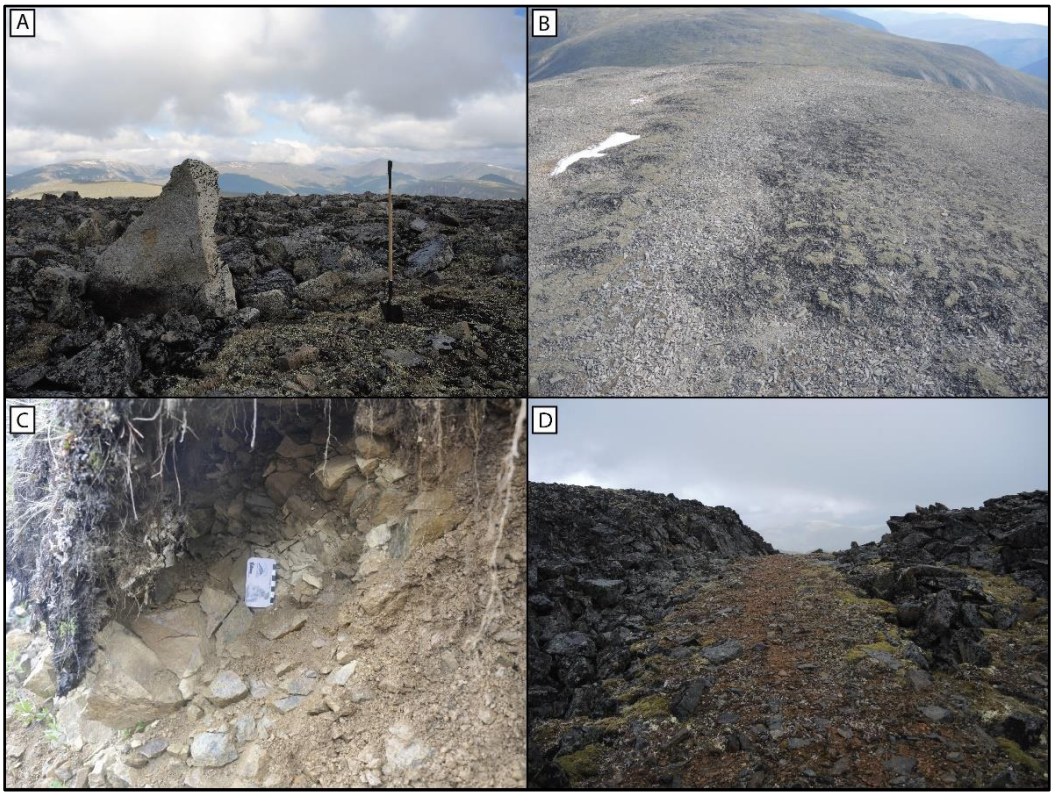

Figure 2.7 Weathered bedrock and associated landforms in the Gladstone map area. A) Felsenmeer on high plateau surface in the east side of the map area. B) Felsenmeer on cryoplanation terraces above Albert Creek. C) Weathered bedrock in Ruby Range cirque. D) Differential weathering of a dyke and granitic country rock on high elevation ridge above Gladstone creek.

Fluvial (F; v, p, t, f)

Fluvial materials (Figure 2.8) are transported and deposited by rivers in nonglacial settings. Fluvial deposits typically consist of well-sorted sands and gravels. Clasts are generally rounded. Fluvial terraces are commonly found up to a few tens of metres above modern fluvial plains in Gladstone and Raft creeks. Fluvial fans occur at most major valley confluences and commonly dissect paraglacial fans. Veneers of silt and sand are common in low energy channels and on floodplain surfaces but are not well-preserved in section.

Figure 2.8 Fluvial deposits and landforms in Gladstone map area. A) A gravel-bedded, active fluvial plain in lower Raft Creek. B) Boulder covered inactive fluvial plain. C) Boulder cobble gravel from a cut bank on a periglacial fan in upper Gladstone Creek. D) Fluvial sands at the mouth of Gladstone Creek.

Glaciofluvial (F^G; t, p, r, b, u, h)

Glaciofluvial materials consist of sediment transported and deposited by glacial meltwater. Glaciofluvial deposition occurs in front of or in contact with glaciers. Glaciofluvial sediment is typically less sorted than fluvial sediment due to rapid sedimentation and aggradation. Glaciofluvial landforms and sediment characteristics vary based on the location of deposition relative to the source glacier. Distal glaciofluvial facies tend to be finer, including silts, sands and gravels, with a higher degree of sorting than proximal facies. Ice proximal glaciofluvial facies commonly contain poorly sorted boulder gravels in a matrix of silt and sand (Figure 2.9).

Late Wisconsin – McConnell (M)

McConnell ice-contact and valley-train glaciofluvial deposits are common in upper Gladstone Creek and form many of the large terraces and plains on the east side of Kluane Lake. Kettle and kame topography is a common expression of these deposits as they accumulated in association with stagnant ice.

Early Wisconsin – Gladstone (G)

Gladstone-aged glaciofluvial material has only been mapped in two locations. One polygon is fan-delta complex at the mouth of meltwater channel, well above the McConnell limit. The other polygon, in a high pass connecting Albert and Gladstone creeks, contains a sandy boulder lag deposit where meltwater washed away most of the finer sediment. Meltwater channels and eskers from the Gladstone Glaciation were mapped as discrete line features.

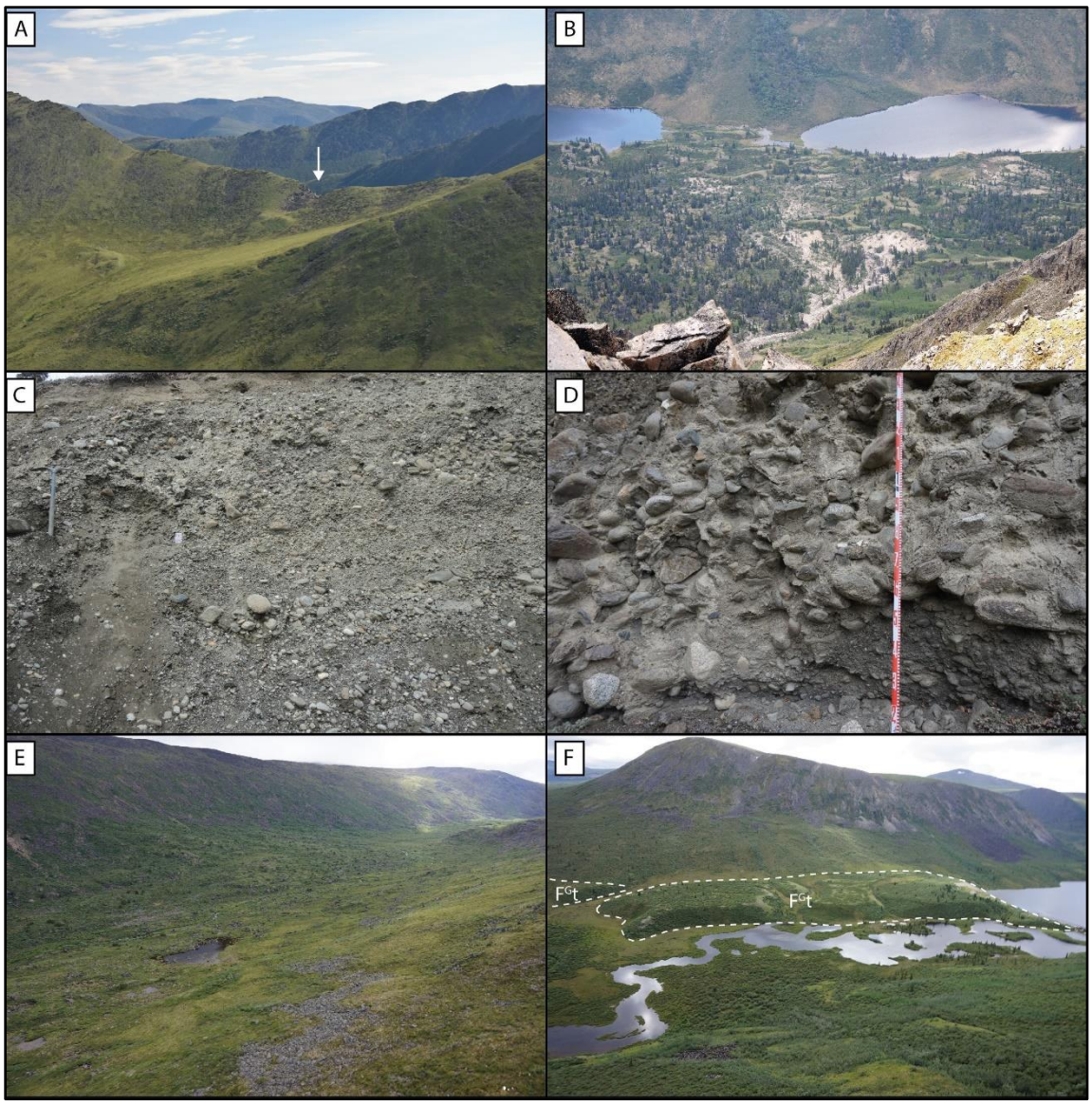

Figure 2.9 Glaciofluvial materials and landforms in the Gladstone map area. A) Meltwater channel formed by glacial meltwater incision through bedrock ridge. B) Esker swarm near McConnell limit in Isaac Creek. C) Glaciofluvial sand and gravel from section GLD-05 D) Poorly sorted glaciofluvial cobble gravel from section GLD-06. E) Remnant boulder lag and scoured bedrock surface from subglacial drainage. F) Glaciofluvial terrace in upper Gladstone Creek from McConnell Glaciation retreat phase.

Morainal (M; b, v, u, h)

Morainal sediment (till) is transported by glacial ice and deposited by either primary or secondary glacial processes (Figure 2.10) and can have highly variable characteristics (Dreimanis and Schlüchter, 1985). Primary processes include lodgement, deformation

and melt-out. Secondary processes include mass-wasting from the peripheries of the glacier (flow tills) and minor sorting by meltwater during deposition. Lodgement, basal melt-out, and deformation tills are commonly expressed as blankets and veneers. Supraglacial melt-out tills commonly have undulating or hummocky surface expressions.

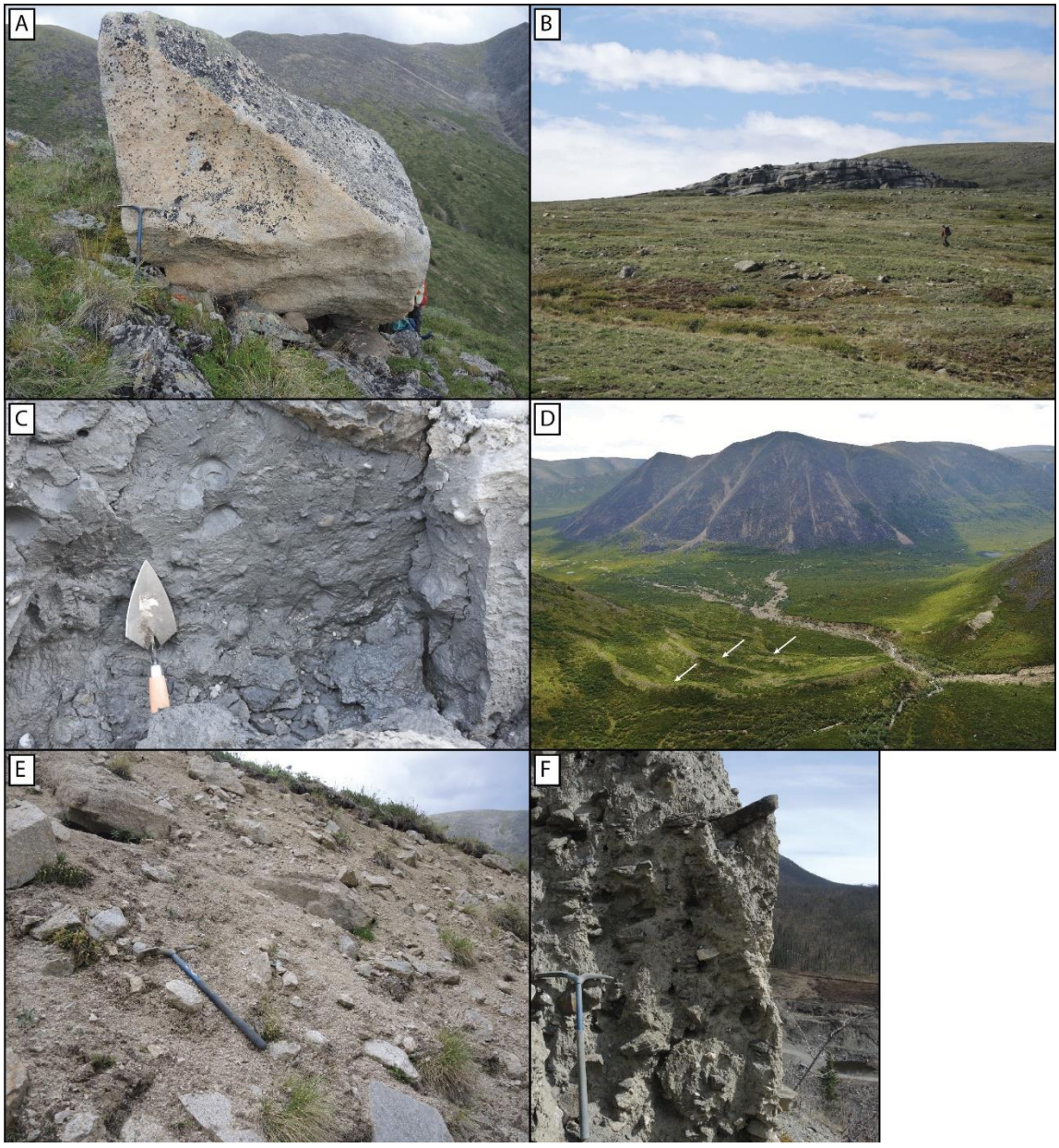

Figure 2.10 Morainal deposits and landforms in the Gladstone map area. A) Granitic erratic perched on gneissic bedrock above lower Rockslide Creek. B) Erratic strewn surface surrounding a streamlined tor on high plateau surface. C) Lodgment till exposed in mine cut in Gladstone Creek (GLD-205). D) Moraine ridges in Albert Creek. E) Cut bank exposure of till blanket in Ruby Range cirque. F) Schist-rich till in lower Gladstone Creek indicative of down-valley ice from cirques above Gladstone Creek (GLD-02).

Till is typically unsorted and massive but rarely displays weak sorting and stratification. Clast sizes range from pebble to boulder and they are commonly striated and faceted. In lodgement and meltout till, the long axes of clasts preferentially align in the direction of flow (Hicock et al., 1996).

Late Wisconsin – McConnell (M)

McConnell till is sourced from both the St. Elias lobe of the Cordilleran Ice Sheet, and Ruby Range cirques and ice caps. McConnell-aged St. Elias lobe till is common in valley bottoms and flanks of Gladstone Creek and lower Raft Creek. Different facies of McConnell till exist in the map area including lodgement, subglacial and supraglacial melt-out. Lodgement till is typically over-consolidated and massive, with 15-60% clasts, in a sandy silt to silty sand matrix. Melt-out tills are generally less compact and have a sandier matrix with rare sorted lenses.

Early Wisconsin – Gladstone (G)

Gladstone till is mapped in the bottoms and flanks of tributary valleys to Gladstone and Raft creeks above the McConnell limit as well as on high plateau surfaces on the east side of the map sheet, proximal to Gladstone Creek. Gladstone till is typically diminished in its fine fraction due to eluviation throughout its prolonged surface exposure. Silt caps are common on clasts. No clasts were found on traverses beyond the Gladstone limit.

Glaciolacustrine (L^G; t, b, v)

Glaciolacustrine sediments are deposited in lacustrine environments in contact with glacial ice or fed by meltwater from glacial ice (Figure 2.11). Deposits are commonly stratified and may contain ice-rafted debris and subaqueous debris flows. Textures range from clays to bouldery diamict depending on proximity to the glacial source. Deposits are typically thickest at valley bottoms, forming plains (p), undulations (u), and hummocks (h). Strandlines (L^Gr), formed by wave action along shorelines, are present in lower Raft Creek (Figure 2.11E). Soft sediment deformation is common in glaciolacustrine material due to rapid deposition on top of saturated sediment.

Late Wisconsin – McConnell (M)

McConnell age glaciolacustrine deposits are common in Gladstone, Raft, and lower Rockslide creeks. Isolated deposits are found in the tributary valleys to upper

Gladstone Creek. Distal and medial facies are most common at the surface and comprise finely bedded, normally graded, silts and sands.

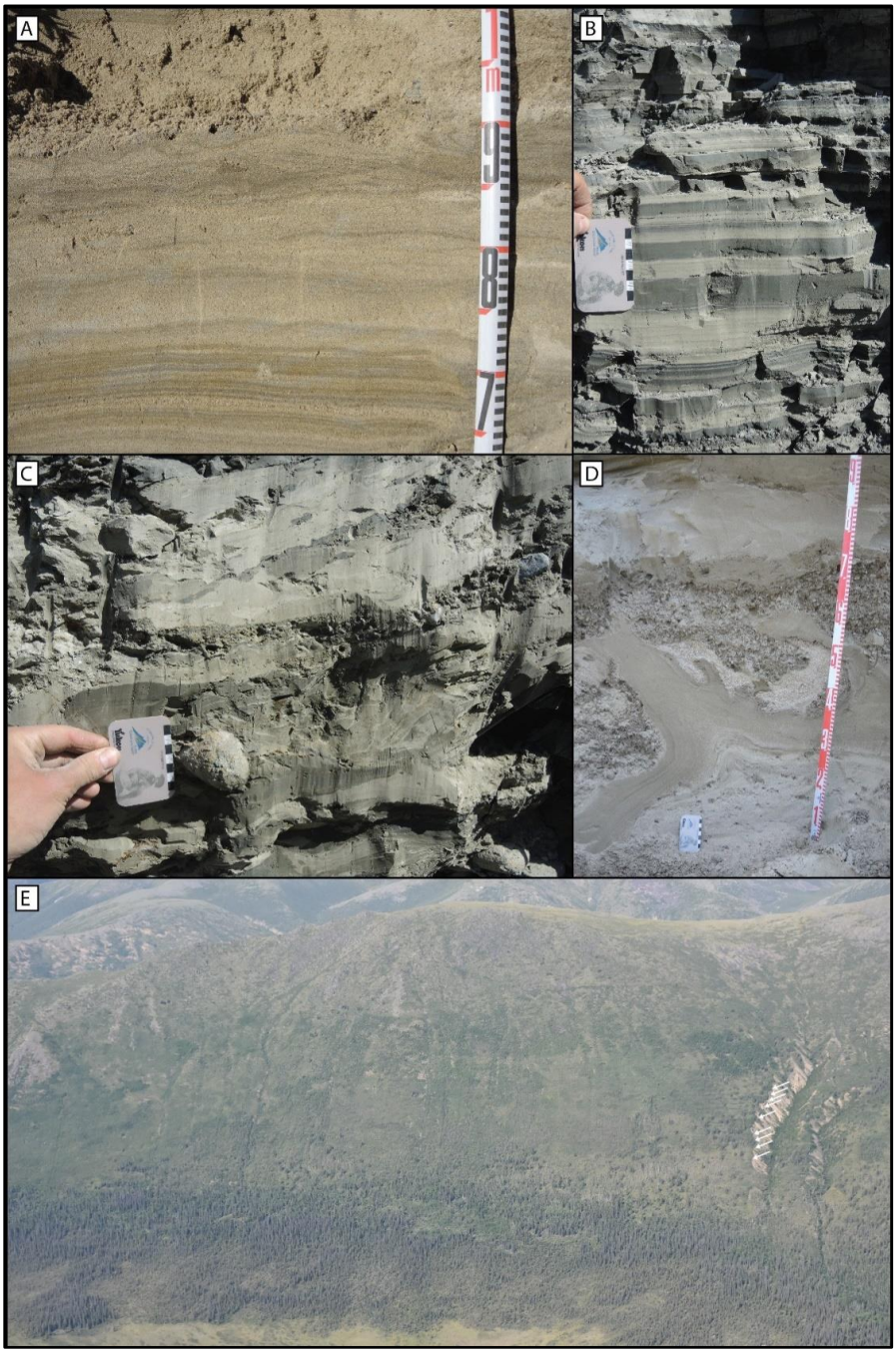

Figure 2.11 Glaciolacustrine sediments and landforms in the Gladstone map area. A) Stratified glaciolacustrine sand from a medial glaciolacustrine environment. B) Distal glaciolacustrine silt and clay in sections in Gladstone Creek. C) Deformed glaciolacustrine silt and clay with dropstones in Raft Creek. D) Soft sediment deformation in glaciolacustrine sediments in Camp Creek. E) Strandlines (arrows) in Raft Creek mark the margin of a glacial lake formed as result of valley impoundment by the St. Elias lobe. These strandlines likely consist of deflated colluvium and till.

Pre-Quaternary

Bedrock (R)

Bedrock in the Ruby Range consists primarily of the Paleocene Ruby Range batholith and the Late Cretaceous Kluane schist metamorphic assemblages (Israel et al., 2011). The Kluane schist is composed of dark grey to black, fine-grained biotite schist, and light to dark gray, fine-grained quartz-muscovite schist. The Ruby Range batholith consists of salt and pepper quartz diorite, light grey to pinkish granodiorite, beige to grey tonalite, and pinkish grey biotite granite. Strongly to moderately deformed equivalents of the Ruby Range batholith are found near its lower contacts. Gneiss in the study area is uncorrelated and may be a gneissic equivalent of the Kluane schist or basement rock to the Yukon-Tanana terrane. Bedrock was not differentiated by age or lithology.

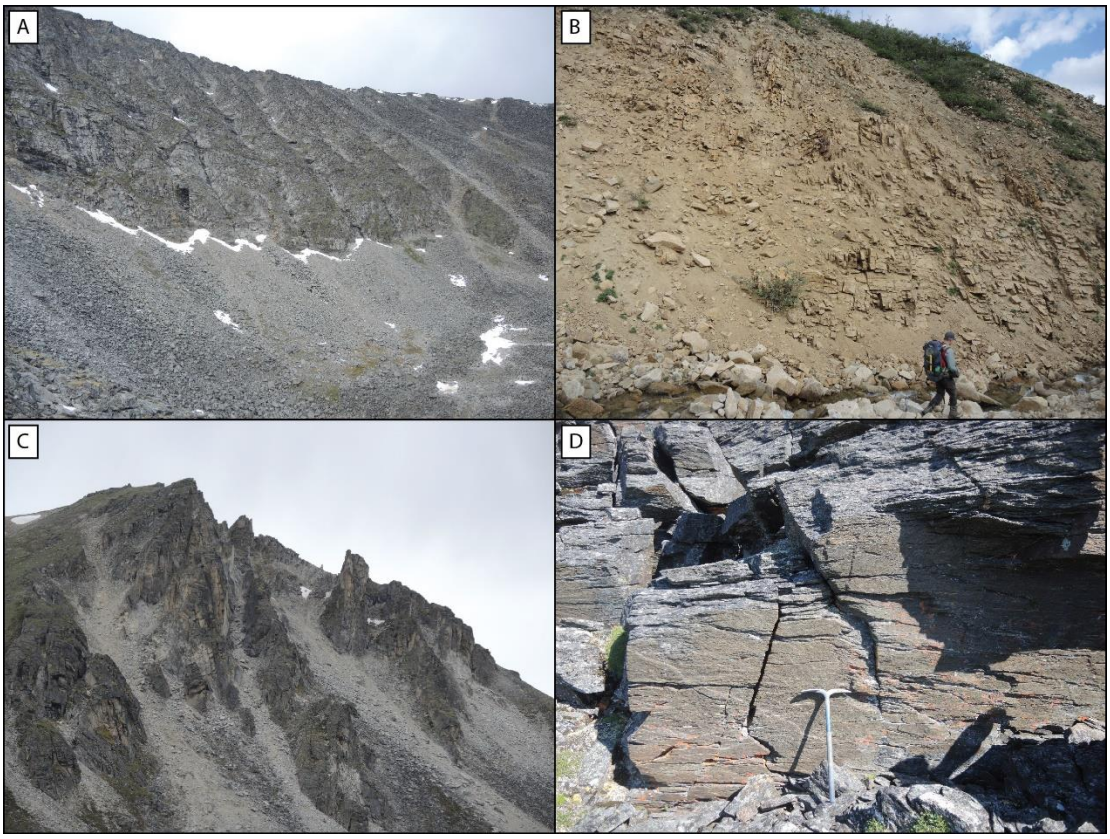

Figure 2.12 Bedrock and associated landforms in the Gladstone map area. A) Steep bedrock from McConnell-age cirque. B) Highly fractured Ruby Range batholith along a fault in Albert Creek. C) Rock ridges and pinnacles on Camp Creek valley wall. D) Kluane schist outcrop on a ridge above lower Gladstone Creek.

Uncorrelated

Undifferentiated (U)

Map units are assigned “undifferentiated” when they consist of a stratigraphic sequence of more than three material types that cannot be separated at the scale of mapping. Undifferentiated materials are mapped on and adjacent to the steep slopes on lower Gladstone Creek that contain complex stratigraphy, too detailed to be shown at the map scale.

2.2.2. **Geomorphic Processes**

Active geomorphic processes in the study fall into four categories: erosional, fluvial, mass movement, and periglacial. These processes are indicated by a capitalized letter following a dash separating the process from the surficial material.

Erosional Processes

Gully erosion (-V)

Gully erosion occurs most commonly on slopes of till and glaciolacustrine sediments where surface water cannot infiltrate, and overland flow occurs, eroding material. Gullying is commonly associated with the degradation of permafrost or debris flow activity. Gully erosion is rare in the map area.

Fluvial Processes

Irregularly sinuous channel (-I)

Most creeks in the map area have irregularly sinuous channels. Meander patterns are typically not repeated. The creeks are commonly confined by thick glacial sediment resulting in flood plains that are typically narrow relative to valley width.

Meandering channel (-M)

Small portions of Gladstone Creek and Raft Creek have a regularly meandering channel where valley bottoms are wide relative to the channel width, and the channel is relatively unconfined by surficial materials. Bends in meandering reaches are regular and repeating in form with a relatively high degree of sinuosity.

Mass Movement Processes

Mass movement processes are gravity driven and divided into rapid and slow based on their rate of movement. Each mass movement label is assigned at least one sub-class. The polygons where mass movements initiated are indicated by a double hash mark (“) following the mass movement label. Mass movement processes are common on steep slopes throughout the study area.

Rapid (-R)

Rapid mass movements include falling, rolling, sliding, or flowing material. Subclasses of rapid mass movement in the area include debris flows (d), debris slides (s), rock falls (b) and rockslides (r).

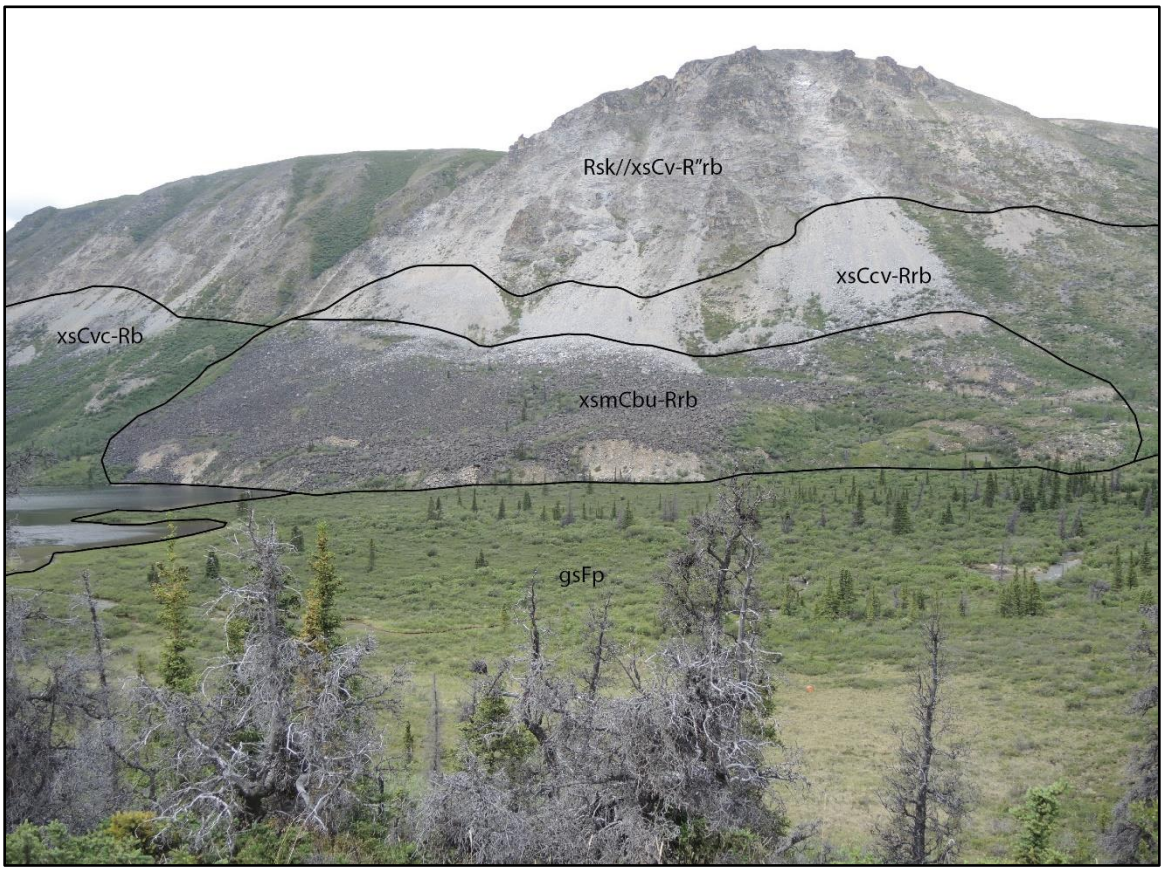

Figure 2.13 Rockslide (-R”r) and rockfall (-R”b) in upper Gladstone Creek. The steep colluviating toe of the deposit suggests active creep of the rockslide deposit.

Slow (-F)

Slow mass movements that move via, sliding, creeping, and settling. Slow mass movement in the map area is limited to rock creep.

Subclasses

Debris flow (d): the most common rapid mass movement process in the map area. Debris flows typically initiate in steep terrain. Many debris flows initiate in response to permafrost degradation.

Debris slide (s): typically occur on steep, open colluvial slopes where debris can fail along a planar surface and move downslope unconfined by topography.

Rock creep (g): occurs in the form of rock glaciers. Rock glaciers are found on a few high, north facing cirques with highly fractured bedrock (Figure 2.15). Rock glaciers are typically found in cirques that display prominent MIS 2 or later moraines, suggesting they may have originated as debris-covered glaciers. It is unknown whether they are ice-cemented or ice-cored. Steep colluviating slopes at the toe of many rock glaciers indicate ongoing activity.

Rockfall (b): Rockfall initiates on steep bedrock outcrops, commonly in McConnell cirques. Persistent rockfall commonly forms blocky colluvial veneers and cones.

Rockslide (r): Rockslides occur rarely, on steep rock slopes, typically where glaciation has oversteepened and destabilized the bedrock.

Periglacial Processes

General periglacial processes (-Z)

Periglacial processes are nearly ubiquitous at high elevations. General periglacial processes are mapped when three or more of solifluction, nivation, cryoturbation, and permafrost processes occur within a single unit. Nivation was not mapped as an independent process.

Permafrost (-X)

Extensive discontinuous permafrost underlies most of the map area (Bonnaventure et al., 2016). The depth of the active layer varies with surficial material type, drainage, slope and aspect.

Solifluction (-S)

Solifluction is common on high elevation slopes of all aspects. Movement commonly occurs along an impermeable permafrost table. Alexander and Price (1980) studied solifluction lobes in the Ruby Range and found a solifluction lobe in upper Gladstone Creek moved at a rate of 7-10 mm/yr.

Cryoturbation (-C)

Cryoturbation, mixing of surficial materials by freezing and thawing, is common at high elevations on all slope aspects and angles. Crude sorting of surficial materials may occur in strongly cryoturbated materials resulting in pattern ground.

Subclasses

Four subclasses can be applied to the polygons containing permafrost (-x):

Segregated ice (i): Segregated ice was only mapped in two polygons, where it was observed in the field. It is likely more widespread in valley bottoms, but its presence is difficult to confirm.

Pingo (n): Open systems pingos were observed in valley bottoms and flanks, typically associated with till or glaciolacustrine sediments. Pingos are identified as point symbols as well as with terrain codes in the polygons.

Pattern ground (r): Occurs in areas of strong cryoturbation and enough sediment cover to allow for sorting of material.

Sheetwash (s): Sheetwash commonly occurs on valley bottoms and flanks where permafrost is near the surface.

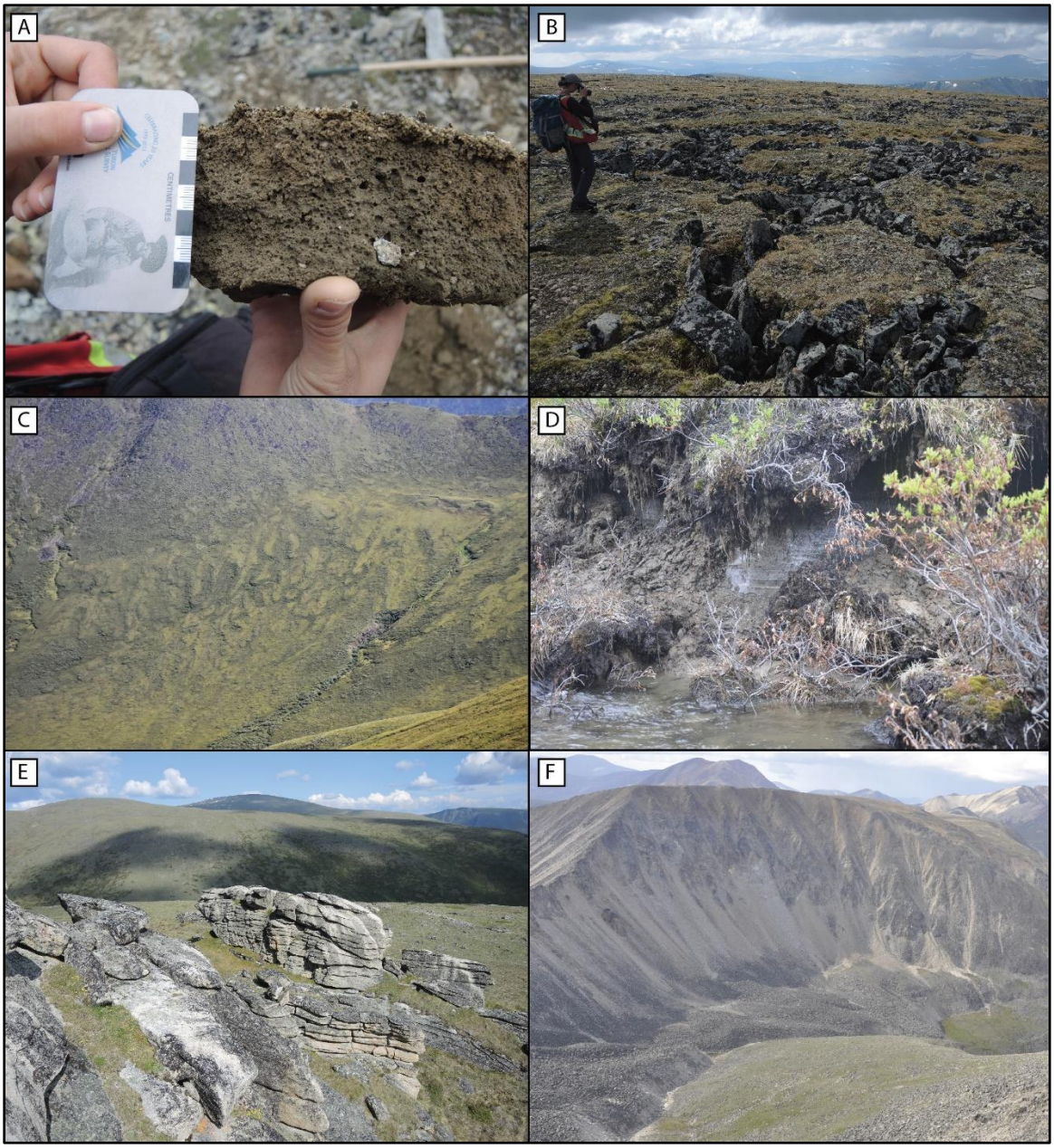

Figure 2.14 A. Vesicular soil from repeated freezing and thawing. B. Patterned ground on weathered bedrock and colluvium surface of Mt Hough C. Solifluction lobes on colluviated till and bedrock above Cyr Creek. D. Massive ice in the cut bank of a small tributary to Gladstone Creek. E. Tors on plateau surface above upper Gladstone Creek formed through periglacial weathering. F. Rock Glacier in upper Talbot Creek.

Deglacial Processes

Channelled by meltwater (-E)

Meltwater channels are common in all glaciated portions of the study area. Meltwater channels are found either at lateral margins, typically incised into bedrock, or at valley bottoms where meltwater flowed subglacially.

Kettled (-H)

Kettled sediments are found where sediments were deposited around or on top of glacial ice which subsequently melted leaving a depression. Kettled sediments occur on the east shore of Kluane Lake and in the valley bottom of Gladstone Creek. Kettles are typically found in glaciofluvial sediments and till.

Ice contact (-T)

Ice contact sediments associated with McConnell deglaciation are common in upper Gladstone Creek and typically consist of convoluted glaciofluvial and glaciolacustrine landforms, including hummocks, ridges, and fans.

Other Processes

Inundation (-U)

Rare areas of dominantly organics are inundated by a seasonally-high water table. Typically, these areas are inundated in the spring during freshet.

2.2.3. **Landforms**

Tors

Tors are bedrock features formed through prolonged periods of weathering at the surface. Their distinctive shapes are the result of increased weathering along joints in the bedrock (Linton, 1955). They are identified on the map as point features. Tors are commonly considered to be indicative of an unglaciated surface due to the length of time required for their formation through subaerial weathering; however, many tors in the map area and further afield have erratics on the surrounding surfaces and even within gnamma developed on their surfaces. This is discussed further in section 2.3.3.

Streamlined Macroforms

Crag and tail features consisting of glacially sculpted bedrock with ridged streamlined till deposited on the lee side were observed in the study area; they indicate ice flow direction (Figure 2.15). Craig and tails are common near Kluane Lake where ice flow velocities were likely higher near the Shakwak Trench due to less obstruction from topography compared to within Gladstone and Raft creeks.

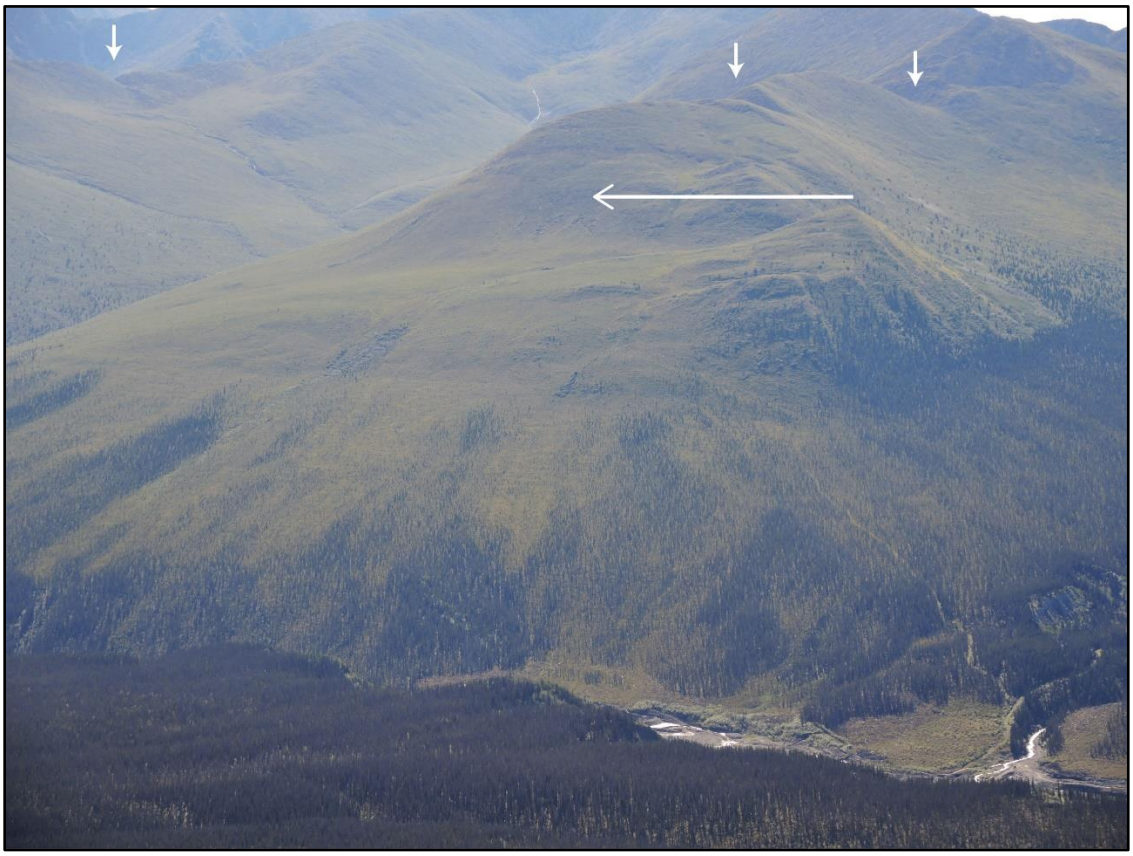

Figure 2.15 A crag and tail feature made of streamlined bedrock and drift indicates up-valley ice flow direction (horizontal arrow) in lower Gladstone Creek above the confluence with Cyr Creek. Meltwater channel notches through bedrock ridges are indicated by vertical arrows.

Eskers

Eskers are elongate, commonly sinuous ridges of glaciofluvial sand and gravel that typically form during deglaciation. Eskers are indicated on the map with line features and symbolized with unidirectional or alternating chevrons, dependent on whether their flow direction is known or unknown. Eskers are commonly found in Gladstone Creek and Raft Creek. One esker was identified on a high plateau surface north of the Gladstone Lakes and is suspected to be a remnant of the Gladstone Glaciation.

Meltwater Channels

Meltwater channels are common in the study area and are commonly the only indicators of glacial limits older than MIS 2. Dykes and faults cross-cutting bedrock are commonly exploited and eroded by glacial meltwater; however, similar landforms can result from differential weathering and erosion, usually along faults or joints, from subaerial processes (Figure 2.7 D; Figure 2.15). These features have similar morphology to meltwater channels and commonly need to be confirmed in the field based on the presence of erratics. It is possible that the desktop mapping by Duk-Rodkin (1999) misattributed subaerially-formed features as glaciogenic when mapping pre-Reid limits in southwest Yukon.

2.2.4. **Glacial Limits**

Glacial limits of different ages can often be distinguished by the morphology or "freshness" of glacial landforms such as moraine ridges. McConnell moraines are typically much steeper than those of older glaciations (Rampton, 1971). Conspicuous glacial landforms are not always present, particularly in areas of steep topography where colluviation causes rapid degradation of landforms. Here, the presence of erratics on the surface and in soil pits can be used to determine if the area has been glaciated. Other more permanent and conspicuous features such as meltwater channels incised in rock can persist for long periods and serve as a marker of minimum ice extent. However, care must be taken to differentiate between meltwater channels and gullies formed through differential erosion at lithological contacts and faults.

Two limits from CIS advances were identified within the study area (Figure 2.16). The fresher, less extensive limit is interpreted to correlate with the MIS 2 McConnell Glaciation. The older, more extensive limit likely correlates with the MIS 4 Gladstone Glaciation based on cosmogenic dates of erratics above upper Gladstone Creel (Ward, 2007). This more extensive limit may be a composite of MIS 4 and 6 limits, which have similar extents elsewhere in southwest Yukon (Turner et al., 2013). Recent mapping by Kennedy (2018) in the Burwash uplands, west of the study area and closer to the St. Elias source areas, also mapped only two advances from the St. Elias source areas supporting the possibility of the MIS 4 limit being locally coincident or more extensive than MIS 6.

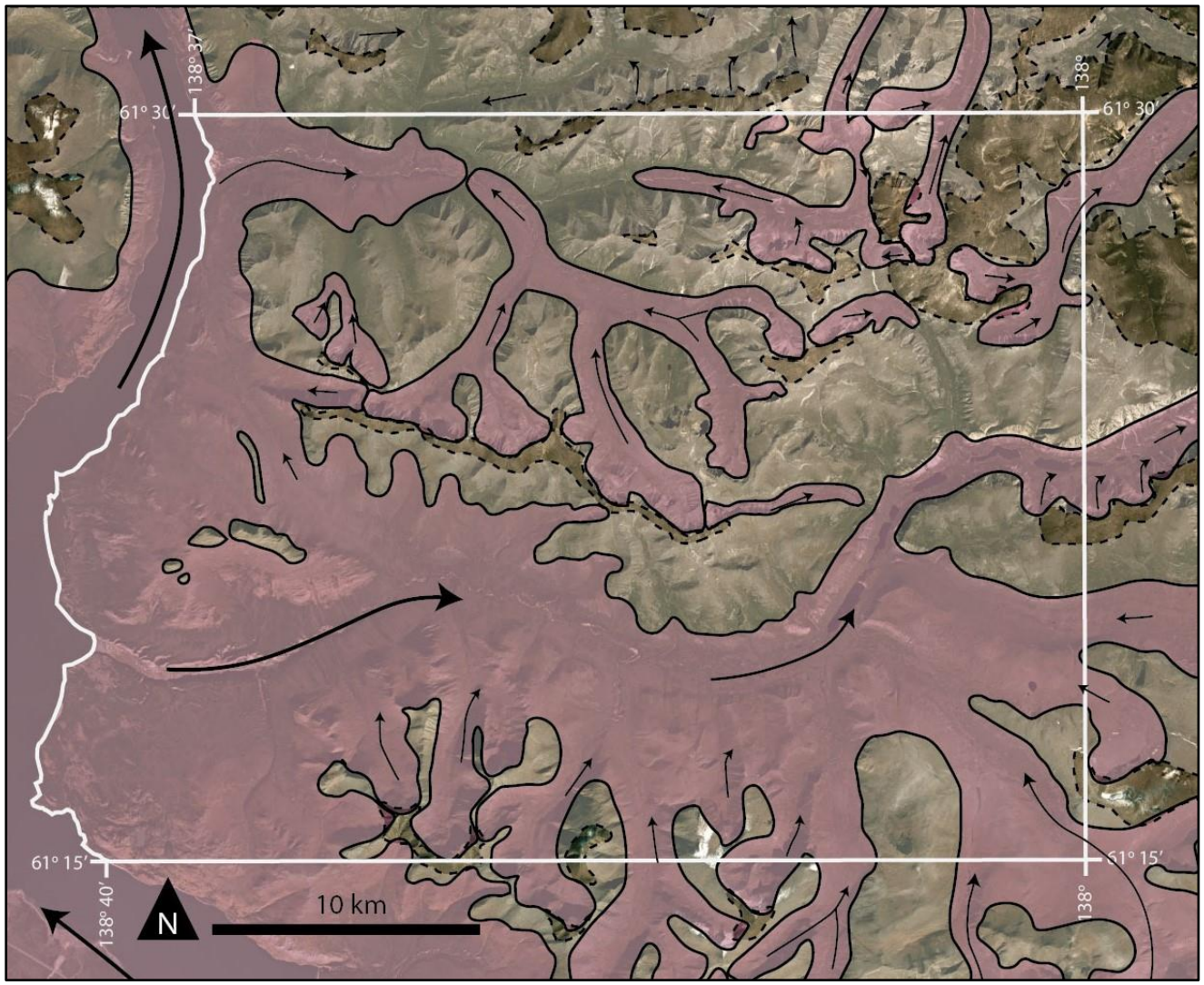

Figure 2.16 Glacial limits in the map area and surroundings based on Cronmiller et al. 2018. The McConnell (MIS 2) limit is mapped with a solid line and purple infill. The more extensive limit, marked with a dashed line and green infill, is likely a composite of Gladstone and Reid (MIS 4 and MIS 6) glacial limits.

McConnell Limit, MIS 2

In the southwest of the map area, near the mouth of Gladstone Creek, the MIS 2 limit is approximately 1700 m asl (Appendix A). The terminal limit in Gladstone valley is located 7 km east of the divide between Gladstone and Isaac creeks at 1200 m. Inferred from elevations of the moraines and trimlines, ice gradient between the mouth of Gladstone Creek and the terminal limit in Isaac Creek is approximately 0.7°.

In Raft Creek the MIS 2 St. Elias lobe limit drops rapidly from approximately 1500 to 1000 m asl. This drop likely is a result of the tight confines of the valley and the valley's orientation at more than 90° to the ice flow direction in Talbot arm of Kluane Lake restricting up-valley ice flow. The terminal limit in Raft Creek is poorly defined; subaqueous fan sediments in sections at this limit suggest a grounding line near the first valley confluence to the north, approximately 7 km above the creek mouth. Ice gradient here may have been as steep as 4°. Valley glaciers descending Raft Creek appear to have come within 1 km of the St. Elias limit, without coalescing. One of the key pieces of evidence for this is the lack of boulders (erratics) in Raft Creek between these limits, which are abundant within the St. Elias lobe and Ruby Range valley glacier limits.

^{10}Be ages from boulders on moraines in Raft and Rockslide creeks date alpine advances to 13.7 ± 0.9 ka (Table 2.1, Appendix D). Relatively fresh moraines from high, north facing cirques and valleys above Gladstone Creek likely correlate with the advances in Raft and Rockslide creeks.

Table 2.1 Cosmogenic ages (^{10}Be) from erratics in the map area. Sample locations shown on Appendix A map. Samples RC-01, RC-02, and RC-03 were collected from boulders on the moraine pictured in Figure 3.31. Insufficient quartz content prevented dating RS-01 using ^{10}Be. Complete field and analytical data used for calculation of ^{10}Be ages is provided in Appendix D.

Sample ID	Age (ka)	Location	
RS-01	Insf. qtz	61.4627° N	138.1459° W
RS-02	16.0 ± 1.0	61.4631° N	138.1563° W
RS-03	13.5 ± 0.8	61.4677° N	138.1525° W
RC-01	14.0 ± 0.9	61.4678° N	138.3747° W
RC-02	13.8 ± 0.9	61.4708° N	138.3835° W
RC-03	13.6 ± 0.9	61.4713° N	138.3826° W

The plateau surfaces in the eastern portion of the map sheet and south of Gladstone Creek appear to have hosted ice caps during the McConnell Glaciation (Figure 2.17). This was initially suggested by Hughes (1987) and is supported by this study. U-shaped valleys descend from these plateaus in multiple directions suggesting radial flow. These valleys likely formed during the earliest glaciations in which the plateau surfaces hosted ice caps, probably during the pre-Reid when deeply weathered bedrock would have been more readily eroded by glaciation. Lateral moraines in the valleys descend toward Gladstone Creek. The moraines descending from the ice caps appear to coalesce with those of the St. Elias lobe, suggesting ice cap growth was roughly synchronous with CIS. Rare erratics are present on portions of the plateau surfaces which may be the result of local plucking or transport from north-flowing ice crossing the plateaus. Low passes in the southwest of the map sheet may have allowed for some connectivity with the Coast Mountain lobe.

Penultimate limit, MIS 4/6

On the west side of the Shakwak Trench, the penultimate glacial limit was previously mapped at approximately 1800 m asl (Muller, 1967; Duk-Rodkin, 1999). Few features confirm the elevation of this limit at the mouth of Gladstone Creek, although based on rare-meltwater channels it appears to have been at approximately the same elevation as reported by Muller (1967). Erratics on a ridge above the confluence of Raft and Rockslide creeks suggest the limit at this location was at least 1650 m asl. Only the highest peaks and ridges in the west of the map area appear to have been nunataks; however, cold-based ice is likely to have occurred in the area, making accurately reconstructing limits difficult. Advances from Ruby Range cirques were more extensive than MIS 2 and occurred at lower elevations and on warmer aspects (Appendix A).

Dated erratics (Ward et al. 2007) on a plateau surface at the east margin of the map sheet suggest the MIS-4 limit at the margin of the St. Elias lobe was somewhere above 1700 m. With ice elevations above 1700 m, it is likely that there was greater connectivity between the Coast Mountain and St. Elias lobes, particularly on the plateau surfaces in the southeast of the study area. These surfaces may have been isolated accumulation areas at the onset of glaciation, but likely would have become incorporated into the CIS and its regional ice flow patterns during the MIS 4 and 6 glacial maxima.

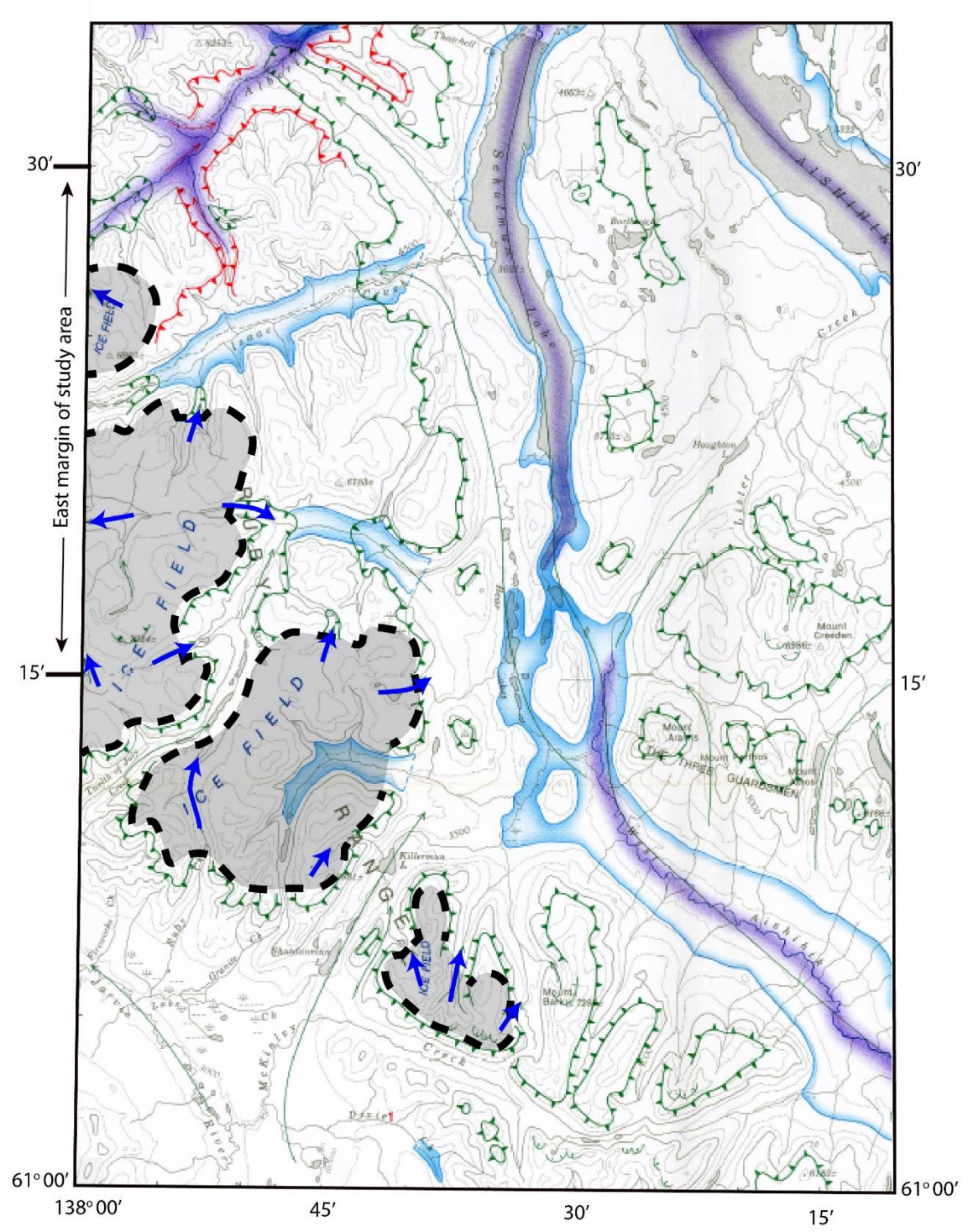

Figure 2.17 Theoretical ice cap extent (gray shading) based on mapping by Hughes (1987)for the area immediately to the east of the study area. Ice cap flow directions are indicated by blue arrows. Because these ice caps do not produce erratics, the most persuasive evidence for their existence comes from U-shaped valleys descending from plateaus in multiple directions, and rare meltwater channels on their surfaces. These ice caps are suspected to extend into the eastern portion of the Gladstone Creek map area, although little evidence definitively confirms their existence.

2.3. Discussion

2.3.1. **Mapping challenges**

Two types of challenges were encountered during mapping. The first type of challenge was associated with hardware, software, and data quality. The second type of mapping challenge was the result landscape complexity and geomorphic activity obscuring older glacial landforms.

The aerial photographs used for mapping were of variable quality. The 1988 photographs had a large blurred portion in the centre of each image due to an issue with the camera lens during the flight. This blurring of images prevented stereo viewing of portions of the centre of each photo in the affected flight lines.

Much of the study area, particularly glacially steepened valley walls, is actively colluviating due to strong periglacial conditions. Colluviation also occurs on low angle slopes through solifluction and soil creep. Frost-shattered bedrock is common, allowing for creep and solifluction even on slopes free of drift. This colluviation obscures marginal glacial landforms such as lateral moraines and meltwater channels.

In areas where glacial landforms are too degraded to identify glacial limits, the presence of erratics can be used to identify the all-time limit of glaciation. The glacial limits in the eastern half of the map area are entirely underlain by the Ruby Range batholith (Figure 1.5). Foreign lithology erratics are rare in this portion of the map sheet because the batholith is so extensive. Erratics must then be determined based on rounded and striated clasts. This however also proves difficult due to the spheroidal weathering of granitic rocks, as well as the difficulty of observing striations on coarser grained rock, especially once weathered.

2.3.2. **Ruby Range ice contributions**

The low angle ice gradient in Gladstone Creek is in stark contrast to the steeper gradient found in Raft Creek. This may be partially attributed to the orientations of Gladstone and Raft Creek confluences being more and less aligned with the local ice flow directions in the Shakwak Trench, respectively. However, the 0.7° ice gradient in Gladstone Creek more comparable with the 0.5° gradient reported for the outermost 50

km of the Selwyn lobe in major trunk valleys (Jackson et al., 1991). The McConnell terminal limits of the Selwyn lobe are located in much broader and shallower valleys than Gladstone Creek. A more satisfactory explanation for the low angle ice gradient is ice contributions from local Ruby Range cirques and ice caps augmenting the St. Elias lobe. No extrabasinal erratics were found during traverses on the east side of the map suggesting penetration of St. Elias lobe ice was minimal due to the presence and gradient of local ice sources.

2.3.3. **Cold-based ice**

The extreme cold temperatures during the last glacial maximum increase the probability of cold-based ice near the lateral and upper margins of the ice sheet, where ice is thin. When ice is frozen to the underlying substrate, little or no erosion takes place, resulting in few defining landforms or materials and preservation of old, fragile surfaces. Erratics and ablation till may be deposited during deglaciation if englacial or supraglacial sediment is present. Meltwater channels beyond the limit of other evidence of glaciation may give evidence of cold-based ice.

Some landforms previously believed to be associated with unglaciated terrain, such as tors (Linton, 1955), have been shown to be able to survive under cold-based ice with little or no erosion (Stroeven et al., 2002; Hättestrand and Stroeven 2002). Tors on an erratic-strewn plateau surface approximately 65 km southeast of the study area have many fragile features formed through weathering incongruent evidence of ice cover given by erratics (Figure 2.18A). Even stronger evidence for their glaciation is the presence of rounded, exotic clasts in some of the gnammas on the tors (Figure 2.18B).

Thin ice near the margins of glaciers in extremely cold environments allows for frozen-bed conditions as the pressure melting point of ice may not be reached where ice is thin. Hattestrand and Stroeven (2002) found that frozen-bed conditions may also occur in areas of thick ice if pre-glacial ground temperatures are cold enough to negate the effects of strain heat release. Areas of divergent flow or underlain by rough topography may reduce ice flow velocities, reducing strain heat release and increasing the likelihood of cold-based ice and hence, subaerial landform preservation (Hattestrand and Stroeven, 2002). Kelman and Stroeven (1997) found that pre-glacial surfaces are best preserved at intermediate elevations, where ice is thin enough to allow for frozen bed conditions but

low enough that they are not affected by cirque glaciation. This may partially explain the preservation of surface features commonly associated with unglaciated terrain on the plateau surfaces in the southeast portion of the map area.

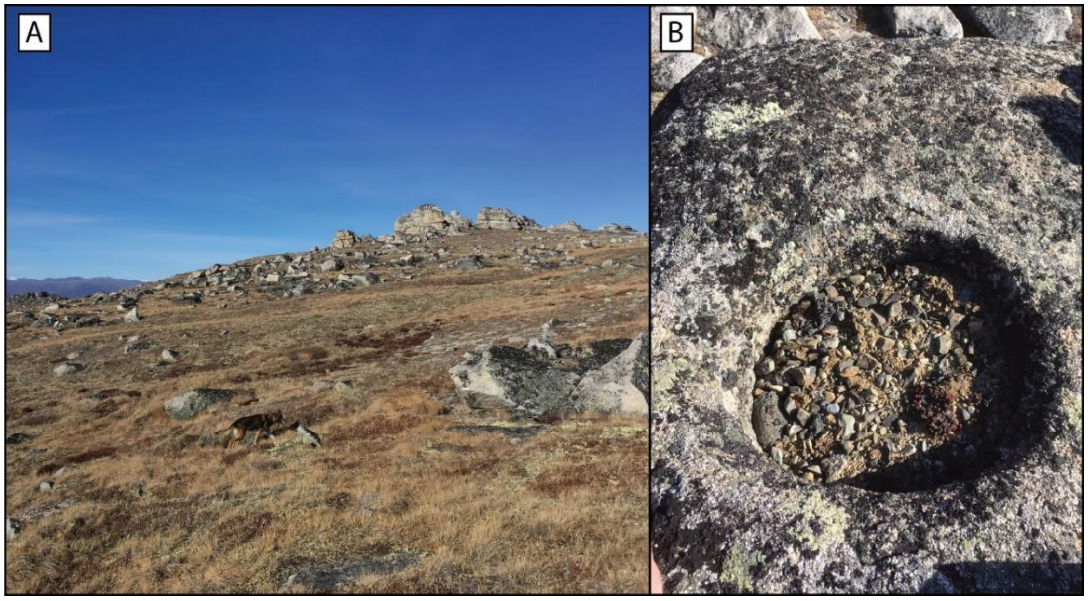

Figure 2.18 A. Tors surrounded by erratics on a plateau surface above the confluence of the Aishihik and Dezadeash rivers, southeast of the map area. B. A gnamma on the top of one of the tors is filled with drift, confirming the tors were, in fact, glaciated. The nearby McConnell limit of the Coast Mountain lobe suggests ice cover would an been thin, allowing for cold-based ice, leaving the tor relatively unchanged.

2.3.4. **Distribution of surficial materials**

The distribution of surficial materials in the Gladstone map area reflects the interplay between local and regional ice sources and ice limits during the last two glacial cycles. Bedrock is exposed in Gladstone- and McConnell-aged cirques and the oversteepened walls of glaciated valleys. Rare bedrock exposures are found on steeper unglaciated peaks and form tors on plateau surfaces. Low angle unglaciated surfaces, mostly located on high plateaus on the east side of the map sheet, are typically covered by weathered bedrock. Colluvium is the most extensive material in the area, most commonly consisting of colluviated bedrock with lesser amounts of colluviated till below glacial limits. Till is found on the flanks of trunk valleys, the bottom and flanks of tributary valleys, and rarely on plateau surfaces. Glaciofluvial material is found in upper Gladstone Creek, rarely in Raft Creek, and along the east margin of Kluane Lake, where meltwater was free flowing at the front of glaciers. In lower Gladstone, Raft, and Rockslide creeks, and their ice-free tributaries, meltwater impounded by the CIS formed pro-glacial lakes.

Glaciolacustrine deposits are found where these lakes existed (Figure 2.19). Fluvial sediments are found in valley bottoms throughout the map area. Deposits are typically more widespread in broader, lower gradient valleys. Eolian material is widespread throughout the study area but typically in thin, non-mappable concentrations of loess. Thick eolian deposits occur on terraces above Kluane Lake and rarely on glaciofluvial terraces in upper Gladstone Creek in the form of clifftop dunes. Organic material occurs on floodplains, low angle areas with shallow permafrost tables, and other areas where high water tables allow for its development. The distribution of these surficial materials and their associated landforms are used to inform the glacial history of the study area as discussed in Chapter 3.

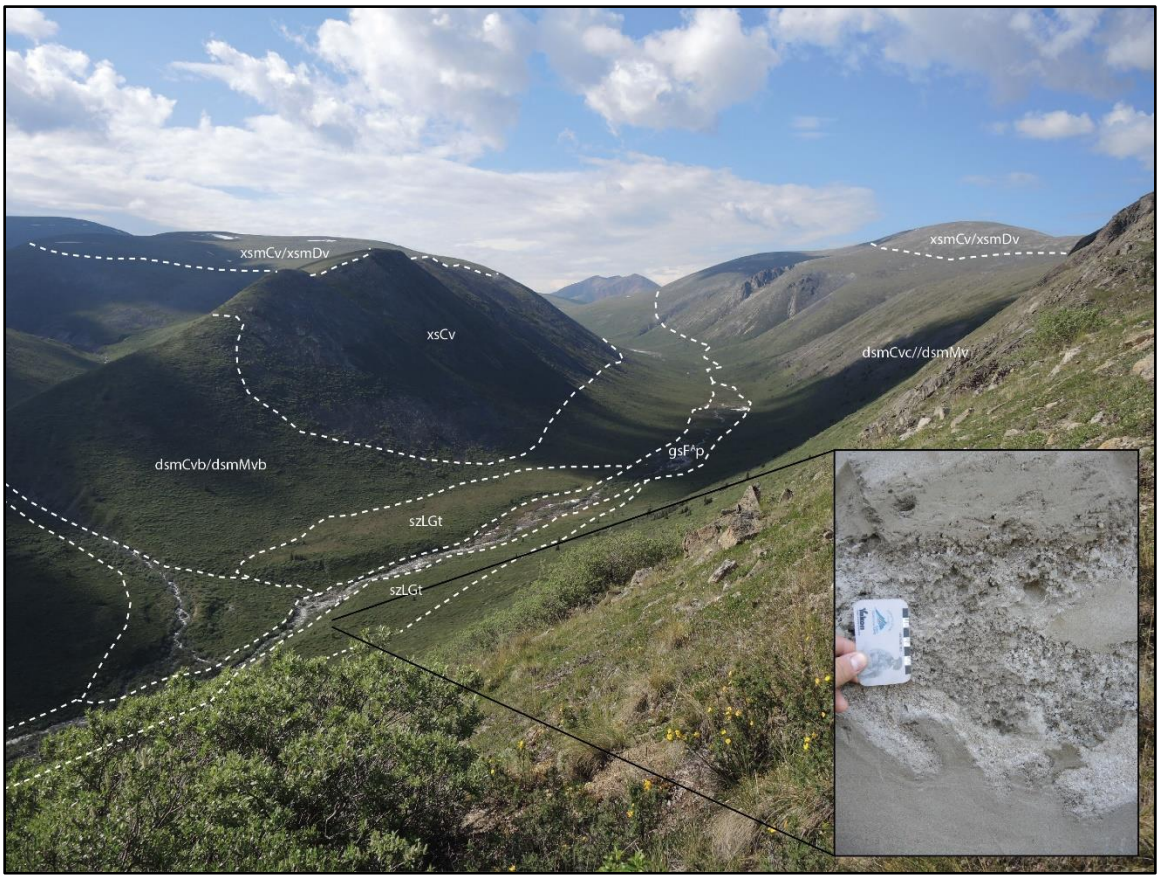

Figure 2.19 Surficial geology in Camp Creek. Inset shows a cross section of glaciolacustrine terrace sediments deposited as the CIS impounded the creek during MIS 2.

Chapter 3. Stratigraphy and Glacial History of the Central Ruby Range, Southwest Yukon

Derek C. Cronmiller and Brent C. Ward
Department of Earth Sciences, Simon Fraser University

Jeffrey D. Bond
Yukon Geological Survey

John C. Gosse
Department of Earth Sciences, Dalhousie University

Britta J.L. Jensen
Department of Earth and Atmospheric Sciences, University of Alberta

Michel Lamothe
Department of Earth and Atmospheric Sciences, University a Quebec du Montreal

Alice Telka
Paleotec Services

3.1. Abstract

The surficial geology and stratigraphy of the central Ruby Range record the complex interplay between opposing glacial advances of the St. Elias lobe of the northern Cordilleran Ice Sheet, and extensive Ruby Range glaciers sourced from cirques and ice caps in the Ruby Range. The style of sedimentation from glacial advances is dictated by alterations to base level resulting from the impounding of Gladstone Creek and the Shakwak Trench. Sections from Gladstone Creek and the Gladstone Creek map area (NTS 115G/7, 8) record two advances of the St. Elias lobe, and at least three advances from Ruby Range source areas. Two glacial limits from St. Elias lobe correlating to MIS 4 and 2 were identified in the map area. The MIS 4 limit is poorly constrained and may be a composite of MIS 6 and 4. Both limits appear to have been significantly augmented by local sources.

3.2. Introduction

The deep valleys of the central Ruby Range are filled with thick packages of Quaternary drift, which have been incised up to 120 m by modern fluvial erosion (Figure 3.1). The resulting terraces contain complex middle- to late-Pleistocene stratigraphic

sequences that arise from the interplay between opposing glacial advances from the cirques within the Ruby Range and the St. Elias lobe of the Cordilleran Ice Sheet. This chapter presents the findings of stratigraphic analyses within Gladstone Creek and the central Ruby Range. The results of the stratigraphic analysis are synthesized with surficial geology mapping from Chapter 2 to provide a more comprehensive picture of the glacial history of the Ruby Range. Stratigraphic sections and sedimentological descriptions are presented in Appendix B, with key sections and an idealized composite section of the stratigraphy in Gladstone Creek also included in-text.

3.2.1. **Setting**

The central Ruby Range comprises most of the study area (Figure 1.2); however, the northeast corner of the study area overlaps with the west margin of the Nisling Range. These mountain ranges were formed by dissection of the Klondike Plateau during uplift in the Late Miocene or Pliocene (Tempelman-Kluit, 1980). The rolling plateau surfaces in the east of the study area represent partial dissection of the initial lower relief surfaces, whereas the rugged peaks in the central and western portions of the study area represent complete dissection of this surface (Figure 1.3, cf. Tempelman-Kluit, 1980). Deep U-shaped valleys, with truncated ridges, separate the peaks of Ruby Range. Well-developed cirques exist at elevations above 1500 m on north aspects. North-draining valleys, that commonly contain cirques, tend to be broader and deeper than south-draining valleys due to the relative effectiveness of alpine glacier erosion compared to fluvial erosion (cf. Montgomery, 2002).

The study area is located at the east margin on the St. Elias lobe during mid- to late-Pleistocene glaciations, which covered much of the study area (Muller, 1967; Hughes, 1969; Duk-Rodkin, 1999). Only small rock glaciers, less than 4 km^2, exist in the study area at present. Trunk valleys, such as Gladstone Creek, are commonly filled with thick drift. Steeper slopes and high elevation surfaces are commonly covered with thin colluvium, weathered bedrock, and rare till.

Kluane Lake forms the western margin of the study area. The lake is bounded by the Duke River fan at the north end of the lake, and Kaskawash glacier's valley train deposits in the Slim's River valley. The water level of Kluane Lake (780 m asl) has varied by tens of metres over the Holocene (Brahney et al., 2008; Clague et al., 2006) and

controls the base-level for Gladstone and Raft creeks, which contain the principal stratigraphic record.

Figure 3.1 Thick Quaternary drift forms the valley walls of lower Gladstone Creek. The complex stratigraphic sequences contained in these deposits record both up-valley (CIS) and down-valley (Ruby Range) advances.

3.2.2. **Previous work**

The penultimate limit in much of Yukon was reached by the MIS 6 Reid Glaciation (Bostock 1966); however, recent work by Ward et al. (2007) and Turner (2013) found the penultimate limit of the St. Elias lobe was reached in MIS 4. Recent work by Stroeven et al. (2014) suggests the penultimate limit of the Coast Mountain lobe may also be MIS 4 in age. This glaciation is known as the Gladstone (Ward et al., 2007) and correlates to MIS 4 glaciation recorded in southern Alaska (Brinner et al. 2005, Brinner and Kaufman, 2008) and the Icefield glaciation in Silver Creek (Denton and Stuiver, 1967; Turner et al., 2016). Turner et al. (2013) found confirmation of an MIS 4 advance of the St. Elias lobe in the stratigraphy along White River. Turner et al. (2013), distinguished Reid and Gladstone limits approximately 4 km apart at the glacial terminus, but lateral limits were separated vertically by only tens of metres.

The most recent glaciation, the McConnell (Bostock 1966), occurred during MIS 2 (Matthews et al., 1990; Jackson and Harington, 1991). Ice began to accumulate in source areas in mountainous regions around 29 ka, with the major ice lobes coalescing to form a contiguous ice sheet sometime after 24 ka (Jackson et al. 1991). The St. Elias lobe reached its maximum extent and began retreat by between 17.7 ± 0.9 ka and 16.6 ± 0.8 ka (Bond and Lipovsky, 2009C; ages corrected since original publication). The McConnell limit is the least extensive continuously exposed limit throughout Yukon, though Gladstone limits are likely less extensive outside of the areas glaciated by the St. Elias lobe, but have not been confirmed in section. Its surfaces are readily distinguished by their relatively well-preserved morphology (Ward et al., 2007).

The sections examined on Silver Creek by Turner et al. (2016), 30 km to the south of the study area, record at least five distinct advances from the St. Elias mountains correlating to MIS 2, 4, 6, and two older glaciations, which occurred sometime before 320 ka. These older glaciations are the only stratigraphic evidence supporting pre-Reid advances of the St. Elias lobe to date. Peat beds between MIS 4 and MIS 2 tills date to MIS 3 and indicate the area, which is closer to St. Elias source areas than the Ruby Range, was ice-free during the last interstadial. This suggests that ice extents in MIS 3 were similar to the present day. It is suspected that during MIS 3, glaciation was confined to cirques in mountainous regions (Clark et al., 1993).

Stratigraphy in Gladstone Creek was previously examined Madsen (2001) as part of an undergrad thesis. Madsen identified three advances of the St. Elias lobe, which she interpreted as MIS 6, and two MIS 2 advances based on radiocarbon ages of 40,510 ± 680 and 34,960 ± 390 ^{14}C yr. BP. This work was completed before the Gladstone Glaciation was identified (Ward et al., 2007), and prior to detailed mapping suggesting substantial ice was produced from Ruby Range source areas (Cronmiller et al., 2018), so the lithostratigraphic model proposed by Madsen requires re-interpretation.

3.3. Methods

Stratigraphic sections were logged at twenty-four sites throughout the Gladstone Creek map area (NTS 115 G07/08; Cronmiller et al., 2018), with most sites along the lower 8 km of Gladstone Creek. Heights recorded on stratigraphic sections use Gladstone Creek as base level. Stratigraphic sections were divided into units based on their sedimentology

and relative age constraints. Clast fabrics were plotted on equal-area, lower-hemisphere stereonets. Clast A-axes were measured in diamicton units to help determine their genesis (till vs colluvium) on the basis of their fabric. Fabrics comprised a minimum of 25 clasts, although rarely fewer were collected due to scarcity of suitable clasts and time.

Infrared stimulated luminescence (IRSL) dating was used where units contained dominantly silt and sand and were likely to have been exposed to sunlight sufficient for a complete bleaching of grains before burial. IRSL samples were collected in PVC and copper pipes driven into the sediment with a mallet. IRSL samples were processed by the LUX Laboratory at Université du Québec à Montréal. Laboratory analysis used a Freiberg Instrument Lexsyg Smart Luminescence System equipped with a 90Sr beta irradiator and a Canberra gamma spectrometer. Analysis generally followed procedures for IRSL dating on potassium feldspars as outlined in Duller (2008). A single aliquot regenerative protocol modified according to Forget Brisson et al., (submitted) was used to determine the equivalent dose. The annual dose was calculated using gamma spectrometry and analysis of water content.

Where units contained organic material, samples were collected for identification and radiocarbon dating. Bone samples were sent to Dr Grant Zazula with Yukon Government for processing and identification. Insect macrofossil samples were sent to Alice Telka at Paleotech Services in Ottawa for identification and isolation of carbon samples for dating. Radiocarbon dating was completed by the Keck Carbon Cycle Laboratory at University of California and A.E. Lalonde AMS Laboratory at University of Ottawa.

Tephra samples were collected from sections. The tephras were collected in plastic sample bags, then sieved on a shaker to isolate the fraction finer than 125 µm. The fine fractions of samples were sent to Dr Britta Jensen at the University of Alberta for chemical analysis and comparison of the major element composition of glass shards to a database of known tephra samples. Glass shards were analyzed using electron probe microanalysis on a JEOL 8900 SuperProbe by wave-dispersive spectrometry. Standards of Lipari obsidian (3506) and Old Crow Tephra were analyzed at the start and end of each run to ensure the accuracy of calibration.

3.4. Results

3.4.1. Gladstone and Cyr Creek Stratigraphy

Eighteen sections were logged on Gladstone and Cyr creeks (Figure 3.2). Stratigraphic sections and unit descriptions from these sites are shown in Appendix B. Sections on the north side of Gladstone Creek range from 35 - 115 m in height. Sections on the south side and valley bottom of Gladstone Creek and on Cyr Creek are generally less than 40 m thick and mostly exposed in mine cuts. Exposures are commonly poor and interrupted by colluvial cover, requiring lateral traversing and extensive digging to log complete sections. Despite extensive digging, many sections still have covered intervals. It is possible that laterally discontinuous stratigraphic units were not identified, or the stratigraphic order of these units is incorrect. These covered areas, both within and between sections, combined with cut and fill through repeated cycles of glaciation and fluvial erosion, make correlation between sections challenging. The following is a best effort at the interpretation of stratigraphy and glacial history mainly from the exposures Gladstone Creek, but also throughout the study area.

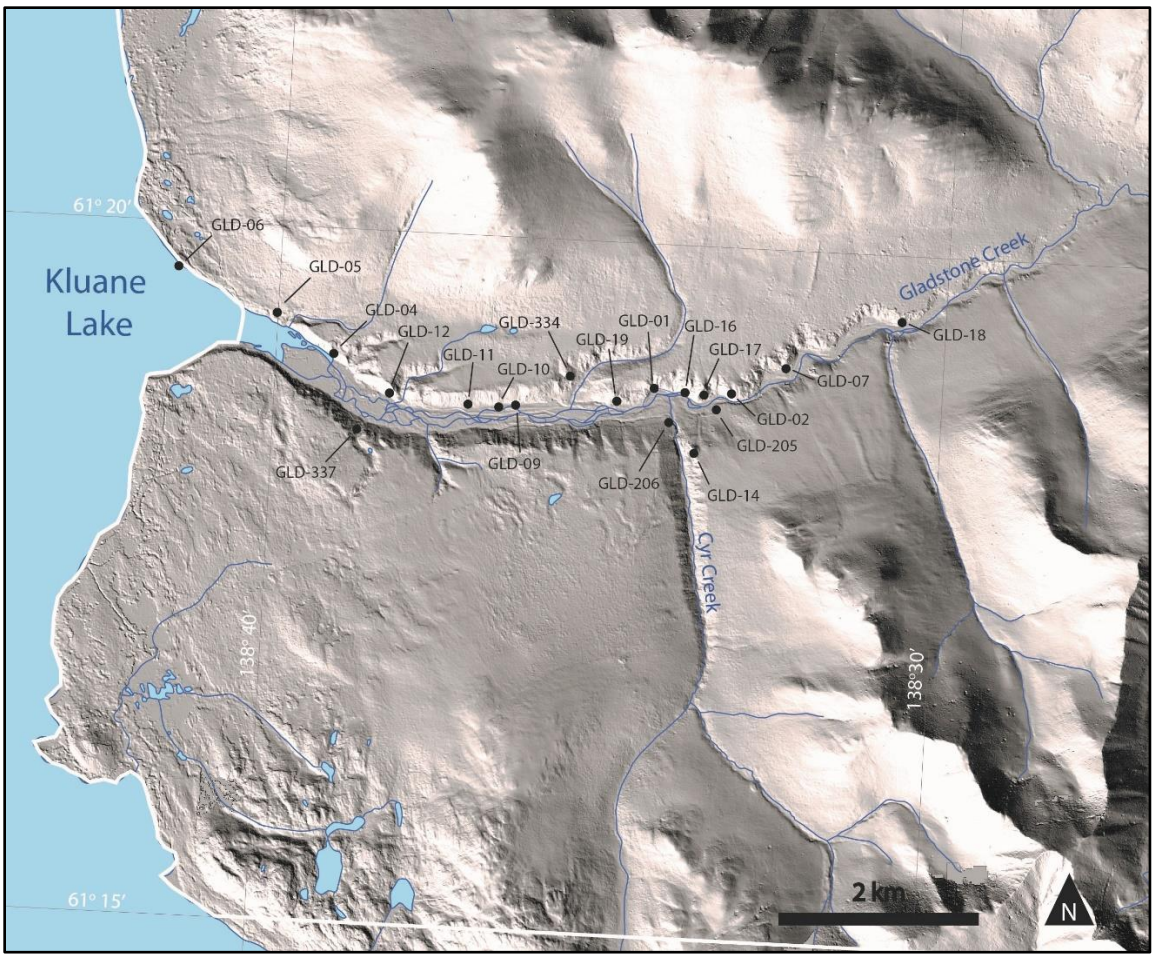

Figure 3.2 Locations of stratigraphic sections on Gladstone and Cyr creeks. The surficial mapping boundary is shown by the white line. Hillshade derived from 2 m Arctic DEM (Porter et al., 2018).

Lithostratigraphic units

An idealized composite section composed of units exposed in Gladstone Creek comprises 16 lithostratigraphic units (Figure 3.3 and Appendix B). Each lithostratigraphic unit represents a unique time and depositional environment in Gladstone Creek's history. Unit descriptions vary slightly between sections. Also presented here are certain key sections vital for geochronology and geologic history. All sections and detailed descriptions are listed in Appendix B. The correlation of lithostratigraphic units between section on Gladstone Creek is also shown in Appendix B.

Unit 1 – Bedrock

Unit 1 is Kluane schist composed of dark grey to black, fine-grained biotite schist, and light to dark gray, fine-grained quartz-muscovite schist. This Late Cretaceous bedrock unit floors lower Gladstone Creek, although it was only exposed at the base of mine cuts near the outlet of Cyr Creek, and in a river-cut canyon upstream of GLD-02. Where exposed, the bedrock surface is typically undulating. This unit is only shown in the composite stratigraphic section (Figure 3.3) as it did not appear in any logged sections. This bedrock is suspected as the primary source of placer gold in Gladstone Creek.

Unit 2 – Gravel

Unit 2 is gravel of unknown age and genesis. This unit was not observed during field visits for this thesis, but was it observed by Gladstone placer mine operator Alan Dendys as well as Jeff Bond of the Yukon Geological Survey during previous site visits. This unit likely consists of advance glaciofluvial gravels associated with Unit 3. It is possible that pre-glacial fluvial gravel is preserved on top of the Kluane schist wherever glacial erosion was limited (e.g. in the lee of bedrock features). Unit 2 may consist of advance glaciofluvial or glaciolacustrine gravels as well as pre-glacial fluvial gravels.

Unit 3 – Ruby Range till, MIS 6 or older

Unit 3 is dense, compact blue-grey diamict with abundant clasts of Kluane schist. Clast content averages 10%, comprising 90% pebbles and 10% cobbles. Clasts are sub-rounded to sub-angular. The matrix is clayey silt with minor sand. This unit was exposed in the bottom of mining excavations on the right (GLD-01, observed by miners) and left banks (GLD-205, Figure 3.5) of Gladstone Creek and forms a resistant, false bedrock layer for placer gold to accumulate on. The lower contact was not observed. Local placer miners have excavated through this unit and report a typical thickness of 3 to 5 m.

Unit 3 is interpreted to be till from Ruby Range alpine glaciation due to the lack of thick glaciolacustrine sediments bracketing the unit. Gravel was observed below the unit, but it is possible the till could have eroded advance glaciolacustine sediments, giving the unit a higher matrix content than other till units. Bedrock is exposed in nearby mining cuts, suggesting little sediment underlies the till. This unit is not well constrained but was likely deposited during MIS 6 or earlier. The interpretation of deposition by Ruby Range rather than St. Elias ice is due to the high schist content and relatively minor accumulation of

advance-phase sediments below the till compared to the thick accumulations expected from up-valley St. Elias advances (*cf.* Unit 13).

Unit 4 – Subaqueous outwash, MIS 6 or older

Unit 4 comprises a complex of interbedded silt and sand, gravel, and diamictic layers. Unit 4 is 8 to 14 m thick. Unit 4 is exposed at GLD-01 and possibly GLD-16. Silt rip-up clasts are common within gravel beds. Bedding is commonly laterally continuous with many gravel beds having erosive lower contacts, and few if any beds with cross-stratification. Gravel beds are variably sorted with sandy to sandy-silt matrixes. Sand and silt beds are also laterally discontinuous and drape underlying sediments. Silt and sand beds are rhythmic and commonly normally-graded with rare ripple-stratification. Clast content of diamict beds varies from 5-40%. All beds are commonly deformed.

Unit 4 is interpreted as subaqueous outwash associated with either the overlying or underlying Ruby Range tills based on the intebedding of silt, sand, and gravel beds, and common normal grading (*cf.* Rust, *1977)*. The subaqueous setting could be the result of impoundment behind a moraine left by the underlying Ruby Range advance or an elevated base-level from an advanced position of the St. Elias lobe. Alternatively, Unit 4 could be interpreted as a proximal glaciolacustrine deposit from a St. Elias advance, although the lack of finer grained sub-aqueous deposits is problematic.

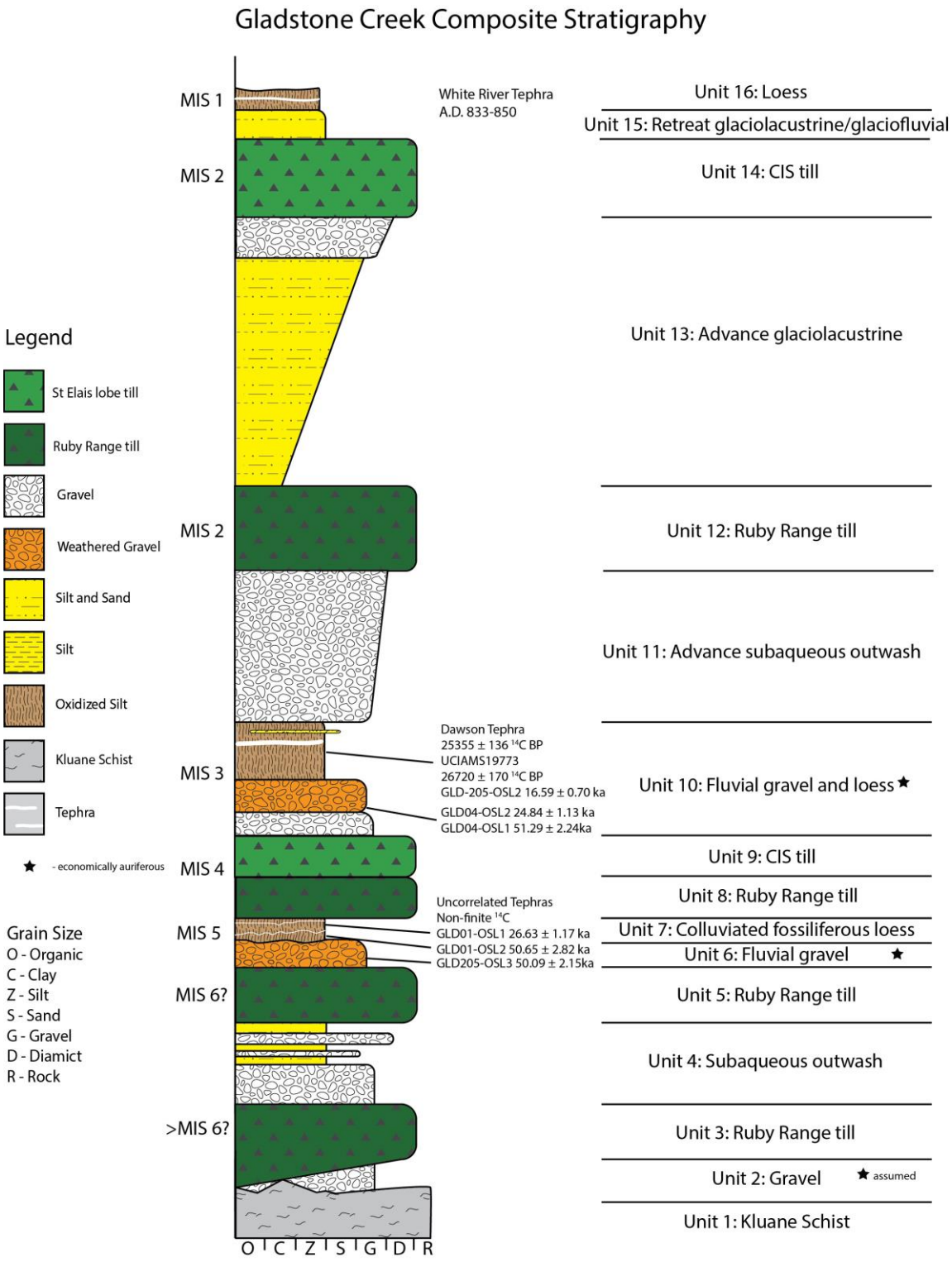

Figure 3.3 Idealized composite section of lithostratigraphic units from exposures on Gladstone Creek. Photos units are shown in Figure 3.4 and Figure 3.14.

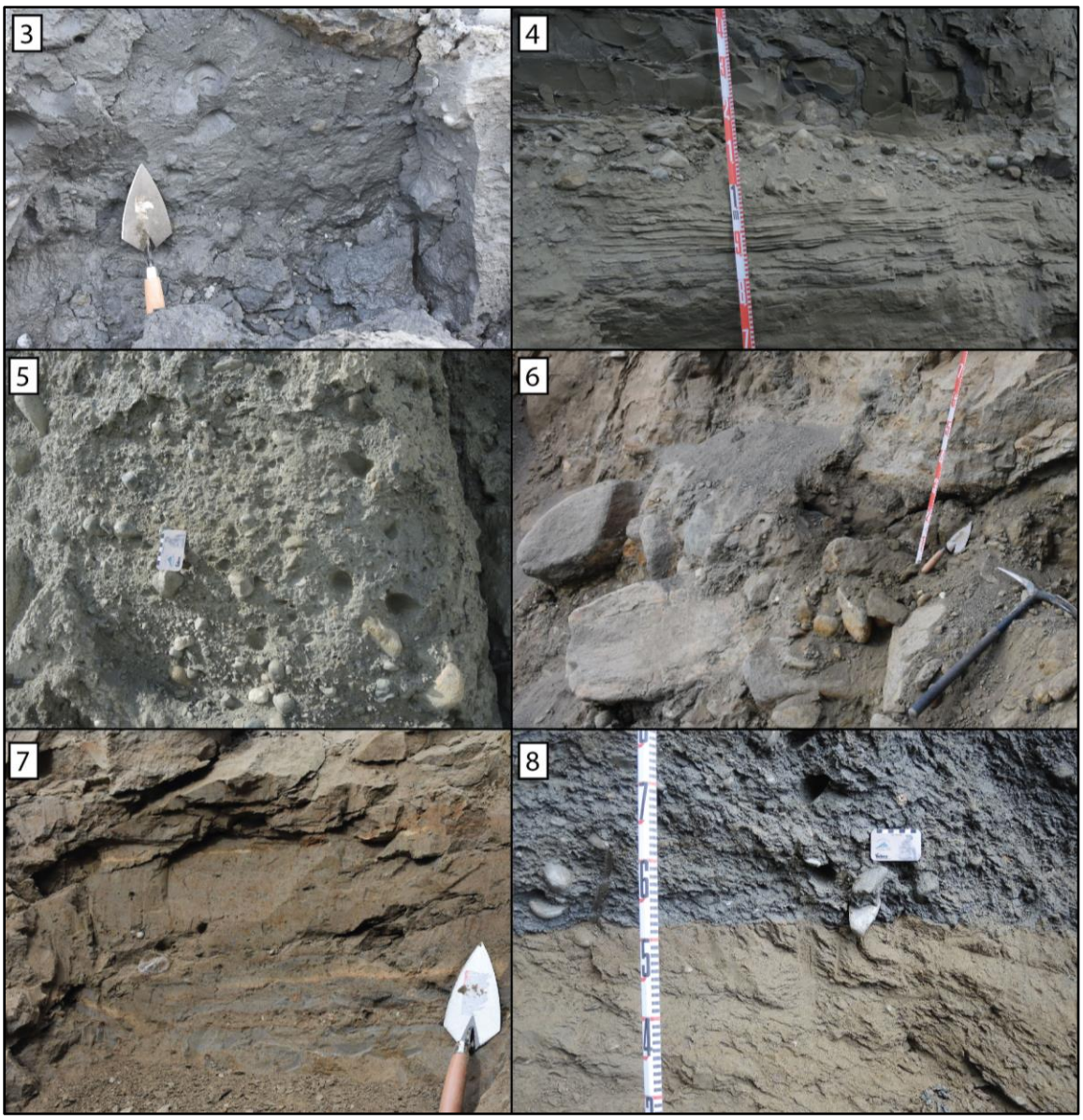

Figure 3.4 Photographs of lithostratigraphic units 3-8 from Gladstone and Raft creeks. Numbers on the photographs correspond to the lithostratigraphic unit number. Units 1 and 2 were not photographed.

Unit 5 – Ruby Range till, MIS 6

Unit 5 is a dense blue-grey diamict. The unit is laterally discontinuous with a thickness of 6-10 m. Clast content averages 15%, comprising 85% pebbles, 15% cobbles. Clasts are angular to rounded. The matrix consists of sandy silt with trace amounts of clay and rarely displays contorted stratification. The lower contact is gradational with the

proximal outwash sediments of Unit 4. Unit 5 was poorly exposed and only described in section GLD-01 (Figure 3.6).

Unit 5 is interpreted to be till deposited by a Ruby Range advance prior to MIS 4. Unit 5 is only separated from Unit 3 by outwash sediments and may represent a re-advance or oscillation of the ice front rather than a separate glacial event given the lack of non-glacial sediments or obvious unconformities.

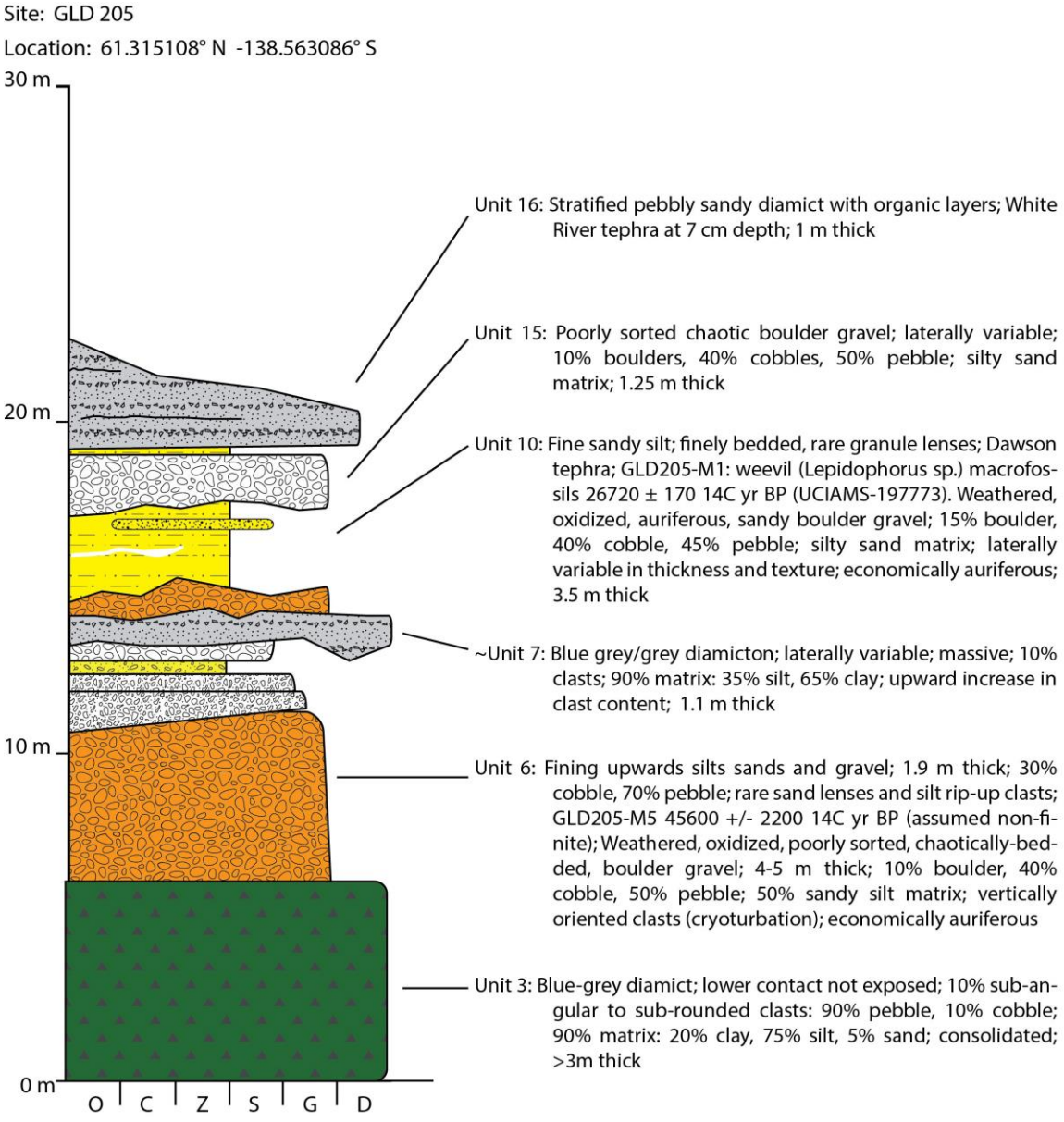

Figure 3.5 Stratigraphy of GLD-205. Legend in Figure 3.3. A gravel unit below Unit 3 was exposed in a mine cut prior to site visits for this study. This section contains two of the three identified economically auriferous units, Units 6 and 10. This section is discussed further in Chapter 4.

Site: GLD-01

Location: 61.316321°N -138.571477°W

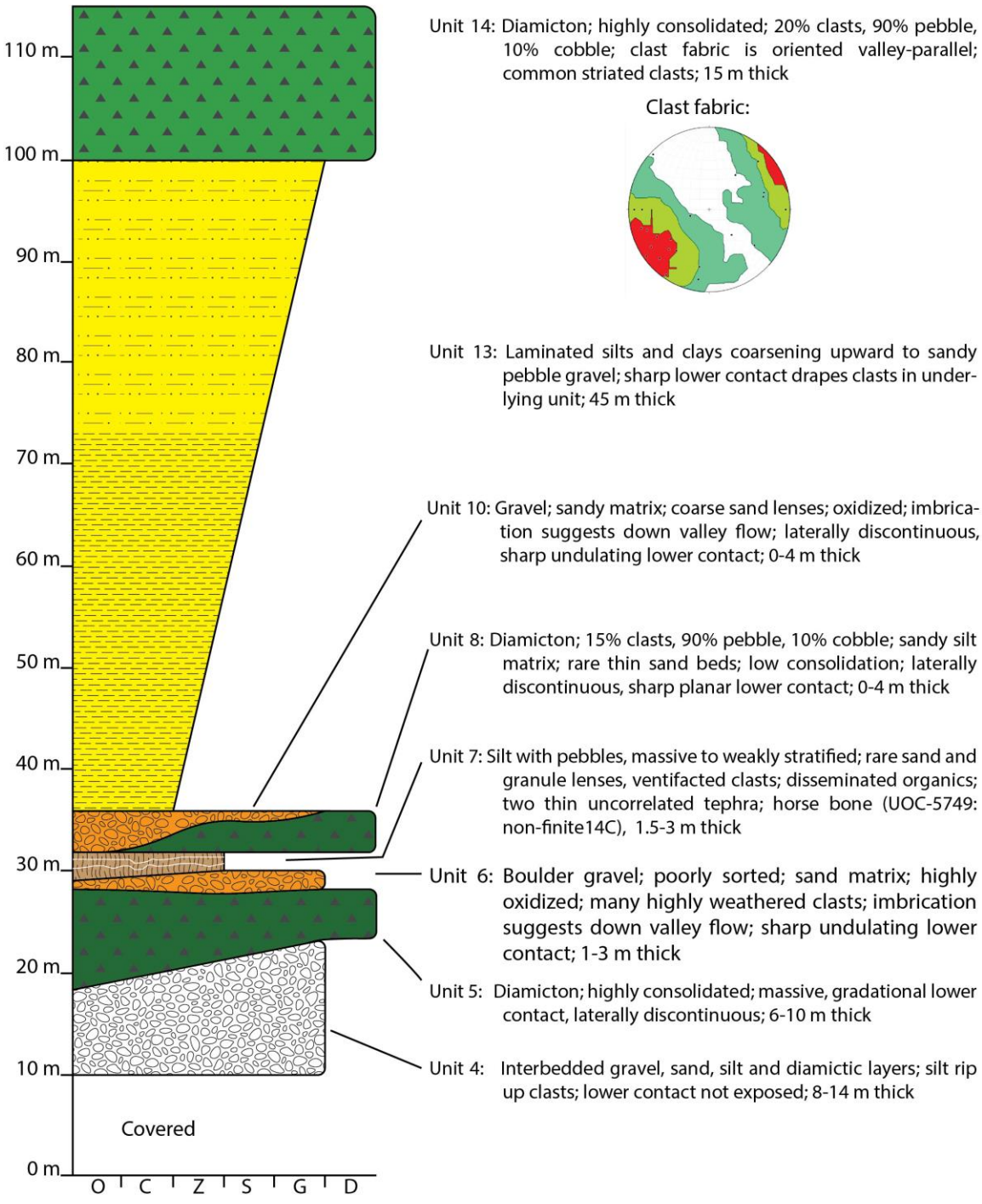

Figure 3.6 Stratigraphy of GLD-01. Legend in Figure 3.3. This section contains the only exposure of Units 7 and 8. Below Unit 4, immediately downstream of this section, another till and gravel layer were observed by TIC Exploration and Jeff Bond of YGS.

Unit 6 – Fluvial Gravel, MIS 5

Unit 6 is a strongly oxidized, poorly- to moderately-sorted boulder to cobble gravel with rare silt and sand interbeds and lenses. Many clasts are weathered and grussified. Matrix content varies from 10-50%. Where matrix content is higher, it consists of sandy silt. Where matrix content is lower, it consists of coarse sand and granules. The gravel varies from crudely- to well-sorted, with an upward increase in sorting rarely observed. Imbricate clasts indicate down-valley flow. Unit 6 ranges from 0.5 - 6 m thick. The lower contact is typically sharp and undulating and likely eroded retreat-phase sediments that would overlie Unit 5 (GLD-01, Figure 3.6). Unit 6 was described in GLD-02, GLD-07, GLD-09, and GLD-205. Beetle (*Pterostichus sp.*) elytra were recovered from silt beds and yielded an age of 45,600 ± 2200 ^{14}C yr. BP (GLD-205-M5, Figure 3.7, Table 3.1). This radiocarbon date may be non-finite as the sample is near the useful limit of the method; however, a complimentary IRSL age (GLD-205-OSL 3) suggests the age may be credible. A non-finite interpretation is favoured based on the stratigraphy and correlation to adjacent sections. When found lower in section (GLD-205), this unit tends to be thicker (*cf*. GLD-01).

This unit is interpreted to be fluvial gravel, likely deposited during MIS 5. This unit occurs at varying elevations due to down-cutting and terrace development during its deposition during a period of adjustment to a lower base level. Where the unit is found lower in section it likely represents the centre of MIS 5 Gladstone Creek; where found higher in section it represents terraces on the margins. In GLD-205 this unit appears to have eroded further down to overlie Unit 3. Two IRSL samples from this unit (Figure 3.8, Table 3.2) give complimentary ages of 50.09 ± 2.15 ka (GLD-205-03) and 51.29 ± 2.24 ka (GLD-04-OSL1). These IRSL samples suggest an alternative interpretation as MIS 3 interstadial gravels. Unit 6 contains economic concentrations of placer gold.

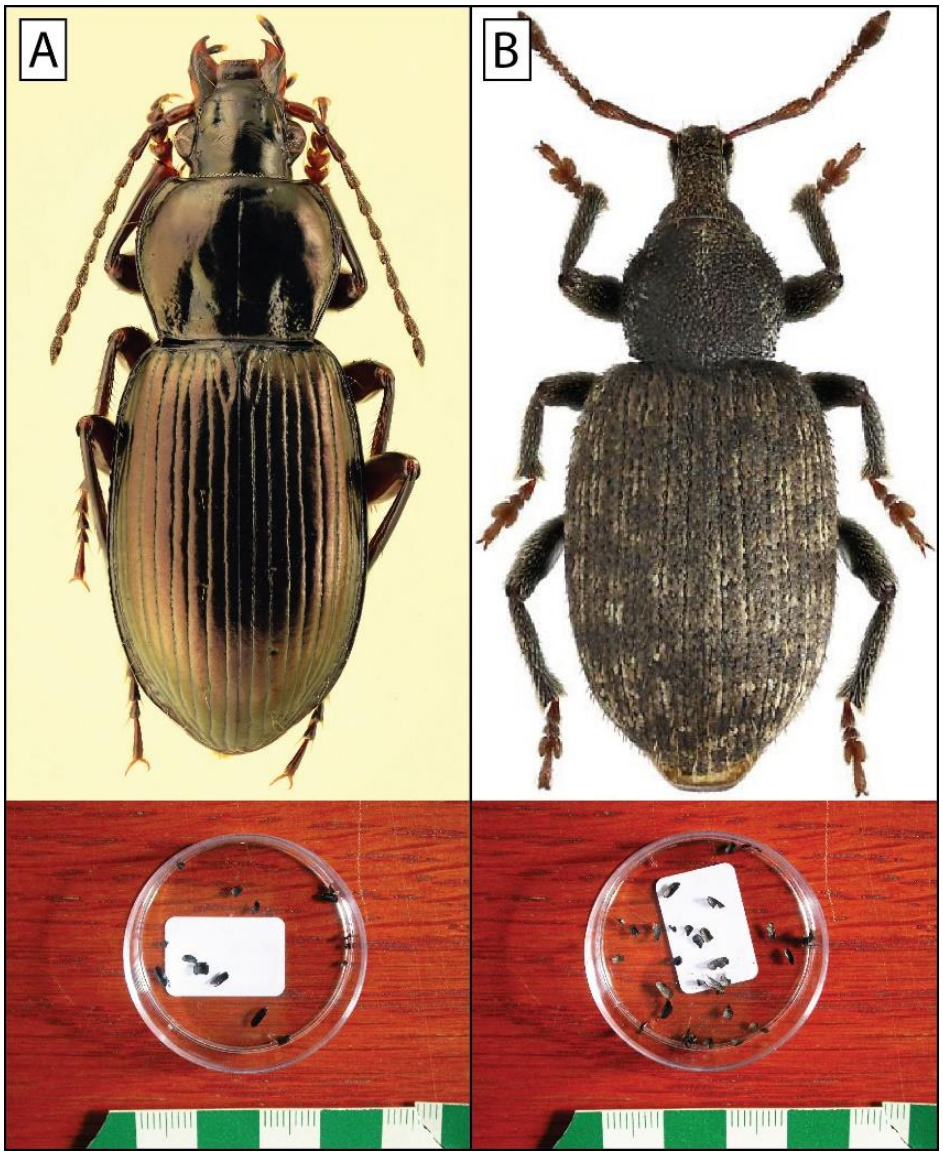

Figure 3.7 Elytra recovered from silts in GLD-205. The radiocarbon ages from these samples are shown in Table 3.1 A) Pterostichus sp. and elytra collected from Unit 6 (GLD-205-M5) B) Lepidophorus sp. and collected elytra from Unit 10 (GLD205-M1).

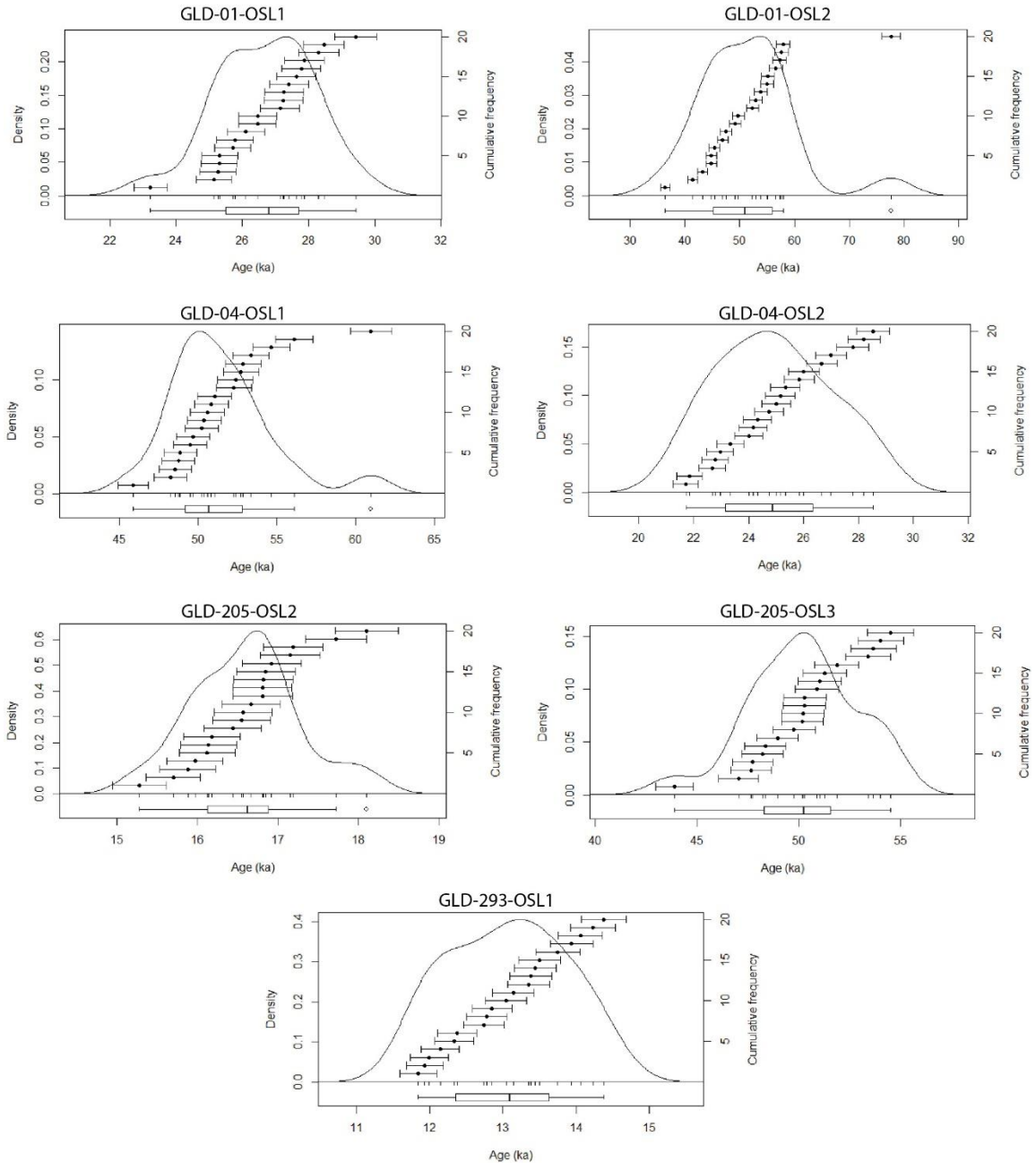

Figure 3.8 IRSL age distribution results for samples from sections on Gladstone and Raft Creek. Sample locations are shown on stratigraphic sections in Appendix B.

Table 3.1 Radiocarbon ages and data from samples collected in Gladstone Creek. Horse bone samples were taken from GLD-01, Unit 7. Repeat sampling showed ages older than the lab's reference blank, confirming an infinite radiocarbon age. The comparable age and fraction of ^{14}C of sample GLD-205-M5 suggest it may also be infinite.

Sample	Lab ID	Material	^{14}C yr BP	$F^{14}C$	Cal BP	Note
YHB-17-03	UOC-5749	Horse bone	46361 ± 1023	0.0031	47800 (95.4%)	Infinite
YG 598.1-BU-1	UOC-5906	Horse bone	>45900	<0.0033	>48340 (95.4%)	Infinite
YG 598.1-BU-2	UOC-5907	Horse bone	>45900	<0.0033	>48340 (95.4%)	Infinite
YG 598.1-BU-1	UOC-5941	Horse bone	>48100	<0.0025	>47510 (95.4%)	Infinite
YG 598.1-BU-2	UOC-5941	Horse bone	>48100	<0.0025	>47510 (95.4%)	Infinite
GLD-205-M1	UCIAMS197773	Weevil (Lepidophorus) elytra	26720 ± 170	0.0359	29200(95.4%)	Finite
GLD-205-M5	UCIAMS197774	Beetle (Pterostichus) elytra	45600 ± 2200	0.0034	45600 (95.4%)	Suspected infinite

Table 3.2 Dose rate calculations, anomalous fading, and corrected age results for IRSL samples.

Sample	Annual Dose Rate (Gy/ka)	Error	*g* -value(%/decade)	Error	CAM Uncorrected De	Error	CAM Corrected De (Gy)	Error	Corrected Age (ka)	Error
GLD-01-OSL1	2.22	0.09	1.60	0.33	50.10	0.97	59.12	0.71	26.63	1.17
GLD-01-OSL2	1.95	0.08	1.45	0.21	85.04	3.29	98.61	3.47	50.65	2.82
GLD-04-OSL1	2.58	0.11	2.89	0.19	94.17	1.86	132.06	1.79	51.29	2.24
GLD-04-OSL2	2.52	0.11	1.26	0.24	54.63	1.28	62.58	1.12	24.82	1.13
GLD-205-OSL2	2.57	0.11	2.76	0.29	32.15	0.57	42.64	0.37	16.59	0.70
GLD-205-OSL3	2.42	0.10	2.24	0.14	93.87	1.76	121.41	1.40	50.09	2.15
GLD-293-OSL1	5.47	0.22	3.75	0.19	45.44	0.90	66.97	0.89	12.25	0.52

Unit 7 – Colluviated Loess, MIS 5

Unit 7 is a fossiliferous, reddish-brown silt. The silt is dense, oxidized, and weakly stratified. Unit 7's lower contact is gradational with Unit 6 and comprises alternating beds of silt and sand transitioning to silt. This unit contains horse bones, ventifacts, and two tephras. Disseminated organics are common throughout the unit. This unit is only exposed in section GLD-01 (Figure 3.6).

A metacarpal bone and two phalanx from a "Klondike horse" *(caballine Equus*) (Figure 3.9) obtained from Unit 7 at GLD-01 yielded a non-finite radiocarbon age, indicating the animal died > ~50,000 ^{14}C yr. BP (Table 3.1). The length and breadth of the bones were plotted against a database of horse bones collected in Yukon to determine the species (Figure 3.10*,* Figure 3.11)*.* Generally, the larger *caballine Equus* are from the last interglacial or earlier as it is thought that horses became smaller towards the late Pleistocene (Dr Grant Zazula, pers. comm. March 2019).

Figure 3.9 Metacarpal and phalanx bones of a caballine Equus "Klondike horse" recovered from GLD-01. Photo courtesy of Dr Grant Zazula, Yukon Government Heritage Resources. Bone lengths are plotted in Figure 3.10 and Figure 3.11.

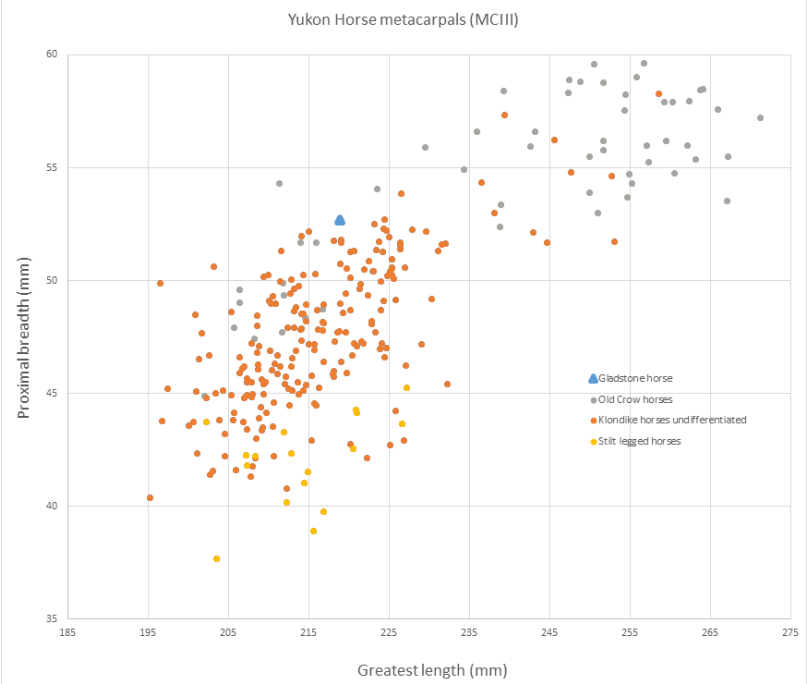

Figure 3.10 Comparison of length and breadth of metacarpal bone recovered from GLD-01 to a database of horse bones recovered in Yukon. Unpublished morphometric data courtesy of Dr Grant Zazula.

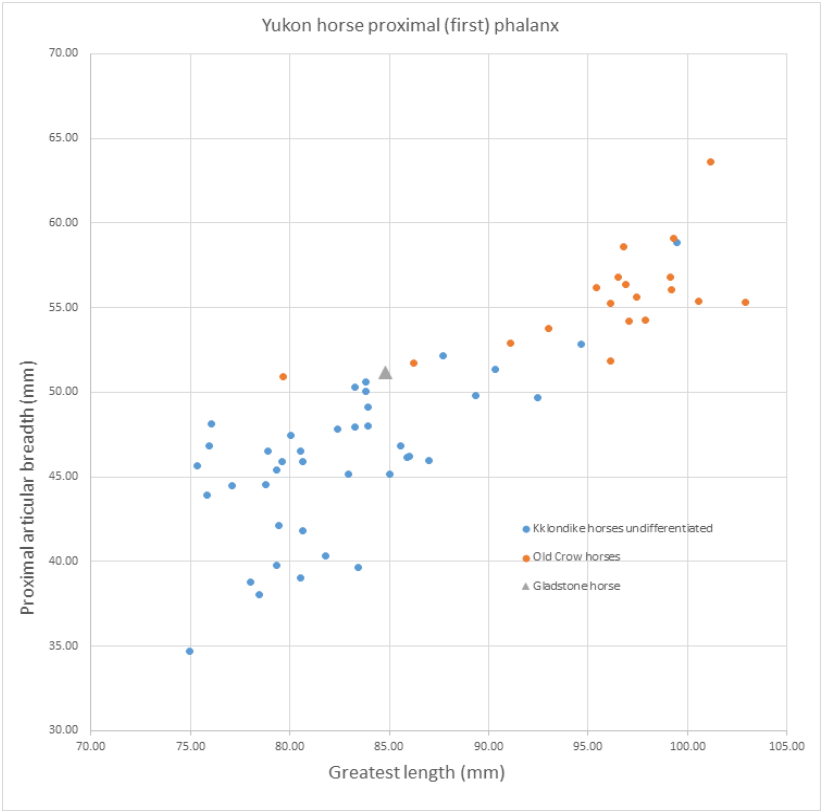

Figure 3.11 Comparison of length and breadth of proximal phalanx bone recovered from GLD-01 to a database of horse bones collected in Yukon. Unpublished morphometric data courtesy of Dr Grant Zazula.

The tephras in Unit 7 (Figure 3.12) do not correlate with reference tephra in the University of Alberta's database. The horse bones give a non-finite radiocarbon age (>48340, UOC-5907). Two IRSL samples from this unit give ages of 26.63 ± 1.17 ka (GLD01-OSL1) and 50.65 ± 2.82 ka (GLD-01-OSL2). These IRSL ages suggest continuous loess deposition throughout MIS 3, however stratigraphically this interpretation is suspect. This unit is preferably interpreted as colluviated loess deposited during the later stages of the last interglacial (MIS 5).

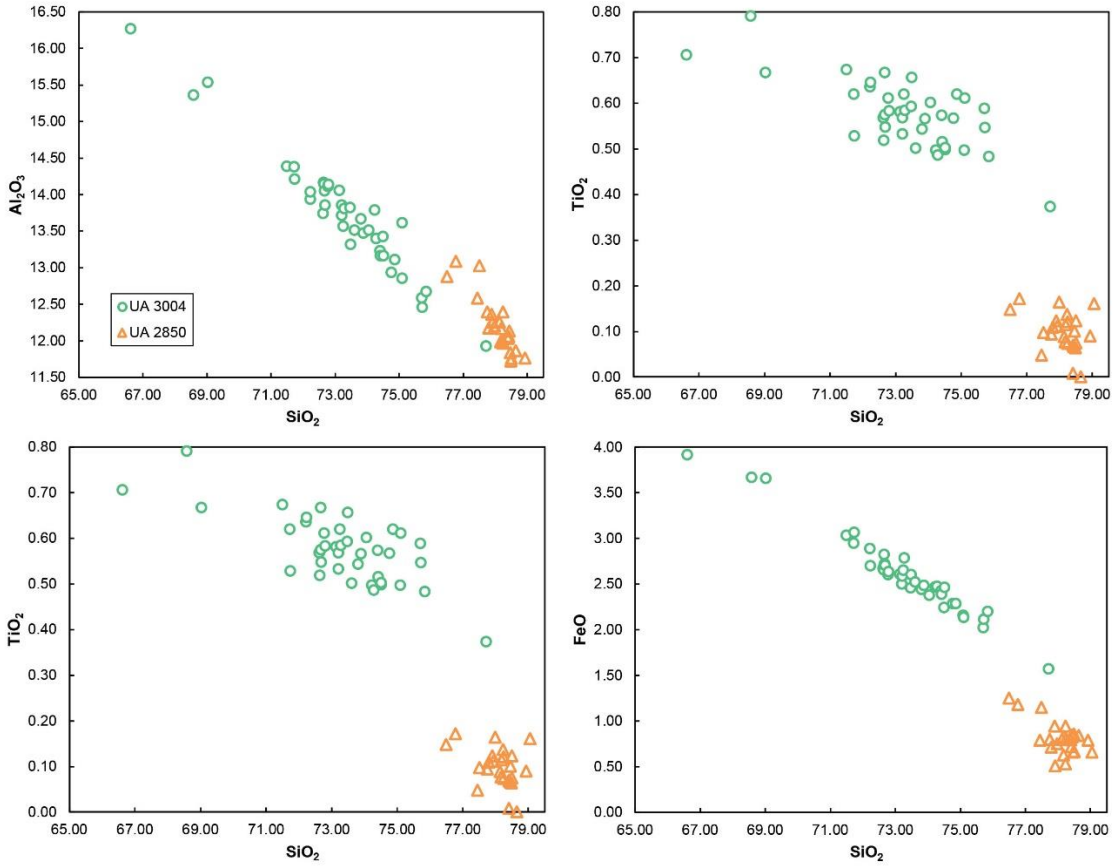

Figure 3.12. Oxide variation diagrams of unknown tephra samples GLD-01-T1 (UA3004) and 15JB87-T1 (UA 2850). These tephras do not match reference tephra in the University of Alberta's database.

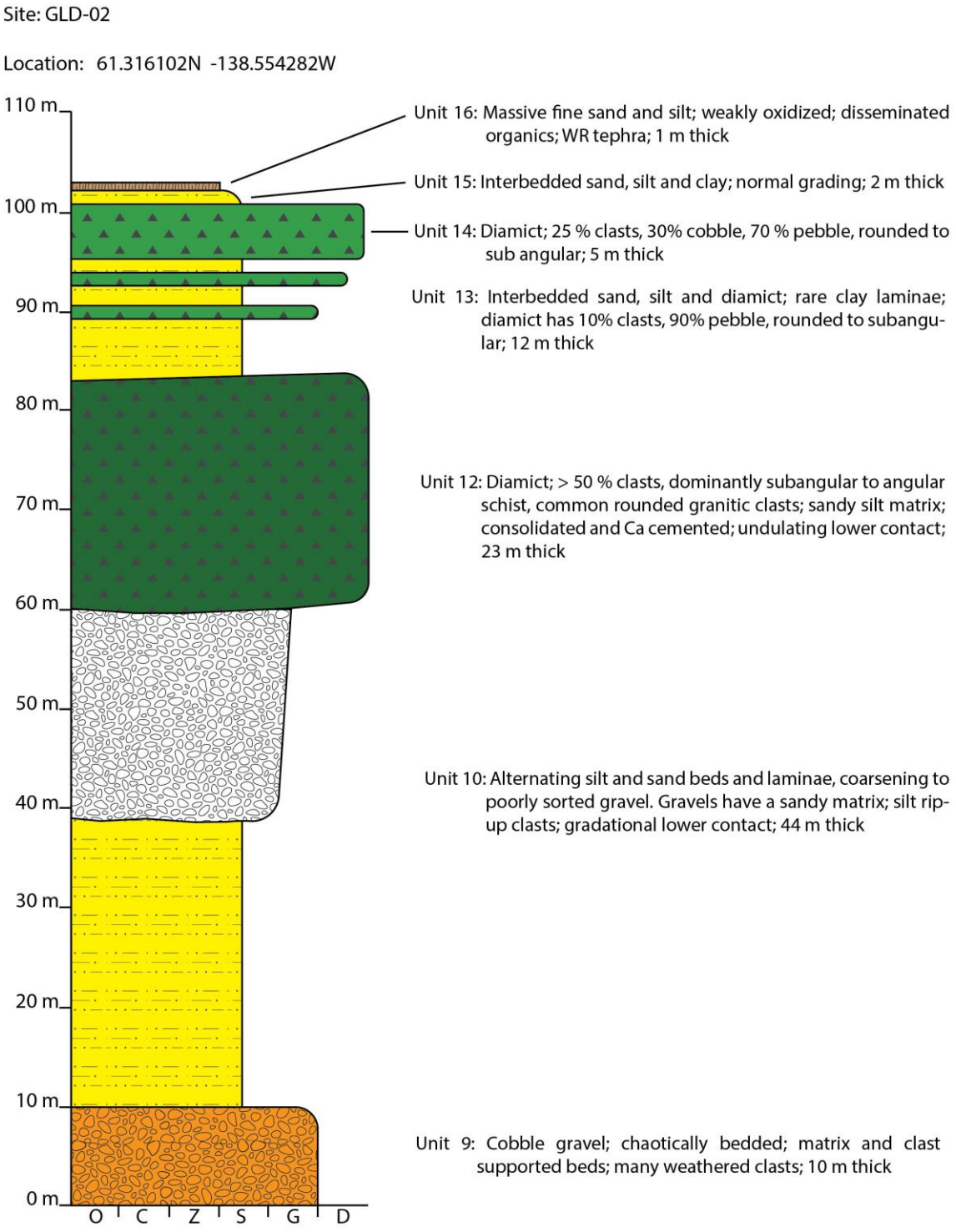

Figure 3.13 Stratigraphy at GLD-02. Legend in Figure 3.3. Unit 12 is schist-rich diamict distinctly different from the diamict in units 12 and 13. Unit 12 is interpreted to be a local till from Ruby Range cirques. The relative absence of foreign clasts, the clast abundance, and coarse grain size support a short transport distance. The stratigraphic relationship suggests advances from local cirques preceded the arrival of the St. Elias lobe.

Unit 8 – Ruby Range till, MIS 4

Unit 8 is a grey-brown diamicton. Clast content averages 15%, with 90% pebbles and 10% cobbles. The matrix is sandy silt. Rare thin sand beds and lenses are present. This unit is less consolidated than other diamictons described, likely due to moisture content where the unit is exposed. This unit is only described at GLD-01. The unit has a sharp planar lower contact. Unit 8 is laterally discontinuous due to erosion by Unit 10, and up to 4 m thick. Unit 8 is interpreted as Ruby Range till from an MIS 4 advance.

Unit 9 – St. Elias till, MIS 4

Unit 9 is a compact grey diamict containing 25-60% casts. The matrix is composed of sandy silt. A clast fabric was completed in this unit showing ice flow direction parallel with the Talbot Arm of Kluane Lake. The lower contact of the unit was not exposed. Unit 9 was described at GLD-06. This unit is approximately 5 m thick on average.

Unit 9 is interpreted to be a St. Elias-sourced till deposited during the MIS 4 Gladstone Glaciation based on its stratigraphic position and the orientation of the clast fabric aligned with the Talbot Arm of Kluane Lake Figure 3.17. This unit is difficult to correlate across sections and could alternatively be interpreted as an initial MIS 2 advance rather than a separate glaciation, as suggested by Madsen (2001).

Unit 10 – Boutellier fluvial gravels, loess, and colluvium, MIS 3

Unit 10 comprises weathered sandy boulder and cobble gravels overlain weakly stratified silt and rare diamict beds. Gravel beds are 1- 4 m thick with sharp lower contacts. This unit was described at sections GLD-01, GLD-02, GLD-04, GLD-10, GLD-11, and GLD-16. At GLD-01 this unit appears to have eroded units 8 and 9. Insect macrofossils and disseminated organics in the silts suggests these are interstadial. Radiocarbon dating of weevil (*Lepidophorus sp.*) (GLD-205-M1) elytra recovered from the unit at section GLD-205 gives an age of 26,720 ± 170 ^{14}C BP. Previous work by Madsen obtained radiocarbon ages of 40,510 ± 680 and 34,960 ± 390 ^{14}C yr BP from bones in this unit. Tephra was found in Unit 10 at GLD-205 and positively correlated to a reference sample of Dawson tephra (Figure 3.15). The Dawson tephra was deposited approximately 25,355 ± 136 ^{14}C yr. BP from an Aleutian arc-Alaska Peninsula eruption (Westgate, 2000; Froese et al., 2002; Preece et al., 2011). Dawson tephra is an important stratigraphic marker, present throughout much of southern Alaska, and central and southern Yukon (Westgate, 2000;

Froese et al., 2002), marking the transition from non-glacial to glacial conditions at the end of MIS 3. It has been suggested that deposition occurred during the winter and its thickness is a result of re-sedimentation during snowmelt (Froese et al., 2006). Dawson tephra in stratified silts at the top of this unit confirms a late MIS 3 age. An IRSL age (GLD-205-OSL2) for this unit gives a much younger age of 16.6 ± 0.7 ka and is considered erroneous. Unit 10 is interpreted as fluvial gravels with rare loess deposited during the MIS 3 Boutellier interstadial. This unit contains economic concentrations of placer gold at GLD-205 and GLD-09.

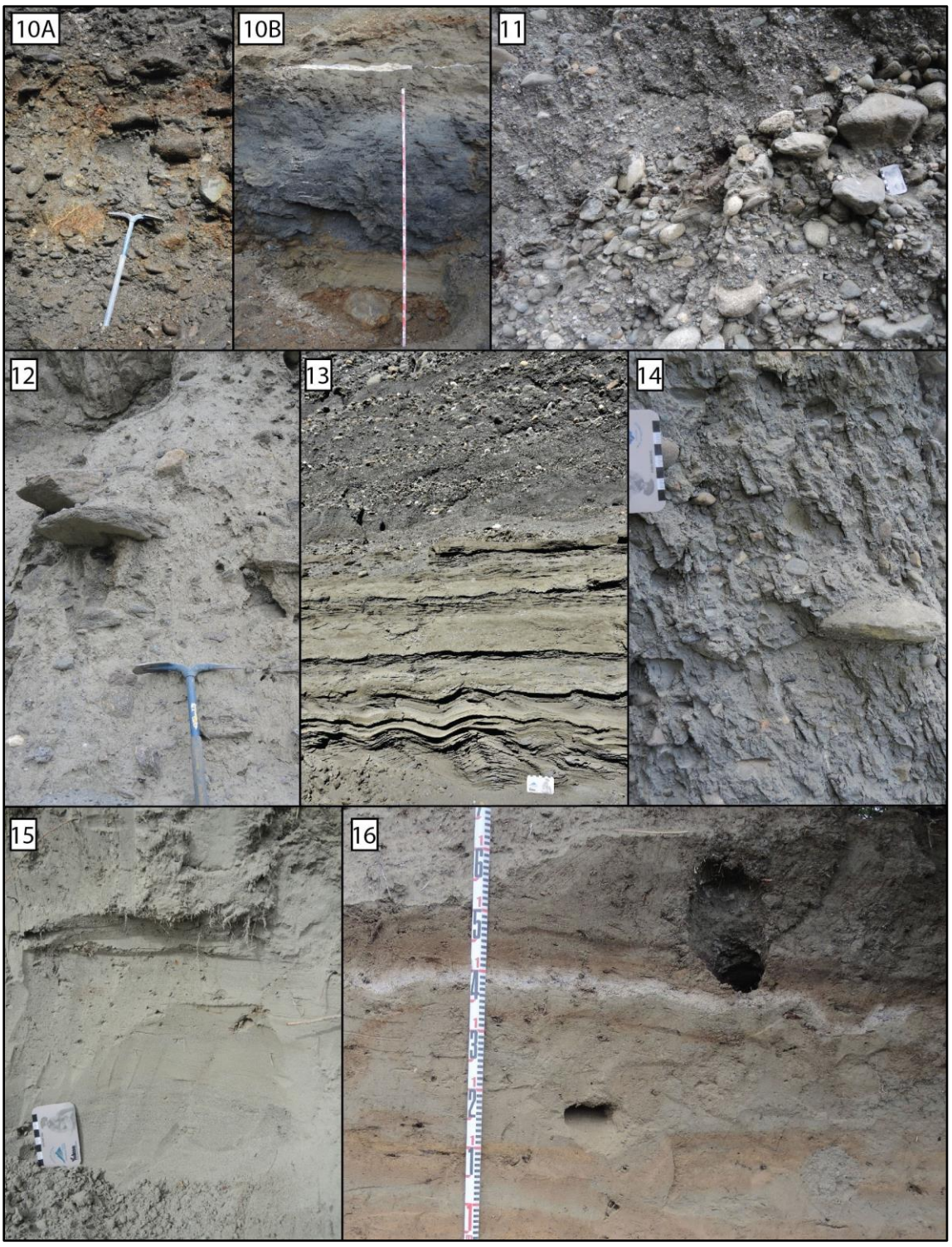

Figure 3.14 Photographs of lithostratigraphic units 9-15.

Unit 11 – Ruby Range advance subaqueous outwash, MIS 2

Unit 11 is a coarsening-upward sequence of silt, sand, and gravel. The thickness of the unit is up to 54 m, though highly variable between sections. Sorting decreases upwards in the unit. Lower contacts of coarse beds commonly erode underlying rhythmically bedded fines. Coarse beds are commonly matrix-supported. Rare clastic dykes and faulting are present throughout the unit. Rip up-clasts and diamicton lenses are common in the top half of this unit. The top of this unit is a poorly-sorted schist-rich boulder gravel similar in character to Unit 12. This unit was described at GLD-02, GLD-07, GLD-11, GLD-12, and GLD-17. Unit 11 is interpreted as subaqueous outwash deposited during a Ruby Range advance at the beginning of MIS 2. This interpretation is supported by the intebedding of silt, sand, and gravel beds, common normal grading and laterally continuous bedding, rarely eroded by coarse beds. (*cf.* Rust, *1977)*. Clastic dykes and extensive faulting within the unit support the interpretation that the unit was overridden by ice post-deposition. The presence of thick sub-aqueous outwash sediments underlying a Ruby Range advance suggests base level must have been higher than present during the advance.

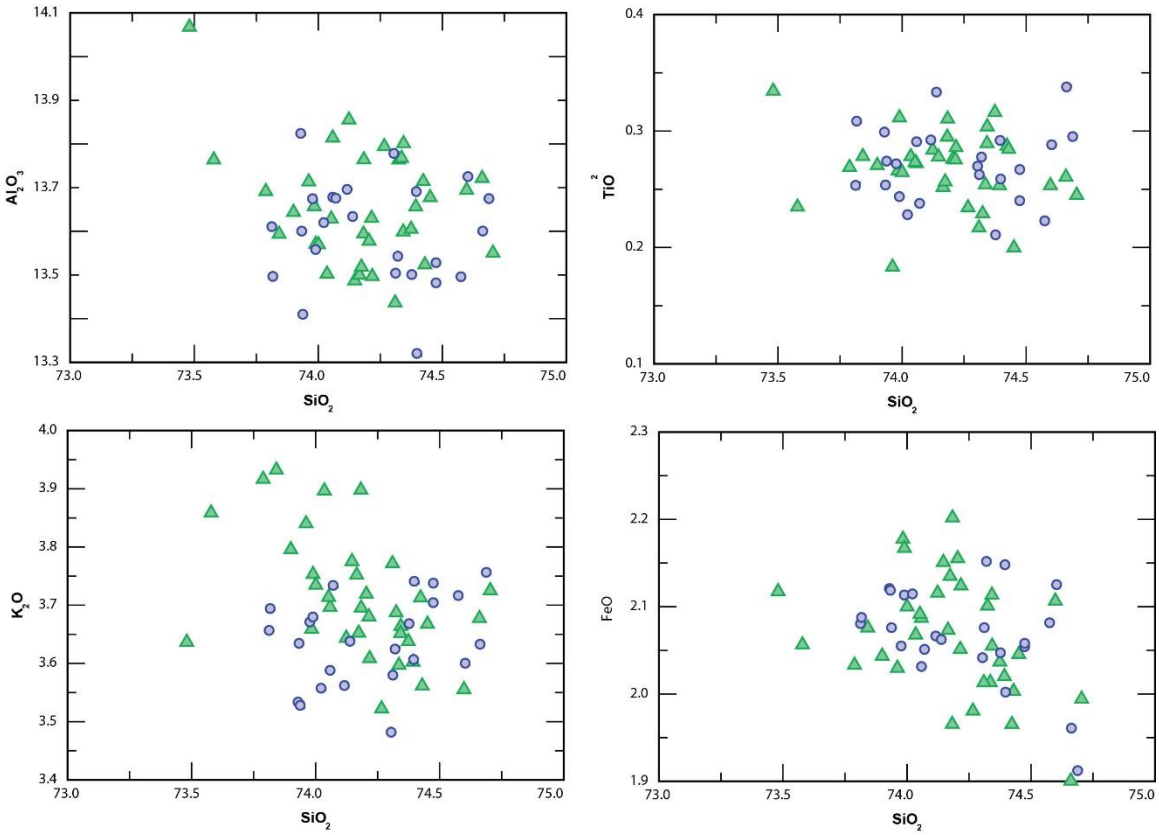

Figure 3.15 Oxide variation diagrams comparing sample GLD-205-T1 (UA3046, blue dots) to a Dawson reference sample from Sulphur Creek, Yukon. These results confirm the correlation between the tephra at GLD-205 and Dawson tephra.

Unit 12 – Ruby Range till, MIS 2

Unit 12 is a dense grey diamicton capping the coarsening-upward sequence of Unit 11. Clast content varies from 35% to >50%, with schist comprising more than 90% of clasts. The matrix is sandy silt with rare clay. Unit 12 is distinctive from other diamicton units due to the high concentration of angular schist. Platy schist clasts commonly lie flat, in crude stratification. Rare clast supported lenses are crudely sorted. The unit is typically 10-15 m thick. Unit 12 is similar in character to the very poorly sorted boulder gravel capping Unit 11 in GLD-07. A scarcity of elongate clasts and pervasive Ca cementation prohibited a clast fabric analysis. The correlation of this unit downstream of GLD-17 is challenging as the distinctive clasts were not observed. Unit 12 was described at GLD-02, GLD-17, GLD-18, and possibly at GLD-01, GLD-04, GLD-11, and GLD-12. This unit is interpreted as till deposited by a Ruby Range valley glacier preceding the advance of the St. Elias lobe during MIS 2. At sections GLD-02, GLD-17, and GLD-19 this till may

represent an end moraine from the cirques above and adjacent to Cyr Creek. Alternatively, the blocky clasts in the till could be the result of a rockslide deposit incorporated into the till though the stratification is harder to explain with this interpretation. Unit 12 is best exposed in section GLD-02 which also contains thick advance glaciolacustrine and subaqueous outwash deposits underlying Unit 11 (Figure 3.13). At sections GLD-01, GLD-04, GLD-11, and GLD-12, Unit 12 more closely resembles a typical lodgement till.

Unit 13 – St. Elias advance glaciolacustrine and glaciofluvial, MIS 2

Unit 13 is a coarsening-upward sequence of laminated and interbedded clay, silt, sand, and gravel. Normal grading is present within beds and laminae as well as at the scale of the entire unit. Rare pebbles and cobbles in silt depress the underlying beds. Soft sediment deformation is common. Beds become poorly-sorted near the top of the unit. Unit 13 varies greatly in thickness from 2 m to 45 m. This variable thickness likely has to do with where Gladstone Creek eroded sediments in MIS 3, creating accommodation space in the valley bottom. An IRSL age from the top of this unit gives an age of 24.84 ± 1.13 ka (GLD-04-OSL2; Table 3.2, Figure 3.8). This unit is rarely interbedded with Unit 14. Unit 13 was described at: GLD-01, GLD-02, GLD-04, GLD-05, GLD-06, GLD-07, GLD-11, GLD-12, GLD-17, and GLD-18.

Unit 13 is interpreted as an advance glaciolacustrine sequence deposited during an MIS 2 advance of the St. Elias lobe. At the mouth of Gladstone Creek (GLD-04 and GLD-05) deposition occurred before impoundment of the creek, producing advance glaciofluvial sediments rather than glaciolacustrine (Figure 3.17 and Figure 3.18). Here, this unit comprises moderately-sorted pebbly cobble gravels with poorly sorted lenses. Weak bedding dips shallowly up Gladstone Creek at GLD-05. The glaciolacustrine sediments indicate that Ruby Range glaciers did not occupy lower Gladstone Creek valley when the St. Elias lobe advanced to the mouth of the Creek.

Unit 14 – Polygenetic (Ruby Range and St. Elias) till, MIS 2

Unit 14 is a dense grey diamict ranging from 5-15 m thick. Clast content averages 30%. Striated clasts are common. The matrix consists of sandy silt. Sorted lenses are rare. A strong clast fabric was found in this unit at multiple locations (Figure 3.28). Beyond the mouth of Gladstone Creek clast fabric indicates northward flow roughly parallel with Talbot arm of Kluane Lake. Within Gladstone Creek, clast fabrics indicate valley-parallel

flow. The lower contact varies from sharp to gradational. This unit commonly forms a complex of interbedded diamicton and subaqueous outwash sediments (Figure 3.16). Unit 13 was described at: GLD-01, GLD-02, GLD-04, GLD-05, GLD-06, GLD-07, GLD-11, GLD-12, GLD-14, GLD-17, and GLD-18. Unit 14 is interpreted as till from the MIS 2 McConnell advance of the St. Elias lobe, that coalesced with ice from Ruby Range source areas.

Unit 15 – St. Elias retreat glaciolacustrine and glaciofluvial

Unit 15 consists of two facies. At the mouth of Gladstone Creek, it consists of moderately-sorted cobble gravels with rare diamicton lenses. These gravels range from 5 to 8 m thick and express a hummocky kettled topography along the edge of Kluane Lake. Farther up Gladstone Creek it consists of laminated and finely bedded silt and sands with normal grading and common soft-sediment deformation structures. This facies ranges from <1 to 6 m thick. Unit 15 was described at: GLD-02, GLD-04, GLD-05, GLD-06 GLD-11, GLD-12, GLD-14, GLD-17, and GLD-205. This unit is interpreted as retreat glaciofluvial and glaciolacustrine sediments. Glaciolacustrine sediments occur up-valley of GLD-05 where ice impounded Gladstone Creek and are typically less than 2 m thick. It is possible these thin glaciolacustrine sediments represent localized ponding within an outwash plain. At GLD-05 and down-valley, Unit 15 comprises glaciofluvial outwash gravels.

Figure 3.16 Photo (courtesy of Jeff Bond) of section GLD-05. Person circled for scale. This section represents the advance and retreat of the St. Elias lobe in Gladstone Valley during the McConnell Glaciation. This section is located where the St. Elias lobe began to impound drainage in Gladstone Creek as the St. Elias lobe advances indicated by the bracketing of till units with glaciolacustrine rather than glaciofluvial sediments. Here, Unit 14 comprises interbedded diamicton and subaqueous outwash gravels. Sub-units of lithostratigraphic Unit 14 refer to amalgamated units from field notes.

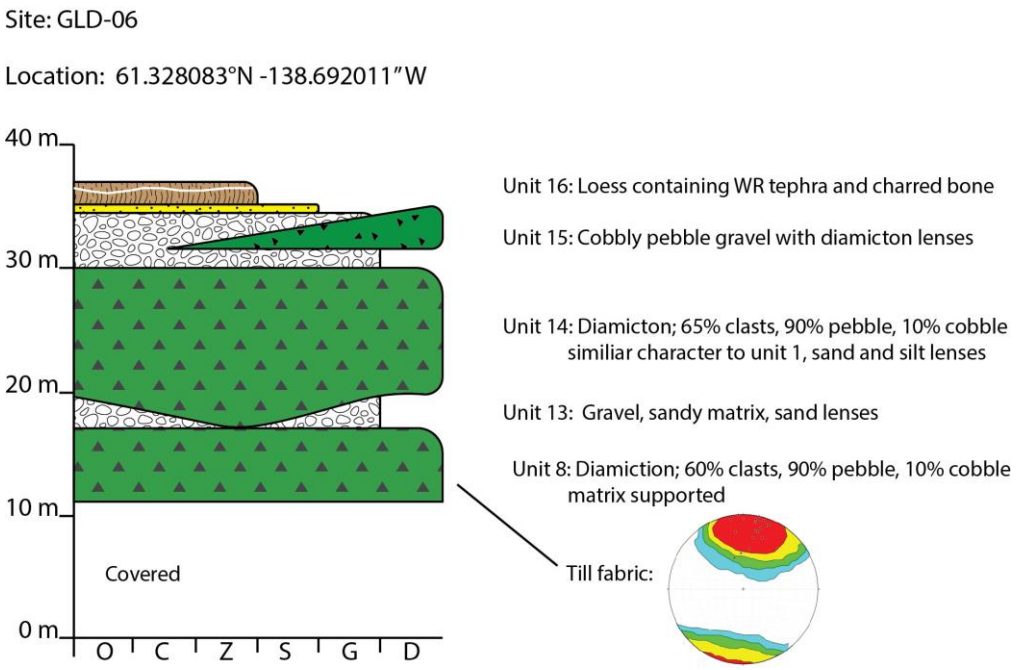

Figure 3.17 Stratigraphy from GLD-06 (Figure 3.18). Legend in Figure 3.3. This section occurs where Gladstone valley opens into the Shakwak Trench. Here the St. Elias lobe is unlikely to impound water and create advance and retreat glaciolacustrine sequences. Units consist of tills and glaciofluvial sediments. The upper till is likely McConnell. The underlying lower till maybe McConnell or Gladstone but lacks geochronology for differentiation. The till fabric from Unit 9 indicates ice flow direction is parallel with the Talbot Arm of Kluane Lake.

Figure 3.18 Structure from motion (SfM) model of GLD-06 with lithostratigraphic units delineated. The SfM model was created from UAV photos (Jeff Bond) using Agisoft Photoscan photogrammetry software. Person for scale (circled).

Unit 16 – Loess, MIS 1

Unit 16 is massive to weakly laminated and bedded silt and fine sand. This unit is commonly oxidized and contains disseminated organics, paleosols, bone fragments, and White River tephra. White River tephra was found capping many sections in Gladstone Creek and forming discontinuous thin veneers at or near the surface of much of the Gladstone map area. The tephra was produced by two separate eruptions of the stratovolcano, Mt Churchill, located in the St. Elias Mountains in eastern Alaska (Clague et al., 1995). The younger of these tephras, dispersed to the east of the eruption site, is present in the study area and was deposited sometime between A.D. 850-833 (Jensen et al., 2014). White River tephra was identified based on visual inspection of its physical characteristics and stratigraphically, as it is typically located at or near the modern surface. Bioturbation from ground squirrels is common in this unit. A paleosol is commonly found underlying the White River tephra. The silt below this tephra is more oxidized than in the top of the unit and is capped by organics. This unit was described at: GLD-02, GLD-05, GLD-06, GLD-14, GLD15, GLD-17 and GLD-18. Unit 16 is interpreted as Holocene loess. The oxidization of the paleosol probably occurred primarily during the Holocene Climatic Optimum, when warmer temperatures would have allowed for greater soil development. The less oxidized loess on top of the paleosol and White River tephra may be from the LIA advance or fluctuations in Kluane Lake level supplying more fine sediment for eolian transport. Abundant charcoal and rare charred bone fragments were found in this unit at GLD-06, suggesting the presence of humans, indicating an age of MIS 1. Several archeological excavation sites located nearby in the unit suggest this interpretation is correct.

Unit 17 – Fluvial Gravels, MIS 1

This unit consists of gravel, sand, and silt of variable thickness (Figure 3.19). Unit 17 occupies the modern valley bottom and terraces along the margins. In main river channels the unit consists of cobble to pebble gravel with a sand matrix. On the floodplain surface surrounding the channels and in minor side channels, the unit comprises sands and silts. Much of this unit has been reworked by placer mining. Rare woody debris and organics are present in this unit. This unit was described at GLD-08 and GLD-206). This unit is interpreted as early Holocene to modern fluvial sediment. Deposits on higher terraces may be associated with incision during deglaciation and could be considered retreat glaciofluvial (Unit 15). This unit commonly contains economic concentrations of

placer gold. This unit is not shown on the composite lithostratigraphic section in Figure 3.3.

Figure 3.19. Unit 17, Fluvial boulder gravels from the mouth of Cyr Creek (GLD-206), and fluvial sands on the Gladstone Creek delta at Kluane Lake (GLD-08).

3.4.2. **Raft Creek Stratigraphy**

Five sections were logged at cut-bank exposures on Raft Creek (Figure 3.20). Sections GLD-221 (Figure 3.21), GLD-222, and GLD-223 represent a proximal subaqueous outwash environment in front of a St. Elias lobe advance. Complete sedimentological descriptions of these sections are contained in Appendix B. The St. Elias lobe impounded drainage in Raft Creek resulting in glaciolacustrine deposition, followed by a fluvial or glaciofluvial setting after the St. Elias lobe retreated beyond the outlet of Raft Creek. Sections GLD-293 and GLD-321 represent the readvance and retreat of an alpine glacier at 13.7 ± 0.9 ka based on ^{10}Be ages on boulders a moraine. An IRSL sample (GLD-293-OSL1) from glaciolacustrine sands impounded behind this moraine confirms the timing of the readvance with an age of 12.25 ± 0.52 ka.

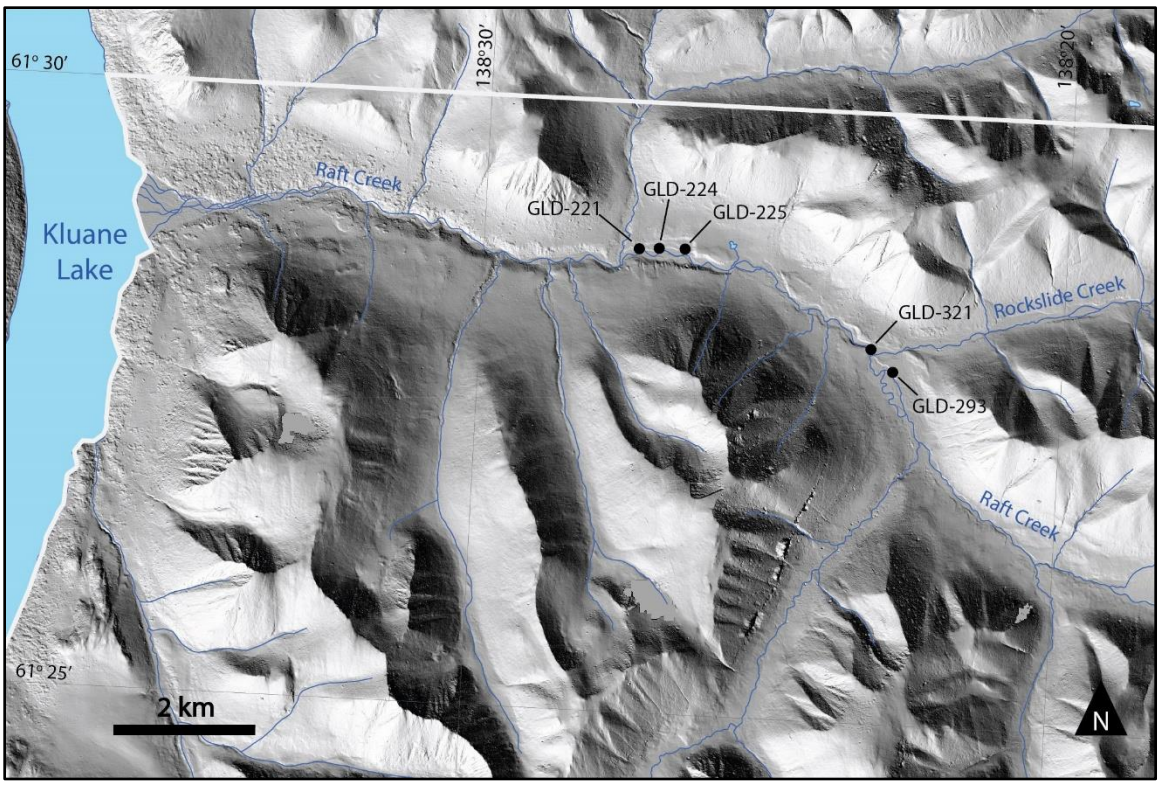

Figure 3.20 Location of stratigraphic sections on Raft Creek. Surficial mapping boundary shown by white line. The hillshade is derived from 2 m Arctic DEM (Porter et al., 2018).

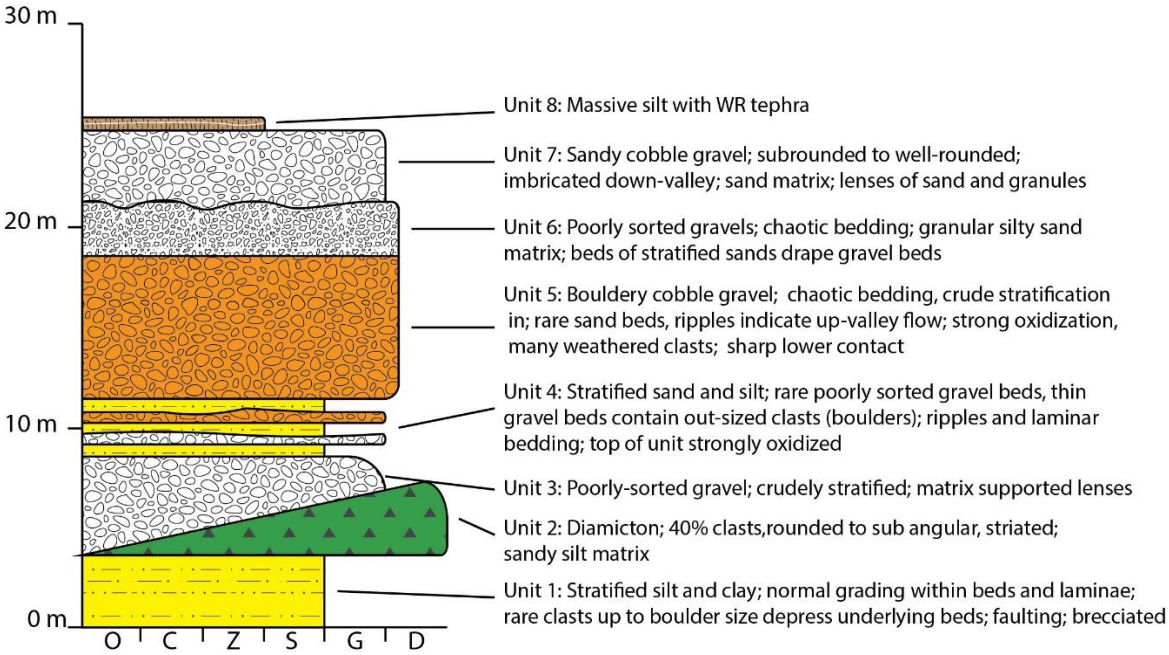

Figure 3.21 Stratigraphy at GLD-221 on Raft Creek. Legend in Figure 3.3. Unit numbers correspond to field notes, not lithostratigraphic units of Gladstone Creek. Units 1-5 represent an ice-proximal glaciolacustrine environment, likely deposited in front of the advancing CIS which impounded Raft Creek. Unit 8 comprises Holocene accumulations of loess and tephra. The location of the section is shown in Figure 3.20

3.4.3. **Other Locations**

During field traverses, small sections were examined in Albert Creek (Figure 3.23C), Camp Creek (Figure 3.20 D), and upper Gladstone Creek typically consisting of few or single units (Figure 3.22). The stratigraphy of these minor sections is

shown in Appendix B. Section GLD-321 in Albert Creek appears to contain two diamict units separated by mottled, sandy silt. This section is located above the MIS 2 limit and is interpreted as MIS 6 and MIS 4 tills separated by interglacial loess. If this interpretation is correct, the mottled loess could be considered a weakly developed Diversion Creek paleosol as it would have formed at the same time. Section GLD-261 consists of a sandy alpine till from cirques in Rockslide Creek. Section GLD-267 comprises a similar till, sourced from cirques in Camp Creek. Section 139 contains glaciolacustrine sand and silt with common deformation structures. This sediment was deposited during

the last glacial maximum when ice in upper Gladstone Creek was sufficiently advanced to impound the drainage of Camp Creek.

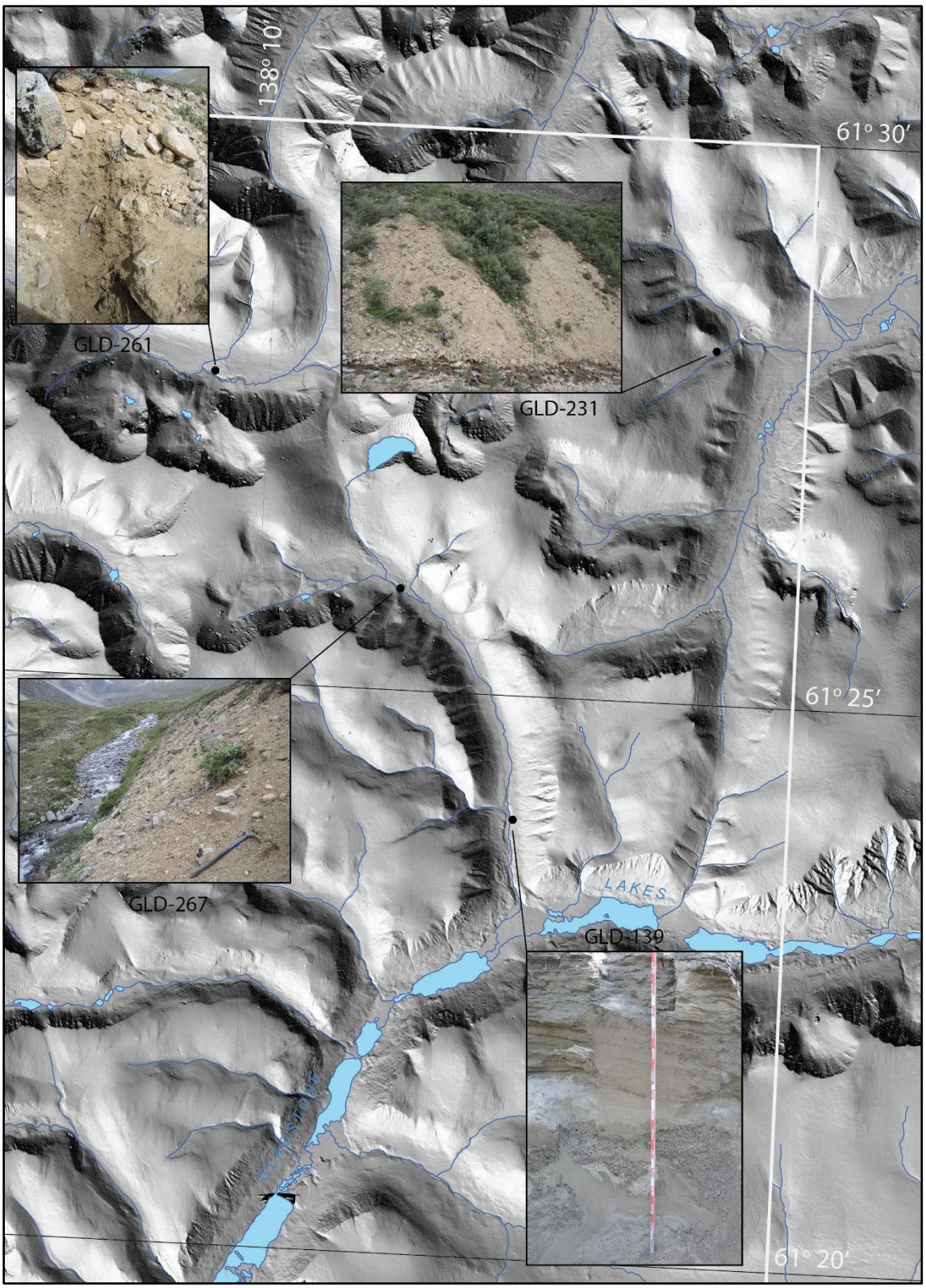

Figure 3.22 Locations and photos of small sections in the northeast portion of the map area. Map boundary shown by white line. Sections GLD-231, GLD-261, and GLD 267 shown in Appendix B.

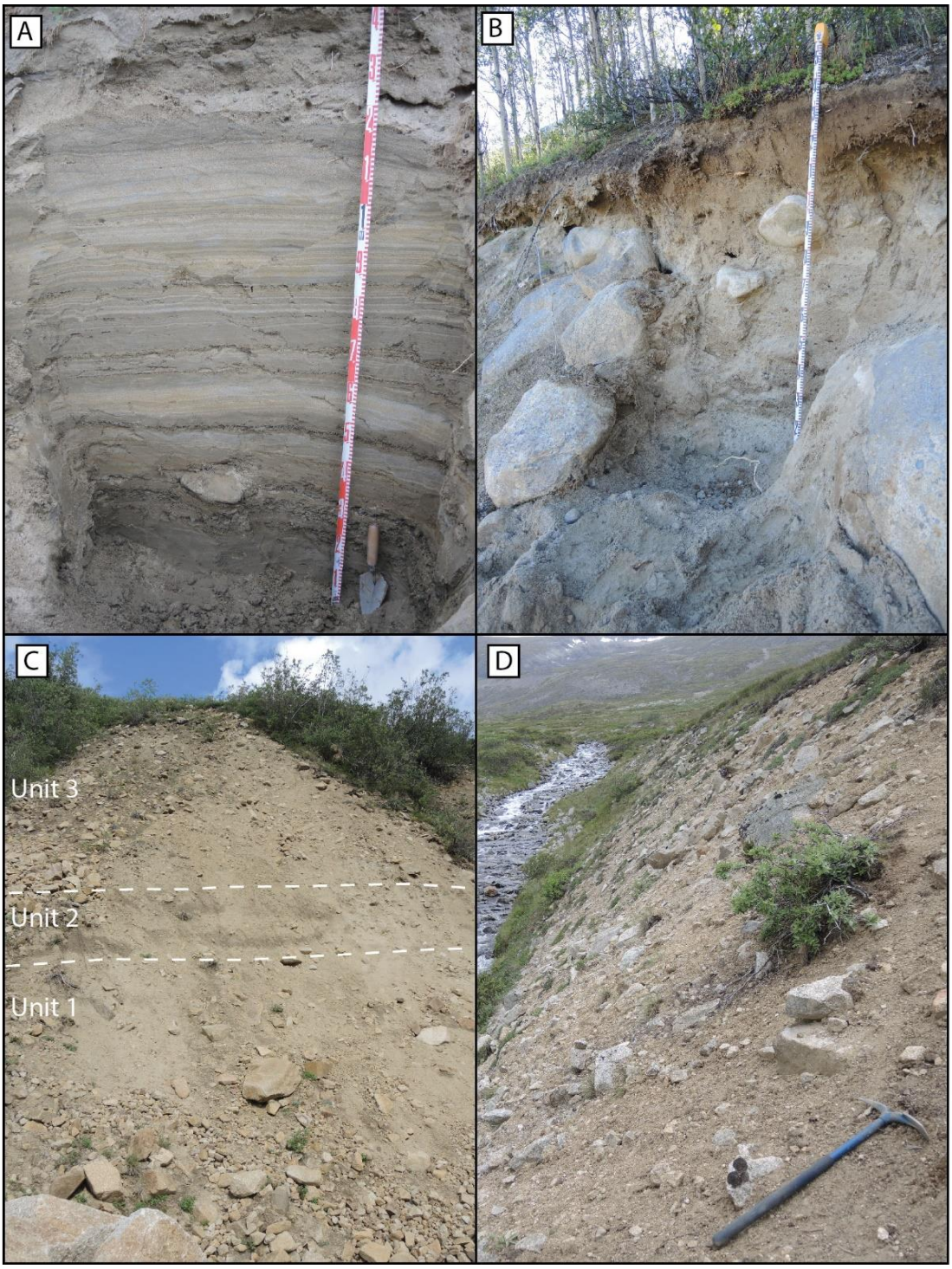

Figure 3.23. Small Sections in Raft (A and B), Albert (C), and Camp (D) creeks. A) Unit 1 of GLD-293 showing rhythmically bedded sands and granules with rare cobbles. This section represents a glacial lake impounded by a moraine (B) that formed as an alpine glacier retreated in Raft Creek. B) A sandy moraine deposited by the advance of an alpine glacier down Raft Creek. This moraine is dated to 13.8 ± 0.9 ka. C) A section exposed in a gulley on Albert Creek. This section contains two similar diamicts separated by an oxidized sandy silt layer (Figure 3.24). These diamicts, interpreted as till, are above the mapped MIS 2 limit and likely correspond to MIS 4 and 6 glaciations. D) Alpine till exposed by fluvial incision below a cirque. This till likely corresponds to an MIS 2 advance from the cirque.

3.5. Discussion

3.5.1. Preferential preservation of Ruby Range-sourced sediments in Gladstone Creek

It is noteworthy that more units from Ruby Range advances are present in section than advances of the St. Elias lobe. Prior to this study it was not expected that extensive ice would have been produced in the Ruby Range given its location in the rain shadow of the St. Elias Range. The preferential preservation of Ruby Range sediments can be explained by the difference in sedimentation and base-level for up-valley and down-valley glacial advances as well as the relative timing of St. Elias lobe and Ruby Range advances. During the McConnell Glaciation, Ruby Range ice appears to have occupied lower Gladstone Creek prior to the St. Elias lobe's arrival but then retreat upstream of Cyr Creek. Alternative to this retreat, it may be that a glacial lake impounded in the Shakwak Trench causing ice from Gladstone Creek to float. Prior to the McConnell Glaciation, Ruby Range glaciers appear to have advanced beyond the mouth of Gladstone Creek, limiting the deposition of St. Elias lobe sediments.

A study of placer sedimentology in the Livingstone Range found that the direction and timing of glacial advances controlled the preservation of placer deposits (Levson, 1992). As glaciers advance up-valley (St. Elias lobe advances) and retreat, they impound the drainage and form proglacial lakes. This impoundment results in rapid deposition of glaciolacustrine sediments due to the rapid drop in energy from transitioning from the glacial to glaciolacustrine environment. This rapid deposition buries previously deposited materials under thick, coarsening-upward packages of sediment. The thick advance deposits result in up-valley till units deposited high above the pre-advance base level. If post-glaciation base levels return to a similar or lower position than pre-advance levels, the up-valley deposits have high erosion potential.

Ice sourced from the Ruby Range does not alter base level conditions independent of the position of the St. Elias lobe; therefore, they may have a net erosional effect rather than the thick net deposition of up-valley advances. The resulting sediments typically lack the low energy deposition of medial and distal glaciolacustrine settings. These packages of down-valley advance and retreat sediments are much thinner than up-valley, leaving them closer to non-glacial base levels which gives them a higher preservation potential.

The lower elevation cirques believed to have been occupied in glaciations prior to MIS 2 suggest that local ice production may have been more extensive during earlier glaciations. Increased local ice production may have caused Ruby Range glaciers to advance into the Shakwak Trench prior to the arrival of the St. Elias lobe, preventing the incursion of the CIS into Gladstone Creek. Ruby Range advances preceding CIS arrival allows Ruby Range glacial deposits to dominate the stratigraphy of lower Gladstone Creek.

3.5.2. **Base level and the character of glacial advance sedimentation**

The relative preservation potential of up-valley and down-valley glaciations may explain the less common presence of MIS 4 St. Elias sediments and the lack of sediments from the MIS 6 advances of the St. Elias lobe. However, alternative interpretations of the stratigraphy are possible which interpret one or both of the lowest two till units as MIS 6 St. Elias lobe sediments given the unknown composition of the gravels underlying the lowest till, and the subaqueous outwash between Unit 3 and 5 tills. However, given the uncertainty of pre-Holocene base-level and drainage patterns in the Shakwak Trench, it is possible that a lake could have been present. If drainage at the time was through the Alsek River, advances of the Kaskawulsh glacier would impound drainage in the Shakwak Trench soon after the onset of glaciation, prior to St. Elias lobe arrival at Gladstone Creek, allowing for subaqueous outwash sediments associated with Ruby Range advances.

3.5.3. **Reliability of IRSL ages**

The IRSL ages presented in this thesis commonly conflict with ages provided by other dating methods. For example, in lithostratigraphic Unit 10, an IRSL sample underlying Dawson tephra, which is well constrained at 25,355 ± 136 ^{14}C yr. BP, gives a much younger age of 16.6 ± 0.7 ka. Conversely, at GLD-293, an IRSL sample with an age of 12.2 ± 0.5 ka was taken from glaciolacustrine sands impounded behind a moraine dated to 13.7 ± 0.9 ka using ^{10}Be. These results generally agree with each other, adding credibility. Because of conflicting ages obtained with ^{14}C and tephrochronology, the IRSL ages are not given precedence over results from other dating methods and stratigraphic correlations. Therefore, some interpretations presented conflict with IRSL ages.

It is possible that some of the difficultly in obtaining consistent IRSL ages is due to the variability in water content of the dated units. A higher ground water content will lower the calculated age of the sample (Duller, 2008). Water content in the units would change over time through climatic changes associated with glaciations, as well as the affect of cut and fill on the groundwater table.

3.5.4. **Glacial History of the Ruby Range**

During the Quaternary, at least three glaciations significantly modified the physiography of the Ruby Range and distribution of surficial materials. Resolution of glacial limits and timing decreases with age. Relatively little is known about pre-Reid Glaciation in the Ruby Range, whereas advance, maximum, and retreat phases of the McConnell Glaciation can be resolved to varying degrees.

Pre-Reid, Pliocene to mid Pleistocene

No limits are mapped for pre-Reid Glaciation, nor was definitive evidence of pre-Reid advances found in sections at Gladstone Creek. The lowest till in section is poorly constrained and may be pre-Reid. Turner et al. (2016) found stratigraphic evidence of pre-Reid advances from Kluane Range cirques on the west flank of the Shakwak Trench. The advances may have been similar in extent to the neo-glacial St. Elias advances identified by Muller (1967). Early regional glacial limits mapping by Hughes (1969), did not identify a pre-Reid limit associated with the St. Elias lobe. This absence of a most extensive pre-Reid limit was contradicted by mapping by Duk-Rodkin (1999), but further supported by Turner et al. (2013), Bond and Lipovsky (2008), and this study. It is possible that Duk-Rodkin misidentified differential erosion at geologic faults as pre-Reid meltwater-channels.

It is unknown whether pre-Reid alpine glaciation occurred within the Ruby Range. It is likely that some degree of cirque or even ice-cap glaciation occurred in the Ruby Range during pre-Reid glaciations given the advances found in the Kluane Range by Turner et al. (2016). Several features resembling degraded cirques exist in the map area which may be pre-Reid cirque, although they have not been mapped as such as this requires further analysis. Work by Nelson and Jackson (2003) found that morphology can be used to determine whether a feature is a cirque and its age. These potential cirque features occur at lower elevations and on warmer aspects than Gladstone and McConnell-

aged cirques, suggesting Ruby Range-sourced glaciers may have been most extensive during the pre-Reid.

Before the first CIS advances, the Ruby Range likely looked similar to portions of the Nisling Range beyond the all-time limit of the CIS. Drainage density would have been higher with primary erosion coming from alpine glaciation, and periglacial and fluvial processes. Periglacial features such as tors, felsenmeer and cryoplanation terraces would have developed over this time.

Reid Glaciation, MIS 6

It was not possible to distinguish between Reid and Gladstone glaciations during field and desktop mapping. Mapping at the northern margin of the St. Elias Lobe along White River found that Reid and Gladstone limits were separated by approximately 4 km horizontally and 200 m vertically (Turner et al., 2013). It is possible this separation is even less in the central Ruby Range, or that the Reid Glaciation was less extensive than the Gladstone. Features associated with Reid Glaciation were not identified definitively within the map area. It is assumed that glacial extent in MIS 6 was similarly or less extensive than in MIS 4 (Figure 3.25). It is possible that some features identified as Gladstone-age are in fact Reid-age.

Stratigraphy in Gladstone Creek does not contain evidence of a St. Elias advance during MIS 6. The stratigraphy does, however, contain till (Unit 5) interpreted to belong to an advance from Ruby Range cirques. It is possible that this till is polygenetic, resulting from an initial advance from the Ruby Range, later being overwhelmed by the St. Elias lobe. Section GLD-261 in upper Albert Creek may contain the only Reid-aged St. Elias lobe till observed in section (Figure 3.23C, unit 1).

Last Interglacial, MIS 5

Two lithostratigraphic units, Unit 6 and Unit 7, are suspected have been deposited during the last interglacial. Unit 6 is a moderately sorted fluvial gravel that likely incised through deglacial sediments previously overlying Unit 5. This unit is strongly oxidized, with highly weathered clasts, suggesting prolonged exposure at or near the surface. Unit 6 is economically auriferous. A long interglacial period would have allowed for the concentration of placer deposits as Gladstone Creek incised through the MIS 6 and older drift that filled the valley. Unit 7 is a colluviated fossiliferous loess with ventifacted clasts

and disseminated organics. This unit may represent a cooler stage within MIS 5, where lower Gladstone Creek would have been occupied by a tundra environment, suitable for grazing horses. The ventifacted clasts and loess suggest strong winds and high sediment availability, possibly a result of the growth of glaciers during this stage. Soils developed during MIS 5 are called Diversion Creek paleosols. A weakly developed version of this paleosol may be present in section GLD-231 (Figure 3.24). The weathering of Unit 6 gravel in Gladstone Creek could have occurred at this time.

Figure 3.24 Oxidized and mottled silty sand between two diamict units. This site (GLD-231) is located above the MIS 2 limit, suggesting the diamicts belong to MIS 4 and 6 advances. If this interpretation is correct, this unit may be a weakly expressed Diversion Creek paleosol formed during MIS 5.

Gladstone Glaciation, MIS 4

Gladstone glacial limits are sporadically defined within the map area. Rare meltwater channels, erratics, till, and glaciofluvial deposits occur above the McConnell limit; these are assumed to correlate to the Gladstone Glaciation. It is possible that some of these features correspond to MIS 6, although no data within the study area currently supports this interpretation. It is expected that this advance (Figure 3.25), was similar to

MIS 2, with early ice-growth from local cirques and ice caps followed by intrusion of the St. Elias lobe. The initial MIS 4 advance of Ruby Range glaciers is represented by Unit 8. St. Elias till is represented by Unit 9, which was deposited in Gladstone Creek sometime after the advance of Ruby Range ice. Ice flow in the southeast portion of the map sheet was likely also influenced by the Coast Mountain lobe. In upper Gladstone Creek, ice spilled over the high valley walls and onto the surrounding plateau surfaces depositing rare erratics that were dated by TCN (Ward et al. 2007). Low passes through the plateau surfaces may have allowed ice from Gladstone Creek to enter the Albert Creek drainage, augmenting the advances from cirques.

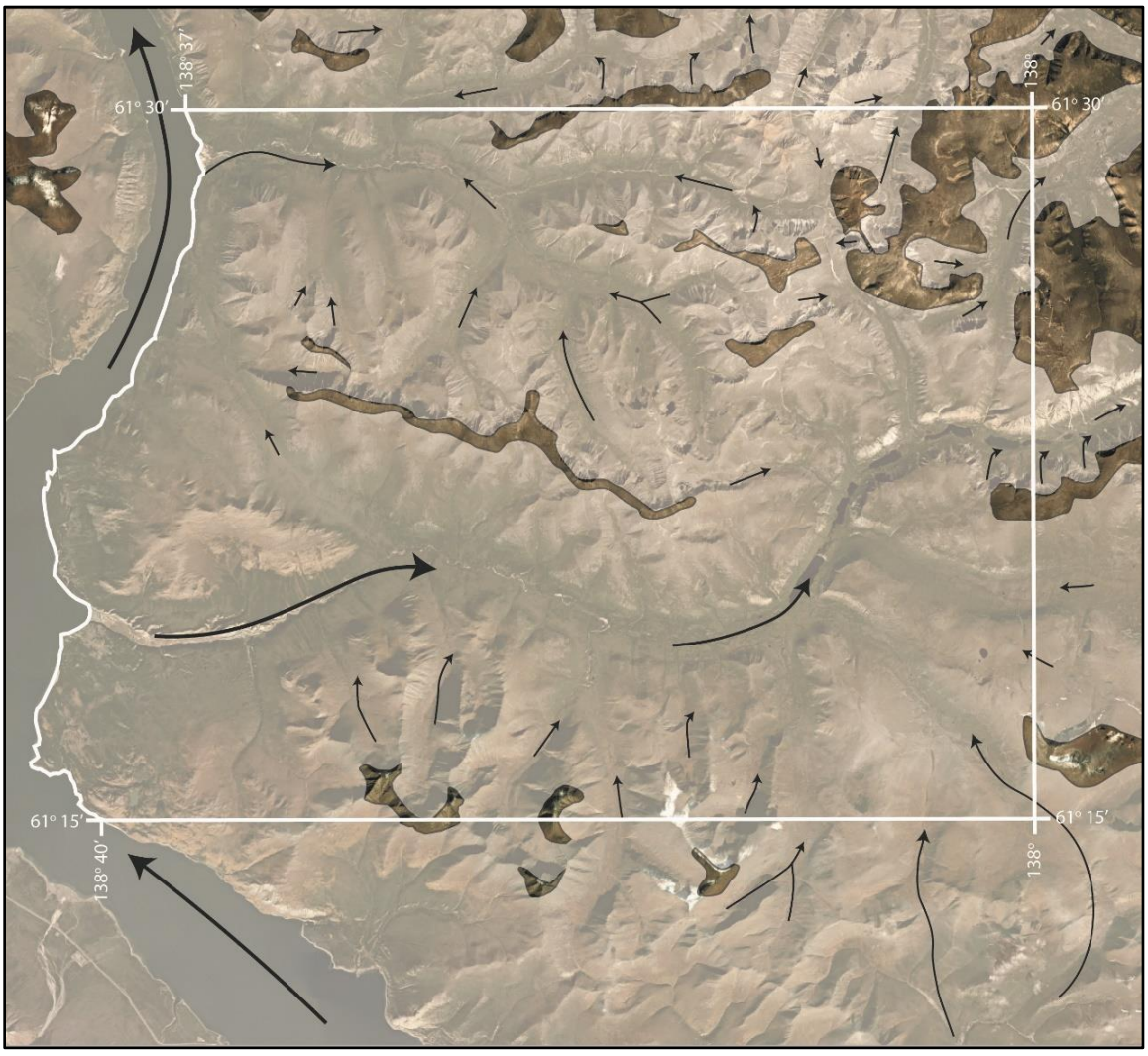

Figure 3.25 Approximate extent of the St. Elias lobe during MIS 4 and MIS 6 glaciations based on interpolation between rare glacial sediments and landforms above the MIS 2 limit. Exact extents are obscured by colluviation and lack of ice-marginal landforms due to cold-based ice. Ice flow directions (arrows) in the

southeast of the map area were likely influenced by coalescence of the St. Elias lobe with the Coast Mountain lobe.

Boutellier nonglacial interval, MIS 3

The MIS 3, Boutellier nonglacial interval was first interpreted by Denton and Stuiver, (1967) at Boutellier Creek, at the south end of Kluane Lake. Denton and Stuiver (1967) dated the interval from 38,000 to 30,000 ka. Subsequent work at Silver Creek, adjacent to Boutellier Creek confirmed the interstadial and that ice extents were broadly similar to today; the absence of MIS 3-aged glaciolacustrine sediments representing blockage of Kluane Lake, indicates Kaskawulsh Glacier was not significantly more extensive than present (Turner et al., 2016). Pollen samples collected by Turner et al. (2016) reflect a tundra environment with a period of boreal forest expansion, consistent with the Schweger and Janssens' (1980) interpretation of vegetation zones in MIS 3 being located lower than their modern equivalents.

In Gladstone Creek, lithostratigraphic Unit 10 dates to MIS 3. The cobble gravel and overbank silt and sand that compose the unit suggest a fluvial environment at a similar elevation to the modern Gladstone Creek. Unit 10 would have incised through MIS 4 and older drift, leaving fluvial terrace deposits at various elevations during the downcutting. *Pterostichus ventrichosus* elytra found in Unit 10 silts suggest a riparian tundra environment (Ball and Currie, 1997) likely similar, but perhaps cooler than the current riparian woodland conditions. The end of the Boutellier interstadial is marked by the Dawson tephra (Froese, 2002), deposited shortly after the onset of climate deterioration. No map units correlate to MIS 3.

McConnell Glaciation, MIS 2

Growth phase

The onset of the McConnell Glaciation in southern Yukon occurred as early as 29 ka BP (Jackson et al., 1991). North facing cirques at elevations above approximately 1600 m produced significant volumes of ice that flowed down into trunk valleys like Gladstone and Raft creeks (Figure 3.26). Stratigraphy in Gladstone Creek shows alpine glaciers occupied valley bottoms, flowing westward with topography, prior to the arrival of the St. Elias lobe. By 24 ka BP the lobes of the CIS had fully merged (Jackson et al. 1991); in Gladstone Creek, Dawson tephra (25,400 ± 140 ^{14}C yr) and an IRSL age (24.84 ± 1.13 ka) suggest the Cordilleran ice sheet occupied the Ruby Range at approximately this time.

The distinctive, angular, schist-rich till forming lithostratigraphic Unit 12 is interpreted as a Ruby Range advance occurring prior to the McConnell advance of the St. Elias lobe. The coarseness, angularity and homogeneous lithology of the clasts suggest a proximal source, possibly the cirques in or adjacent to Swanson Creek. The underlying Unit 11 comprises a coarsening upward subaqueous outwash sequence which is somewhat enigmatic given the down-valley advance. This could be explained by a high base level at the time of advance caused by a synchronously advancing St. Elias ice and advanced ice from the Ruby Range blocking the Talbot arm of Kluane lake. However, there is no evidence of coalescing advances in section to confirm this (e.g. highly deformed glaciolacustrine sediments overlying Ruby Range till, suggesting supraglacial deposition).

Figure 3.26 Ruby Range advance at the onset of the MIS 2 glaciation. Ice from Ruby Range cirques forms large valley glaciers in Gladstone, Raft, Rockslide, and Albert creeks following topography. The St. Elias lobe expands within the Shakwak Trench, flowing to the northwest. Interpreted ice flow directions are indicated by arrows.

The stratigraphy at GLD-04 (Figure 3.27) suggests that Ruby Range ice advanced nearly to the mouth of Gladstone Creek (Figure 3.26) prior to the arrival of the CIS. The transition between Unit 12 and Unit 13 may be explained by the impoundment of the Shakwack trench causing the Ruby Range ice to float and form a calving ice shelf resulting in deposition of glaciolacustrine sediments prior to the arrival the CIS, which would have been deformed if they had been deposited on top of the Ruby Range ice.

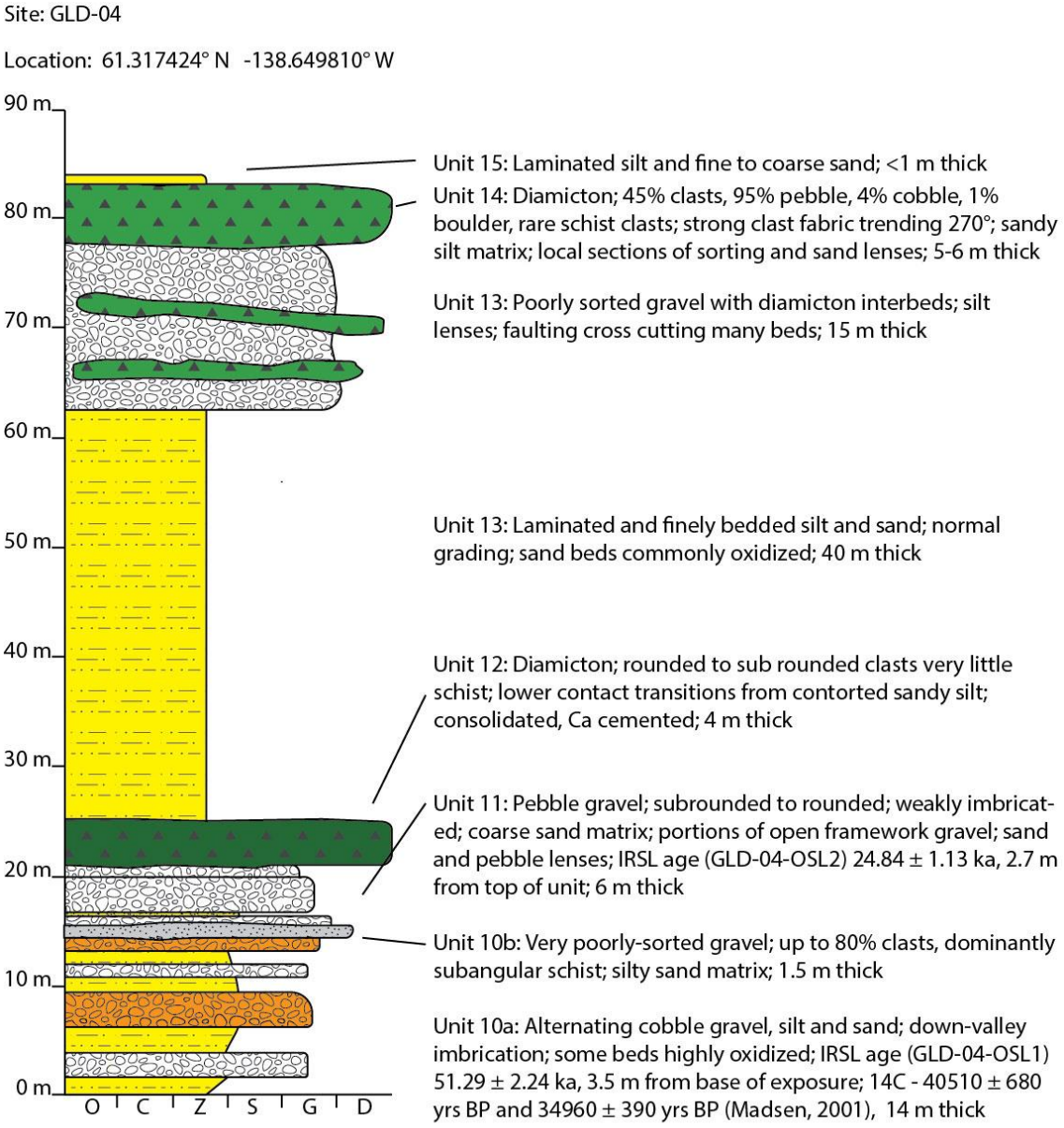

Figure 3.27 Stratigraphy of Section GLD-04. Legend in Figure 3.3.

Last glacial maximum

McConnell limits are the least extensive and most distinct. In Gladstone valley, the St. Elias lobe extended east beyond the Gladstone/Isaac drainage divide. Here the McConnell limit is defined by a valley train deposit where sediment-laden meltwater flowed east down Isaac Creek. Well defined strandlines are present above this limit at 1200 m asl, suggesting the Coast Mountain lobe blocked the outlet of Isaac Creek while ice occupied Gladstone valley and broad synchronicity between advances of the St. Elias and Coast Mountain lobes (Hughes, 1990).

The lateral limits of the St. Elias lobe are sporadically defined by landforms and glacial sediments. Strong periglacial processes have commonly obscured distinguishing features through cryoturbation and solifluction. At high elevations, cold-based ice is probable, though few diagnostic landforms are produced by this style of glaciation, hence the definition of the term. No direct evidence supporting cold-based ice was observed within the map area; however, south of the study, area tors on plateau surfaces have well-developed, fragile gnamma filled with till that suggests little erosion occurred near high elevation lateral limits during the last glaciation.

During the last glacial maximum, St. Elias limits at the west side of the map sheet were approximately 100 m lower than the penultimate limit (Figure 3.29). The same difference in limits was found in the Kiyera Lake map area, north of the Gladstone Creek map area (Bond and Lipovsky, 2009A). The St. Elias lobe did not coalesce with alpine glaciers of the Nisling Range during this glaciation as it did in MIS 4 and 6 (Muller, 1967). Topography strongly controlled ice flow directions (Figure 3.28). Near the Gladstone Lakes, St. Elias-sourced ice was mainly confined to the Gladstone valley. South facing cirques generally produced no or limited ice, which did not coalesce with the CIS advance.

In upper Gladstone Creek, few foreign clasts are available for distinguishing glaciated surfaces. If ice production from local cirques and ice caps continued throughout the McConnell Glaciation, the local ice gradient may have restricted up-valley flow, reducing the influx of extra-basinal material. However, streamlined landforms near the lateral limit in Gladstone Creek suggest ice flowed up-valley during the last glacial maximum.

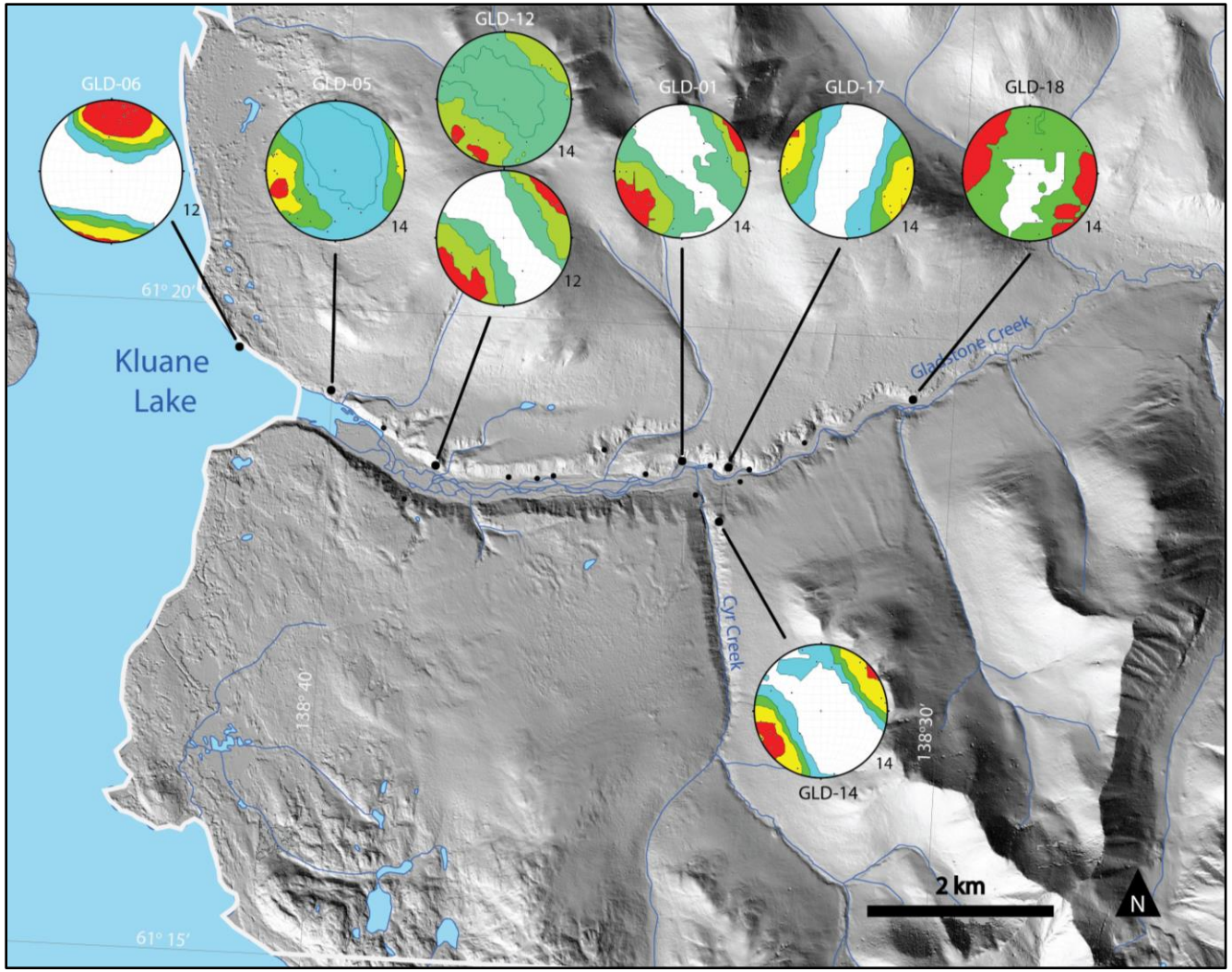

Figure 3.28 Clast fabrics from select diamicton units in Gladstone Creek. Lithostratigraphic unit numbers of samples are displayed beside the stereonet plots. The fabric at GLD-06 indicates ice flow direction parallel with the Talbot Arm of Kluane Lake. The fabrics at all other sections indicate ice flow direction approximately parallel with Gladstone Creek. Clast fabric details are shown in Table 3.3.

Table 3.3. Till clast fabric details. Locations and stereonet plots shown in Figure 3.28.

Section Number	Lithostratigraphic Unit	Clasts Measured	Eigenvector (°)	Mean Plunge (°)	Apparent Ice flow direction (°)	Eigenvalue 1
GLD-01	14	20	239	13.4	59	0.619
GLD-05	14	28	255	16.8	75	0.628
GLD-06	11	20	10	18.4	190	0.892
GLD-12	11	12	234	8.8	54	0.768
GLD-14	14	25	236	4.9	56	0.715
GLD-17	14	25	109	3.0	289	0.803
GLD-18	14	23	307	5.8	127	0.485

Figure 3.29 Extent of glaciation during the last glacial maximum. Valley-bottom topography is overcome by ice gradient in Gladstone Creek. The extent of St. Elias lobe is greatly bolstered by ice contributions from local cirques and ice caps. Limits are approximate due to the likelihood of cold-based ice at glacial margins and lack of diagnostic landforms. Arrows indicate ice-flow direction.

Retreat and Readvance phase

In Talbot Creek, immediately north of the Gladstone map sheet, retreat of the St. Elias lobe from the Ruby Range occurred at approximately 17.2 ka (Bond and Lipovsky, 2009C). It is likely that deglaciation occurred in the study area at approximately the same time, although the significant augmentation of the CIS by local sources could have caused ice to persist for longer, particularly if these sources were out of sync with the St. Elias

lobe source areas. Landforms dated to 13.8 ± 0.9 ka in Raft and Rockslide creeks suggest alpine glaciers in the Ruby Range either continued to produce ice much later than the retreat of the St. Elias lobe, or readvanced. This age fits well with an older group of moraines in the Mackenzie and Cassiar mountains associated with short cooling events within the Bølling-Allerød cooling (Menounos et al., 2017) and ages obtained from boulders in Whitehorse dating the Chadburn readvance of the Cassiar Lobe (Bond, 2004). During the Bølling-Allerød warm periods, ice retreated from its maximum extent and readvanced during cool intervals leaving moraines (Menounous et al., 2017). The moraines in Raft Creek correlate to the Older Dryas cooling event, which was triggered by meltwater discharged by the collapse of the Cordilleran-Laurentide ice saddle at approximately 14.5 ka, weakening the Atlantic meridional overturning circulation leading to widespread hemispheric cooling (Ivanovic et al., 2017). This may also correlate with a 14-12 ka readvance in the Alaska Range, but is considerably earlier than more prominent Younger Dryas advances (12.3-11 ka) observed in the Alaska Range and Ahklun Mountains (Briner et al., 2008). An alpine moraine in the Glenlyon Range was also dated at 13.2 ± 1.2 ka (Stroeven et al. 2010). A retreat from a readvance on Calvert Island on the central coast of British Columbia occurred at 14.2-13.8 ka (Eamer et al., 2017), suggesting the possibility of a climate driver that affected other regions of the CIS. Alternatively, these moraines may represent a standstill in a slow retreat of alpine glaciers, though the drivers for a standstill may be the same as a readvance. Continued ice production in alpine regions compares well with models of glacial decay suggested for the CIS elsewhere, which suggest the onset of decay begins with the reduction but not complete shutoff of ice production in cirques (Clague, 1989; Fulton, 1991).

The northern CIS is precipitation limited rather than temperature limited (Ward et al., 2007). A readvance or standstill during recession could be associated with an increase in precipitation rather than a reduction in temperature required elsewhere in the CIS. It is possible the retreat of the St. Elias lobe and down-wasting in the source areas allowed for more moisture penetration into the Ruby Range. Alternatively, a precipitation driven readvance could have been triggered by eustatic sea level rise which submerged the Bering-Chukchi platform; exposure of which was responsible in part for the aridity of much of Alaska and Yukon during MIS 2 (Briner et al., 2008).

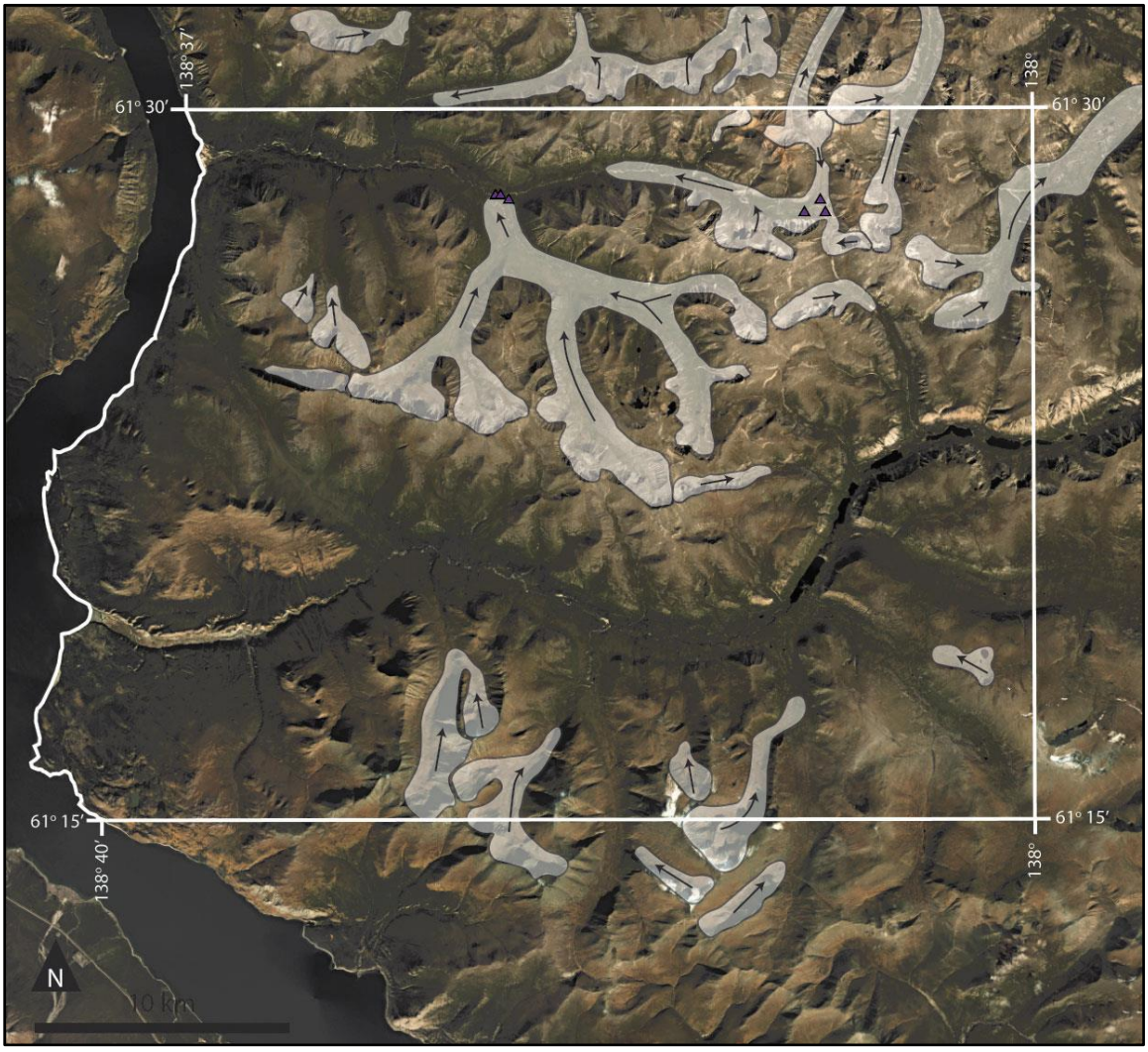

Figure 3.30 Late glacial advance of alpine glaciers at ca.13.8 ka. The timing of the advance is based on cosmogenic ages collected from erratics on moraines (triangles) in Raft and Rockslide creeks. Elsewhere, the advance is inferred from correlation with similar morphological "freshness" of down-valley moraines below Ruby Range cirques. Arrows indicate ice-flow direction.

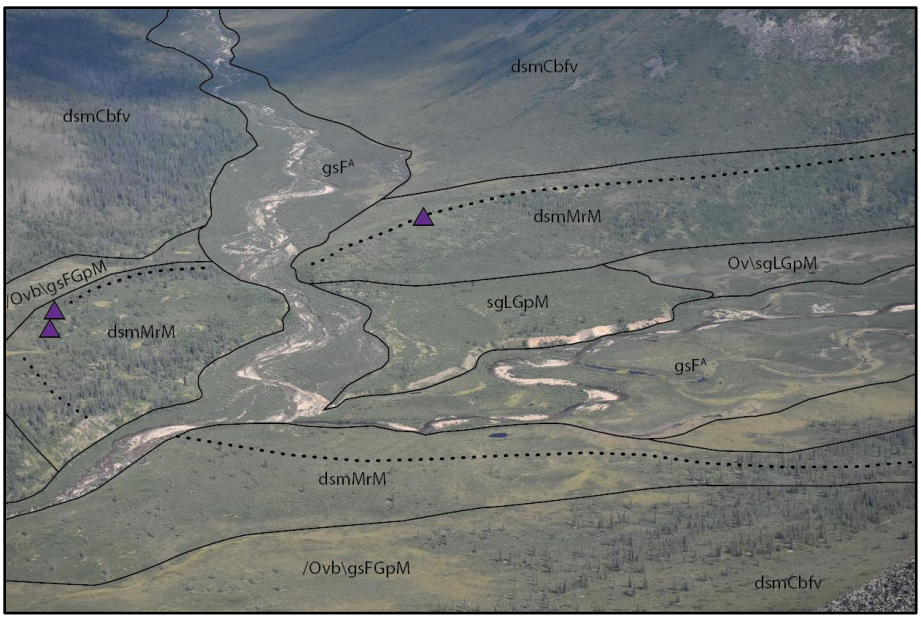

Figure 3.31 Late MIS 2 readvance landforms at the confluence of Raft and Rockslide creeks. A moraine ridge descending from upper Raft Creek is marked with a dotted line. Boulders on this moraine (triangles) give an age of 13.8 ± 0.9 ka. A glaciofluvial outwash plain grew as the glacier advanced down Raft Creek. At a readvance or standstill, the moraine ridge was deposited. As the ice pulled back from the moraine, a small glacial lake formed behind the moraine and deposited sand and gravel. When the moraine was eventually breached, Raft and Rockslide creeks spread fluvial gravels across the valley floor. Organic veneers and blankets accumulating on the low angle glaciofluvial deposits and the valley walls are actively colluviating.

In lower Gladstone Creek, small drainages incise the Quaternary sediments, and run roughly parallel to the creek before deflecting into the modern valley bottom (Figure 3.32). These features appear to be meltwater channels, although the configuration of ice at the time of their establishment is problematic. The stratigraphy best supports the interpretation of up-valley CIS ice persisting last; however, the meltwater channels support the interpretation of down-valley Ruby Range ice outlasting the CIS. The fabrics from the uppermost till (Figure 3.28) are valley-parallel and therefore do not confirm a specific source.

The stratigraphy is somewhat ambiguous as to whether the St. Elias lobe or Ruby Range valley glaciers occupied Gladstone Creek last; however, most of the meltwater channels appear to be associated with down-valley ice flow. The best explanation for this is that the uppermost till in section is polygenetic, representing an initial up-valley advance of the St. Elias lobe and a shift in ice flow direction due to downwasting of St. Elias ice in the Shakwak Trench. The thin lacustrine unit on top of many sections may be the result of a high base level or localized ponding during the retreat of Ruby Range ice. Glaciofluvial gravels only appear above the MIS 2 till below the mouth of Gladstone Creek. Because

gravel units at the top of sections are commonly recessive, they may be present but not exposed at the tops of sections due to erosion and subsequent deposition of loess.

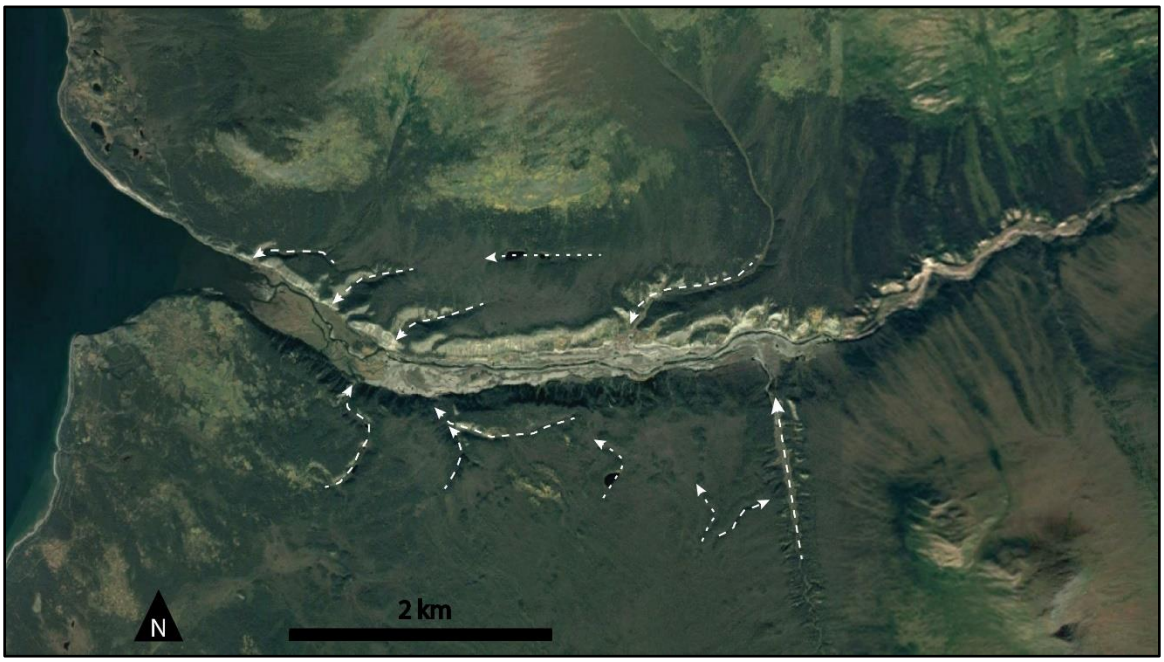

Figure 3.32 Enigmatic drainages in lower Gladstone Creek, that could be interpreted as meltwater channels. The well-developed channels are shown by dashed lines, less developed channels are shown by dotted lines. Cyr Creek is not deflected down-valley, possibly due to occupation by ice from the upslope cirque which persisted after the formation of the other channels.

Ruby Range in the Holocene, MIS 1

Since the end of the last glacial period, the Ruby Range has remained geomorphically active. Periglacial processes are widespread on cold aspects and high altitudes. At lower elevations and warmer aspects, permafrost is warming causing active layer detachments on moderate to steep slopes. Rock glaciers in some of the highest cirques are the only remnant glaciers left in the study area.

Conspicuous nested colluvial fans were observed in upper Rockslide Creek (Figure 3.33). Two interpretations of this feature are possible. The older dissected fans may have formed in contact with a valley glacier and have been dissected after the glacial recession lowered the effective base level allowing for erosion of the original fan surface. Alternatively, the dissected fans may have formed during the paraglacial period following McConnell Glaciation, when sedimentation rates are highest due to availability of sediment and presence of unstable landforms left over from glaciation (Church and Ryder, 1972). The former interpretation is preferred as the catchments feeding the fans appear to be

above MIS 2 glacial limits, which means paraglacial sediment supply would be unlikely within the catchment.

Figure 3.33 Nested colluvial fans in built by debris flows in upper Rockslide Creek. A mining exploration road traverses the modern fan near its toe. Photo by Jeff Bond.

Soil development in the Ruby Range is limited due to cold and dry conditions. The majority of soils are bruisols or cryosols. Brunisols are commonly modified by hillslope processes and periglacial processes, obscuring horizon boundaries (Bond and Sanborn, 2006). Soil sola are typically less than 50 cm thick (Dampier et al. 2008)

Human landscape disturbance within the study area is generally limited to mining and associated activities. Minor exploration roads have been constructed in upper Raft Creek and along the shore of Kluane Lake. Placer mining in lower Gladstone Creek continuous to modify the creek bottom and surrounding valley walls.

Figure 3.34 Brunisolic soil with loess in upper mineral horizon, developing on Gladstone till near a tor above upper Gladstone Creek. This soil may be a cryosol, although permafrost was not confirmed on site. Upper mineral horizon is silt rich from post-glacial deposition of loess.

3.6. Conclusions

Surficial geology mapping and stratigraphic analysis throughout the study area shows evidence of at least two CIS advances of the St. Elias lobe, and three or four advances of ice sourced in the Ruby Range. The most extensive, penultimate limit of the St. Elias lobe may be a composite of MIS 6 and 4 glaciations, or it may be that MIS 4 was more extensive. A more extensive MIS 4 limit has not been observed elsewhere in Yukon and is possible (Ward et al., 2007), but not confirmed by this study.

Stratigraphy in Gladstone Creek is difficult to interpret due to extensive cut and fill. Baseline conditions appear to have varied greatly throughout the Quaternary, due to

glacial advance and retreat, with even minor advances of the St. Elias lobe affecting sedimentation in Gladstone Creek.

The penultimate limit is poorly defined but appears to have overtopped the valley walls of Gladstone Creek and covered much of the surrounding plateau surfaces. Some of these plateau surfaces appear to have also been local sources of ice growth contributing to CIS extent. U-shaped valleys descending from these plateaus suggest ice growth was significant enough for considerable erosion and advances occurred prior to the filling of the Gladstone Creek valley. Tors below mapped limits suggest cold-based conditions likely occurred near ice margins.

The McConnell limit is better defined than the penultimate limit due to better preservation of landforms. This limit is approximately 500 m lower than the penultimate limit at the eastern edge of the map area. Local ice sources contributed significantly to the CIS extent. A readvance occurred from Ruby Range source areas at 13.9 ± 0.9 ka, likely correlating to the Older Dryas and indicating the and Ruby Range ice had already retreated from its MIS 2 maximum.

Only small rock glaciers currently exist in the Ruby Range, within the confines of high cirques. Periglacial conditions are still present throughout the entire study area. Holocene landscape change is dominantly a result of fluvial, colluvial, periglacial, and anthropogenic processes.

Chapter 4. Constraints on the evolution of placer gold deposits from lode gold sources at Gladstone Creek, Yukon

Derek C. Cronmiller and Brent C. Ward

Earth Sciences, Simon Fraser University

Jeffrey D. Bond

Yukon Geological Survey

Daniel Layton-Matthews

Geological Sciences and Geological Engineering, Queens University

Originally published as:

Cronmiller, D.C., Ward, B.C., Bond, J.D. and Layton-Matthews, D., 2019. Constraints on the evolution of placer deposits at Gladstone Creek, Yukon (NTS 115G/7, 8). In: Yukon Exploration and Geology 2018, K.E. MacFarlane (ed.), Yukon Geological Survey, p. 61–74.

4.1. Background

A modified version of this chapter was published in *Yukon Exploration and Geology* (Cronmiller et al., 2018). This chapter addresses the morphology, geochemistry, and stratigraphic dispersion of placer deposits in Gladstone Creek. The stratigraphic unit numbers in this section do not correspond to lithostratigraphic numbers of the previous chapter at Appendix B.

4.2. Abstract

Gladstone Creek hosts a productive placer mine and has been glaciated by the Cordilleran Ice Sheet at least three times. Glaciations eroded bedrock and reworked surficial materials, depositing thick sequences of sediment in Gladstone Valley, which were subsequently fluvially incised during deglaciation and non-glacial intervals. Fluvial incision and reworking concentrated detrital gold in coarse gravels, commonly overlying

bedrock and false-bedrock surfaces. Identifying false-bedrock units in stratigraphy may help placer miners target economical gold deposits perched above the valley bottom.

Gold grain samples were collected from four gravel units on Gladstone Creek. Characterization of gold grain morphology and laser ablation ICP-MS analysis indicates multiple sources of lode mineralization. Based on regional ice flow directions and the stratigraphic and geographic locations of analyzed samples, gold is likely sourced from epithermal and gold-rich porphyry deposits associated with the Ruby Range batholith, and orogenic mineralization in the Kluane schist.

4.3. Introduction

Gladstone Creek is located in the central Ruby Range, southwestern Yukon. The Ruby Range has a long history of placer mining and mineral exploration; placer mining in Gladstone Creek began in the 1910s (Cairnes, 1915). Active and historic placer mines along this creek are well within the limits of the most recent glaciation to affect Yukon, and thus are in a much different setting than placer mines in the unglaciated Klondike.

Stratigraphy and morphology of gold grains in Gladstone Creek were previously examined by Madsen (2001); however, no morphological or geochemical analysis of gold grains has been used to link placer gold to lode gold sources in the Gladstone area. In this paper we present the sedimentological characteristics and commonalities of economically auriferous gravels within Gladstone Creek and how glaciation has affected the development and distribution of placer deposits in Gladstone Creek. We also examine gold grain morphology and geochemistry to determine the likely sources of lode gold based on the style of mineralization in local lithological units. Understanding the mechanisms controlling the distribution of economic placer deposits will help placer miners locate economic gravels in glaciated regions. Determining the provenance of placer gold in Gladstone Creek may also inform future hard rock mineral exploration in the region. The objectives of this paper are to characterize placer gold grain chemistry and morphology to determine potential bedrock sources and how glaciation has affected the distribution and preservation of placer deposits.

4.4. Setting

The central Ruby Range is characterized by rugged peaks greater than 2100 m above sea level (asl), and broad undulating plateaus above 1500 m asl. The peaks and plateaus are drained by deep, U-shaped valleys, such as Gladstone Creek, that drain westward into the east side of Kluane Lake (Figure 4.1). Cronmiller et al. (2018) mapped surficial materials throughout the study area. Upland surficial materials are heavily modified by periglacial processes and comprise colluvium derived from weathered bedrock and thin veneers of till below all-time glacial limits (Cronmiller et al., 2018). Valley bottoms are filled with thick, stratigraphically complex Quaternary deposits comprising glacial and interglacial sediment. In Gladstone Creek these deposits are more than 115 m thick.

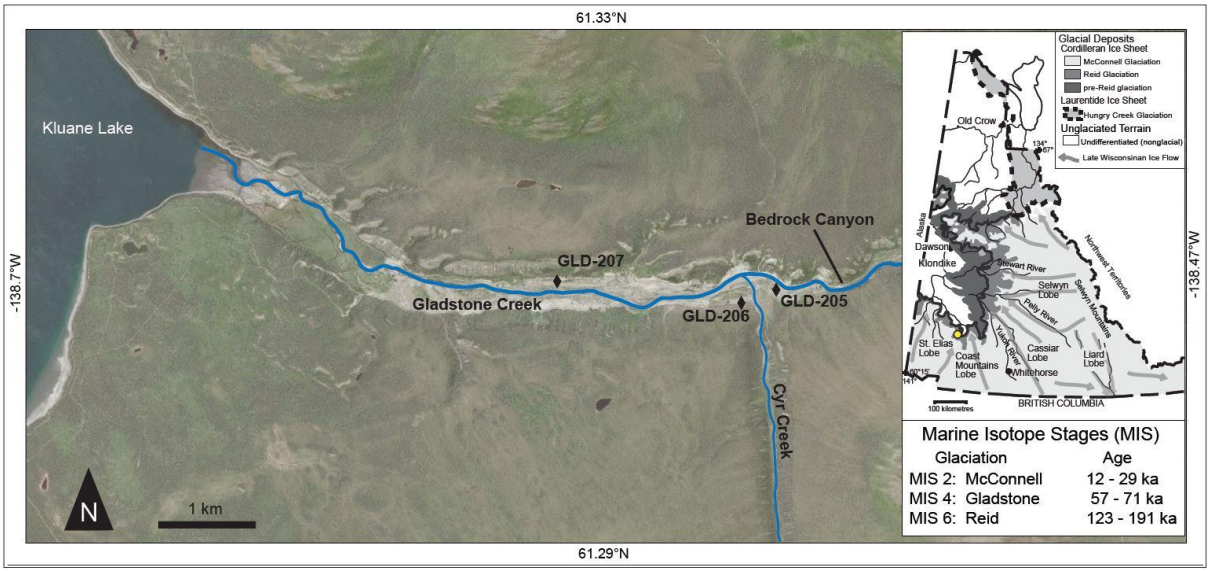

Figure 4.1 Lower Gladstone Creek and Cyr Creek. Sample sites are indicated by diamonds. Location of study area shown by yellow-filled dot on inset map.

4.4.1. Glacial History

Early mapping in southwestern Yukon by Hughes et al. (1969) found evidence of two Cordilleran ice-sheet advances into the Ruby Range, as well as local ice cap formation on the plateau surfaces above 1500 m (Hughes, 1990). Glacial advances were initially suspected to correlate to what we now know are marine oxygen isotope stages (MIS) 2 and 6; however, recent ^{10}Be dating of erratics above Gladstone Creek suggest the local all-time limit may have occurred during MIS 4 (Ward et al., 2007). New field and desktop

mapping (Cronmiller et al., 2018) confirmed the presence of ice caps on plateau surfaces based on the orientation of moraines and meltwater channels as well as descending U-shaped valleys; all of which suggest ice growth extended beyond the high plateaus and into local trunk valleys including Gladstone Creek. In addition, many well-developed cirques are found on high, northerly aspects. Moraines descending from these cirques suggest significant local alpine glaciation coalesced with ice from the St. Elias lobe of the Cordilleran Ice Sheet (CIS; Figure 4.1). Generalized St. Elias lobe ice flow directions are shown in Figure 4.2. Ice caps and cirques may have contributed substantially to the local extent of late Pleistocene limits and could account for the local all-time limit corresponding to MIS 4 advance. Till suspected to have been deposited by westward flowing ice from Ruby Range cirques is observed in sections as far down Gladstone Creek as GLD205 (Figure 4.1). The presence of till in the lower reaches of Gladstone Creek suggests that both east and west-flowing ice could have introduced distal-intrabasinal and extrabasinal auriferous material into Gladstone valley during glaciations.

4.4.2. **Geology and Mineralization**

Gladstone Creek is underlain by two main lithological units: The Ruby Range batholith, and Kluane schist (Figure 4.2). Uncorrelated ortho- and paragneiss are commonly found at the boundary of these two units that are thought to be gneissic or migmatitic equivalents of Kluane schist or the basement rock of the Yukon-Tanana terrane (Israel et al., 2011a). Minor outcrops of ultramafic rock occur in association with the Kluane schist.

Ruby Range Batholith

The Ruby Range batholith is a large multiphase plutonic complex comprising quartz-diorite, tonalite, granodiorite, with minor diorite, gabbro, and granite (Israel et al., 2011a). The batholith contains porphyry Cu-Mo-Au mineralization (Yukon MINFILE 115G070, 115G071) and epithermal Au-Ag mineralization, primarily in the upper crustal part of the batholith. The Ruby Range batholith underlies most of the upper reaches of Gladstone Creek. The main phases of the Ruby Range batholith intrusion occurred between 64 and 57 Ma.

Kluane Schist

The Kluane schist occurs between the Denali Fault on the west side the Shakwak Trench, and the Ruby Range batholith in the east (Figure 4.2). It comprises a metamorphic assemblage of metapelitic quartz-mica schist, rare ultramafic and carbonate bodies, and numerous quartz vein systems (Israel et al., 2011a). Kluane schist contains muscovite-rich and biotite-rich units. The characteristics of gold in Kluane schist suggest orogenic mineralization (Israel et al., 2011a). Deposition of the Kluane schist occurred between 95 Ma and 82 Ma, the onset of metamorphism.

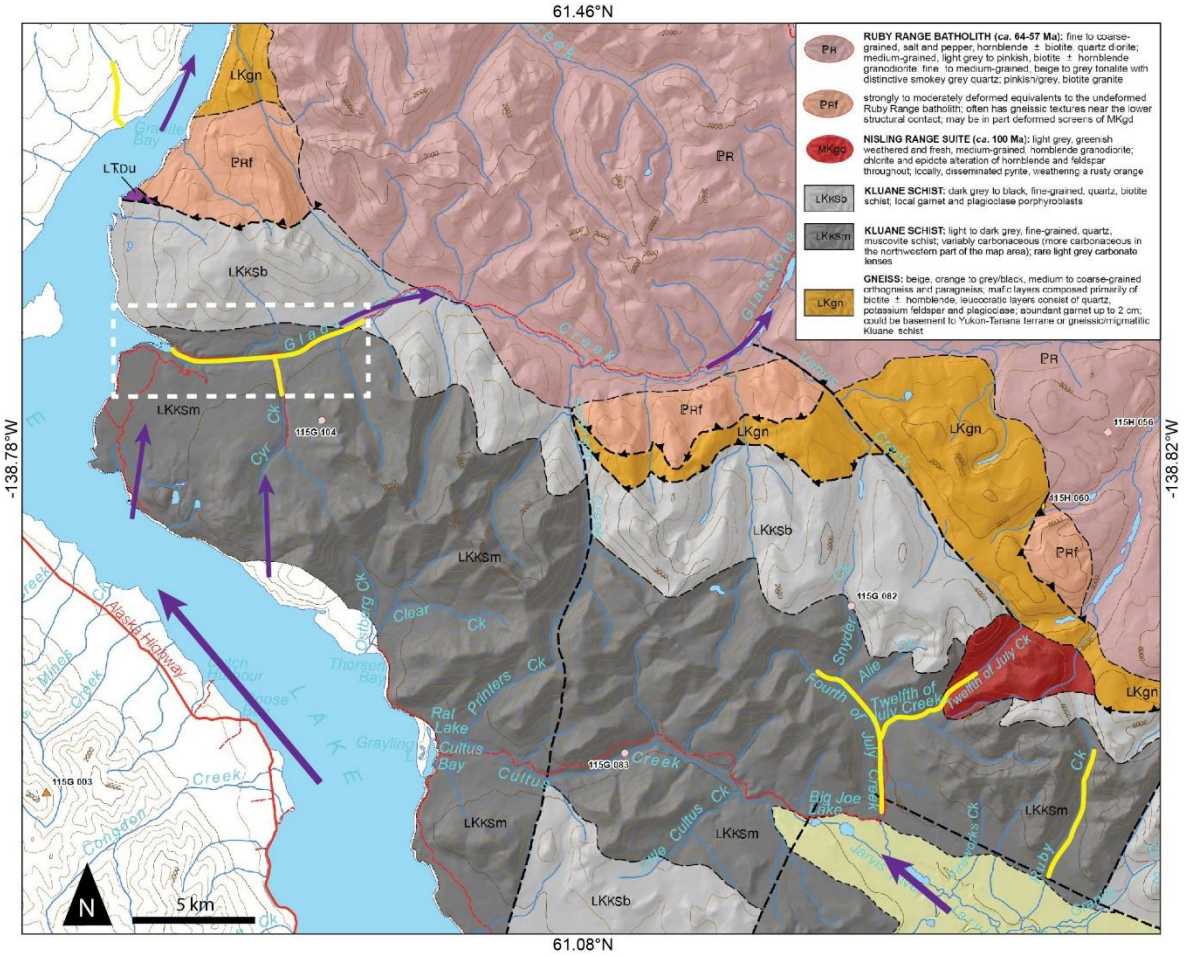

Figure 4.2 Bedrock geology of the west-central Ruby Range (Israel et al. 2011b). The location of Figure 4.1 is shown by dashed white lines. Actively mined placer creeks are shown by yellow lines. Local indicators of St. Elias lobe ice flow direction (Hughes et al., 1969) shown by arrows.

4.4.3. **Mining and Exploration**

Gladstone Creek was first mined in the 1910s below the mouth of Cyr Creek (Cairnes, 1915). The first large-scale operation began with the Kluane Dredge Company, which extracted 5770 ounces of gold from below the confluence of Cyr Creek between 1952 and 1956 (Muller, 1967). The lower reaches of Gladstone Creek and Cyr Creek are now mined by TIC Exploration Inc. TIC Exploration has mined Gladstone Creek intermittently since 1992 (Bond and van Loon, 2018). Mining has focused on the modern flood plain gravels as well as low terraces on the left bank of Gladstone Creek. Pay gravel is sorted with mobile trommel wash plants and sluice runs. The wash plants are moved to the active mine cuts and fed with excavators, eliminating the need for hauling pay gravel.

Numerous other placer mines are currently operating on the west slopes of the Ruby Range, all of which are located in Kluane schist (Figure 4.2). Hard rock exploration has noted similarities between the orogenic mineralization in Kluane schist and the Juneau gold belt (Israel et al., 2011a; Yukon MINFILE 115H 055, 115H 047). Porphyry/sheeted-vein copper-silver-gold-molybdenum mineralization in the Ruby Range batholith is currently being explored at Strategic Metals Ltd.'s Meloy property in upper Rockslide Creek, immediately north of Gladstone Creek.

4.5. Methods

Sites were visited in summer 2017, as part of a larger program to map surficial geology and log stratigraphy of Gladstone Creek and the central Ruby Range. Thirteen sections were described on Gladstone Creek and two at Cyr Creek, three of these are described herein. Sections were divided into stratigraphic units based on sediment type and general sedimentary characteristics. Gold grain samples were collected from two sections on Gladstone Creek (GLD205 and GLD207) and one section at the mouth of Cyr Creek (GLD206). The samples were obtained from gravel units identified by TIC Exploration as being economically auriferous. Gravel was screened using a 4-mesh sieve and sluiced using a portable sluice box (Figure 4.3) to obtain heavy-mineral concentrate. The concentrate was panned to isolate the gold. This process was repeated until a minimum of 25 grains were collected for each sample.

Morphological and chemical analysis of the gold grains was conducted at the Queen's Facility for Isotope Research (QFIR) at Queens University. High-resolution electron backscatter images were produced for each sample using an FEI scanning electron microscope. Gold grain morphology was characterized from the backscatter images using Image Metrology's SPIP™ image recognition software. Laser ablation ICP-MS using aThermo X Series II ICP-MS coupled to an ESI 193 nm Excimer laser was used to determine major, minor, and trace element composition of the gold grains.

Figure 4.3 Collecting auriferous gravel at site GLD207 and sluicing the fine fraction of sieved gravels to obtain gold grain samples.

4.6. Results

4.6.1. **Stratigraphy**

GLD205

Section GLD205 (Figure 4.4) is a mine cut located on the left limit of Gladstone Creek, approximately 200 m downstream of a bedrock canyon (Figure 4.1). A description

of lithostratigraphic units is provided in Table 1. This section contains two economic gravels, Units 2 and 5. Both gravel units overlie consolidated diamicton interpreted to be tills, corresponding to MIS 4 (Unit 4) and MIS 6 (Unit 1) advances of Ruby Range glaciers. This interpretation is based on their dense over-consolidated nature, the presence of extrabasinal, striated clasts, and strong unidirectional clast fabrics. A radiocarbon age of 26,720 ± 170 ^{14}C yr. BP (UCIAMS197773) and Dawson tephra (cf. Froese et al., 2002) in Unit 6 constrains the tills to pre-MIS 3. A radiocarbon age within Unit 3 of 45,600 ± 2200 ^{14}C yr. BP (UCIAMS-197774) is suspected to be non-finite, due to the age being near the useful limit of the technique. Unit 2 is strongly oxidized and contains highly weathered and cryoturbated clasts. Stratigraphy and geochronology indicate Unit 4 is from a MIS 4 advance, suggesting an age of at least MIS 4 for Unit 2. Both economic gravels overlie diamicton, which acts as false bedrock (*cf.* Slingerland and Smith, 1986), where gold is concentrated on an erosionally resistant surface.

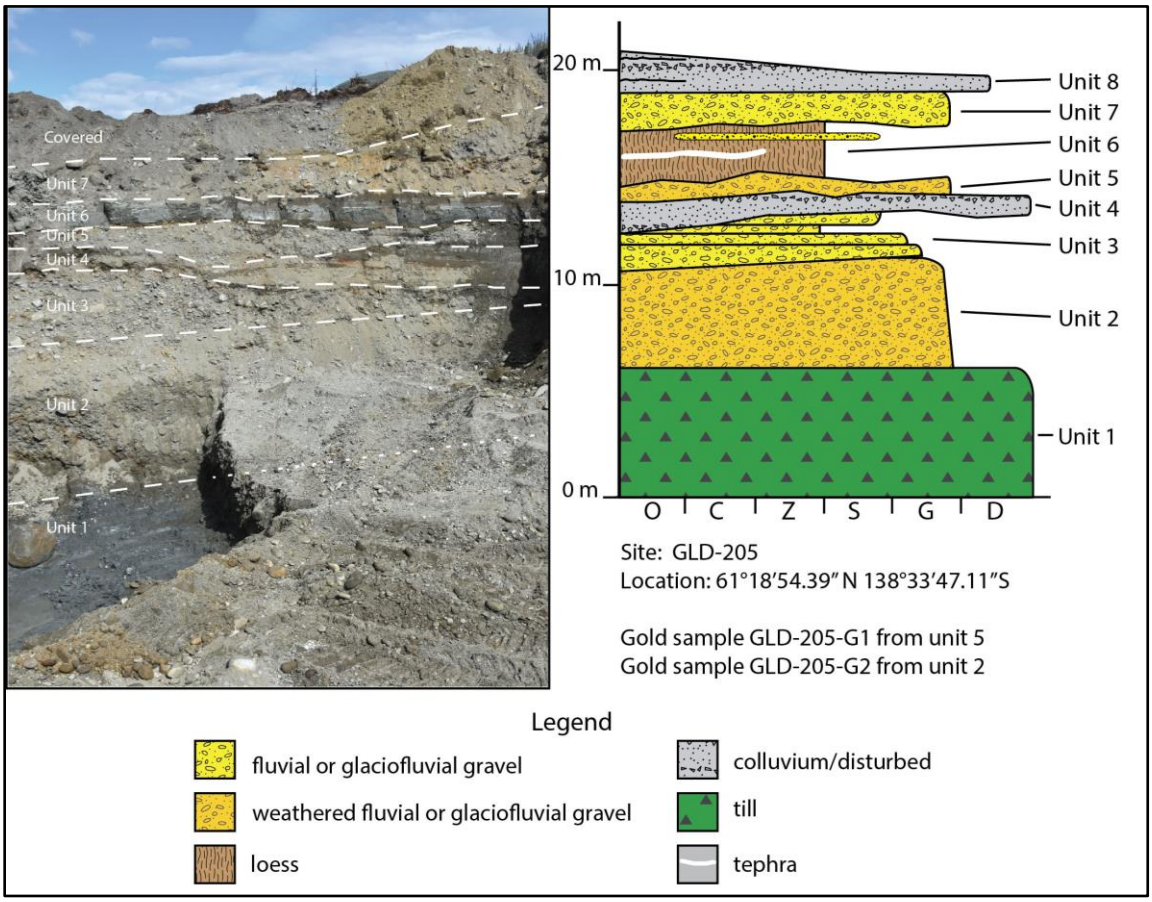

Figure 4.4 Stratigraphy in mine cut on left limit of Gladstone Creek, GLD205.

Table 4.1 GLD205 unit descriptions

GLD205, Unit and interpretation	Description
Unit 9 – Colluvium	Stratified pebbly sandy diamict with organic layers; 1 m thick; White River tephra at 7 cm depth
Unit 7 – Fluvial gravel	Poorly sorted chaotic boulder gravel; 1.25 m thick, laterally variable; 10% boulders, 40% cobbles, 50% pebble; silty sand matrix
Unit 6 – Loess, colluviated	Fine sandy silt; 2.5 m thick; finely bedded, rare granule lenses; 10 cm thick Dawson tephra at 1.6 m above base of unit; GLD205-M1: weevil (*Lepidophorus sp.*) macrofossils 26720 ± 170 ^{14}C yr. BP (UCIAMS-197773)
Unit 5 – Weathered gravel	Weathered, oxidized, auriferous, sandy boulder gravel; 15% boulder, 40% cobble, 45% pebble; silty sand matrix; 1 m thick, laterally variable in thickness and texture; economically auriferous; Gold sample GLD205-G1
Unit 4 – Colluvium	Colluvial diamicton; 1.1 m thick, laterally variable; massive; 10% clasts; 90% matrix: 35% silt, 65% clay; upward increase in clast content.
Unit 3 – Fluvial gravel	Fining upwards silts sands and gravel; 1.9 m thick; 30% cobble, 70% pebble; rare sand lenses and silt rip-up clasts; GLD205-M5: beetle (*Pterostichus sp.*) macro fossils 45600 +/- 2200 ^{14}C yr. BP (UCIAMS-197774) (assumed non-finite)
Unit 2 – Weathered gravel	Weathered, oxidized, poorly sorted, chaotically-bedded, boulder gravel; 4-5 m thick; 10% boulder, 40% cobble, 50% pebble; 50% sandy silt matrix; vertically oriented clasts (cryoturbation); economically auriferous, Gold sample GLD205-G2
Unit 1 – MIS 6 till	Blue-grey diamict; > 3 m thick, lower contact not exposed; 10% sub-angular to sub-rounded clasts: 90% pebble, 10% cobble; 90% matrix: 20% clay, 75% silt, 5% sand; consolidated

GLD206

Section GLD206 is a mine cut on the left limit of the Cyr Creek fan at the confluence with Gladstone Creek (Figure 4.5). The characteristics of stratigraphic units exposed in this section are summarized in Table 2. Bedrock is exposed on both sides of the Cyr Creek valley immediately above this section that constrain lateral migration and downcutting of the channel.

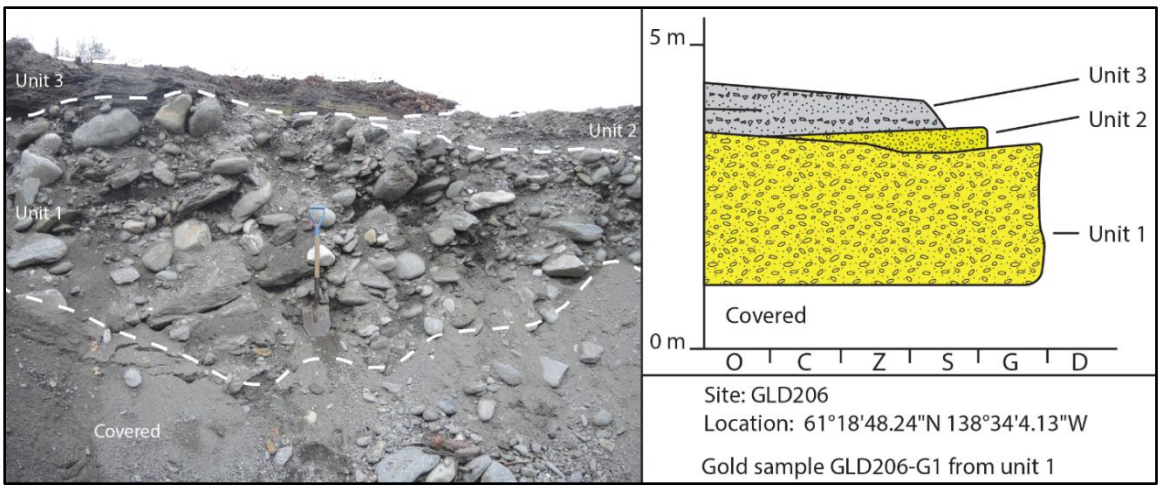

Figure 4.5 Stratigraphy in mine cut on left limit of Cyr Creek, GLD206, near confluence with Gladstone Creek. Section legend in Figure 4.4.

Table 4.2 GLD206 unit descriptions

GLD206 – Unit and interpretation	Description
Unit 3 – Colluvium	Weakly stratified, pebbly sandy diamict with organic layers; 0.6 m thick
Unit 2 – Fluvial pebble gravel	Moderately well-sorted pebble gravel; 0.4 m thick, laterally discontinuous; 75% clasts: 10% cobble, 90% pebble; 10% coarse sand matrix
Unit 1 – Fluvial boulder gravel	Poorly-sorted auriferous boulder gravel; >2.3 m thick, lower contact not exposed; 90% clasts: 40% boulder, 40% cobble, 20% pebble; 10% sand matrix; economically auriferous; gold sample GLD206-G1

GLD207

Section GLD207 (Figure 4.6) is a mine cut on the right limit of Gladstone Creek, approximately 2.7 km downstream from the bedrock canyon. Characteristics of the stratigraphic units are summarized in Table 4.3. Units 1 to 4 are gravels. Unit 3 contains economic concentrations of gold. This unit overlies a consolidated, poorly-sorted, matrix supported gravel (Unit 2), which was likely a paleo-floodplain surface, the age of which is not constrained. Many vertically aligned (Figure 4.6 inset) and frost shattered clasts suggest Unit 2 was exposed to strong periglacial conditions. These conditions may have occurred during a glacial stage, prior to ice arrival in lower Gladstone Creek. The high silt content of Unit 2 may be from loess inputs. Like the diamicton units in GLD205, this unit appears to act as a false-bedrock that limits downcutting due to its consolidation. Unit 5 is modern colluvium from mass wasting of the adjacent valley side.

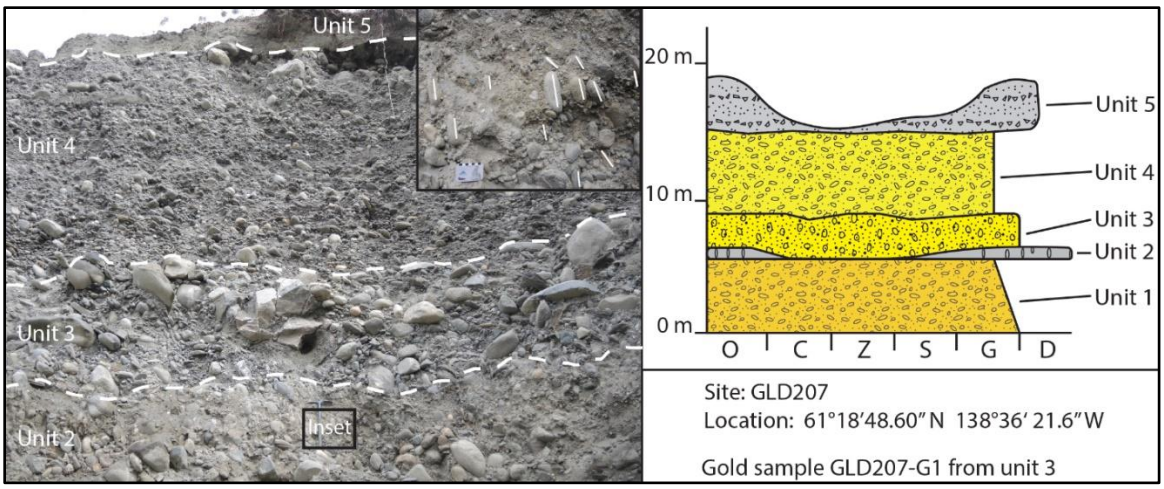

Figure 4.6 Stratigraphy in mine cut on right limit of Gladstone Creek, GLD207. Section legend in Figure 4.4.

Table 4.3 GLD207 unit descriptions

GLD207- Unit and interpretation	Description
Unit 5 – Colluvium	Stratified sandy silt with pebbles; 3 m thick, laterally variable; 90% sandy silt, with 5% pebbles and rare cobbles; 4 weakly-developed buried soils with organics; White River tephra 15 cm from top of unit.
Unit 4 Cobble gravel	Moderately well-sorted cobble gravel; 4.5-5 m thick; 90% clasts: 1% boulder, 40% cobble, 59% pebble; matrix coarse to medium sand.
Unit 3 – Boulder gravel	Chaotic boulder gravel; 1.9 m thick; 98% clasts; 10% boulder, 60% cobble, 30% pebble; 2% sandy silt matrix; down-valley imbrication; economically auriferous; gold sample GLD207-G1
Unit 2 – Cryoturbated gravel	Cryoturbated gravel; 0.7 m thick, laterally variable; 70% clasts: common vertically oriented and frost shattered; 30% sandy silt matrix; highly consolidated
Unit 1 – Weathered gravel	Oxidized, bouldery cobble gravel; >4.3 m thick, lower contact not exposed; 90% clasts, 10% sand matrix; many clasts highly weathered; crudely- to well-sorted; strong down-valley imbrication;

4.6.2. **Gold Grain Morphology**

The roundness of gold grains is commonly used as a proxy for travel distance from lode source (Knight et al., 1999). Well-rounded grains are considered to be more travelled than those exhibiting angular morphologies. Due to their malleability, gold grains round

rapidly in the first three km of fluvial transport, and then more slowly as a stable morphology is achieved (Figure 4.7).

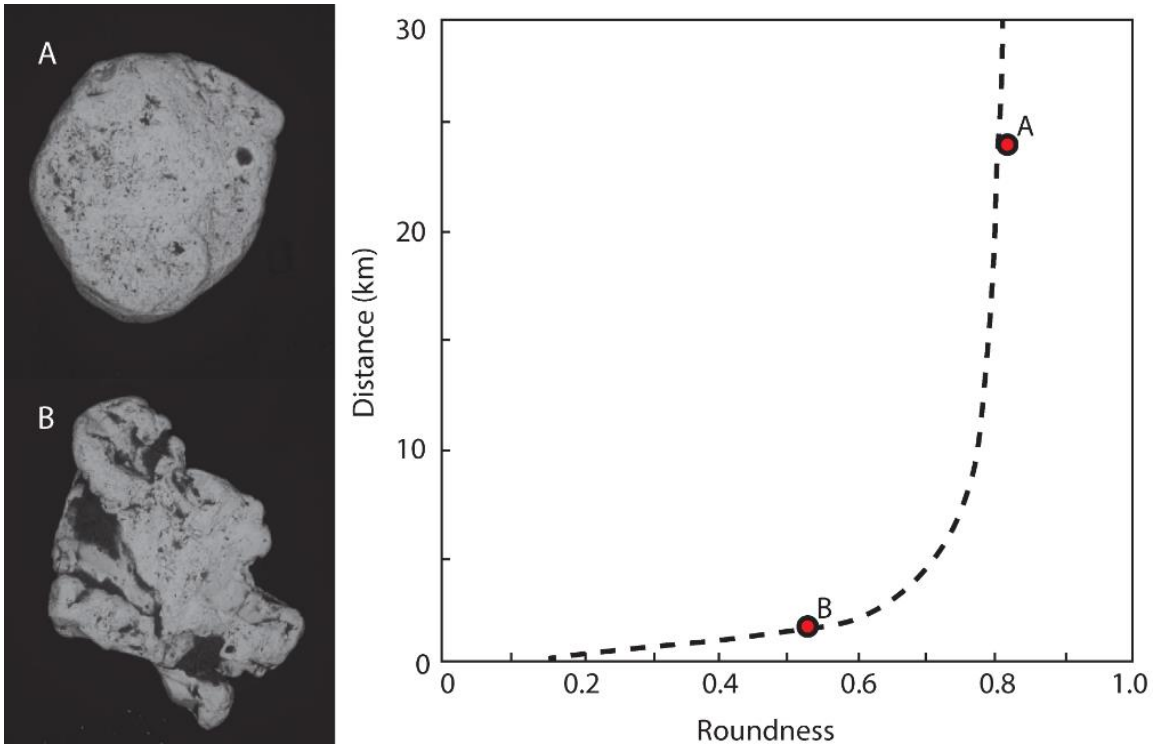

Figure 4.7 Electron backscatter image of high-roundness, well-travelled (top) and low-roundness, less-travelled (bottom) gold grains from GLD205-G1. The more rounded gold grain (0.80) has an estimated travel distance of >10 km, while the less rounded grain (0.53) has travelled approximately 2 km. The roundness-distance curve was empirically determined by analysis of gold grains in the Klondike district (Knight et al., 1999).

The mean roundness of all samples from the Gladstone area is between 0.54 and 0.60; however, considerable variability in roundness is present within each sample (Figure 4.8). Sample GLD06-G1 appears to have a weak bimodal distribution, which may indicate two lode sources have contributed to the deposit. GLD06-G1 also has the lowest average roundness, with a mode of 0.4-0.5, correlating to approximately 1 km of fluvial transport. The low travel distance suggests a gold source is located within the lower reaches of Cyr Creek. Based on an empirically derived relationship between transport distance and roundness (Knight et al., 1999), gold grain transport distances in GLD205-G1 range from 2 km to more than 10 km (Figure 4.7). Madsen (2001) found gold grains were generally flat, indicating longer transport distances are more common. No correlation was found between particle roundness and fineness, %Ag, or %Cu. If gold populations were sourced from discrete zones of mineralization and had simple fluvial transport histories, gold grains within a geochemical population should have a similar degree of rounding.

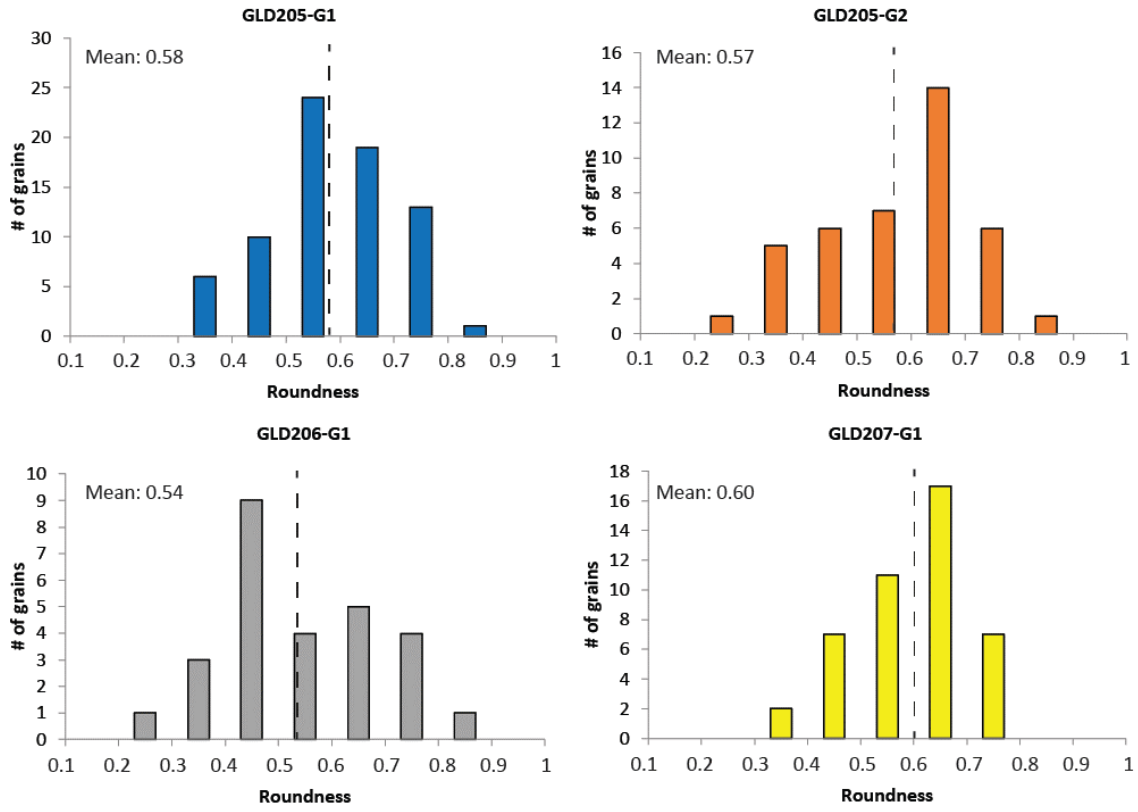

Figure 4.8 Comparison of gold grain roundness at sample sites on Gladstone Creek. Dashed lines show the mean roundness of each sample.

4.6.3. **Mineral Chemistry**

The proportion of gold, silver, and copper varies greatly within, and between samples (Figure 4.9). The fineness (parts per thousand) of analyzed grains ranges from 22 to 947. Three distinct populations are identified: 950-835, 825-690, and 450-350. GLD205-G2 contains only a single grain from the highest fineness population.

There are three distinct populations also identified in the distribution of silver content; 3-12% Ag, 38-48% Ag, and 57-60% Ag. Samples GLD206-G1 and GLD207-G1 have two high-silver content populations not measured in the samples from GLD205. This may be due to high silver content in grains sourced from Cyr Creek, downstream of site GLD205.

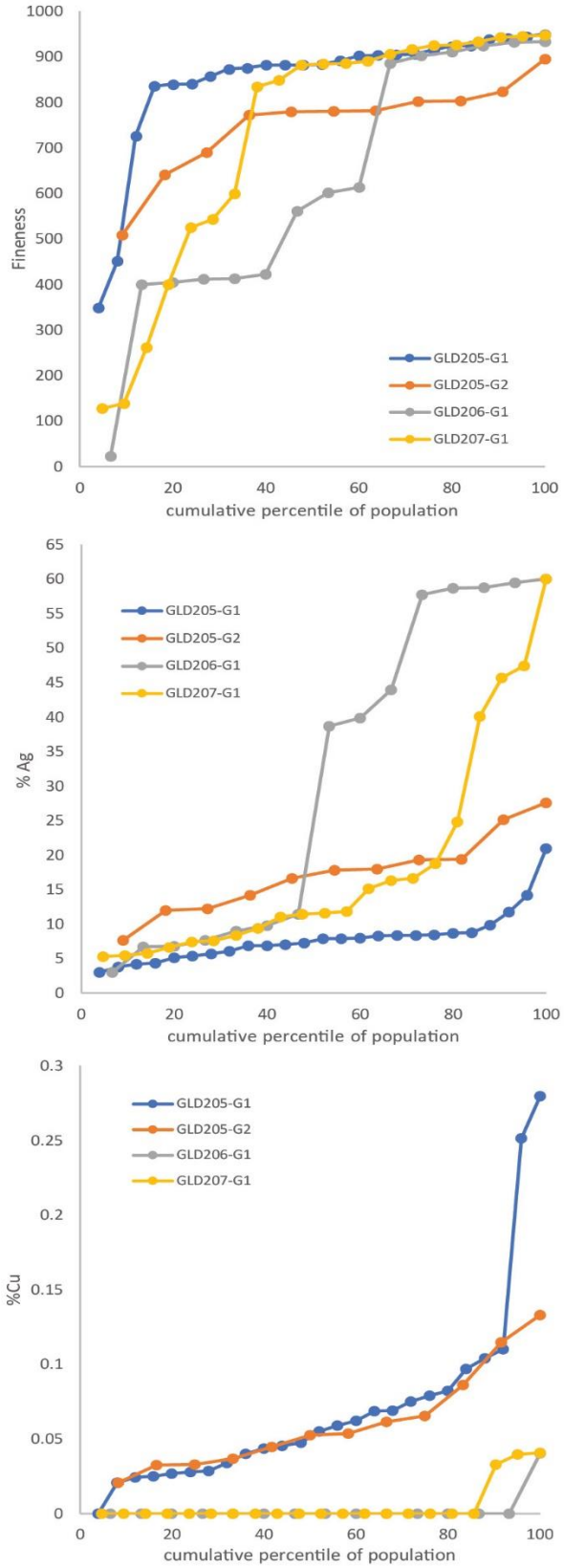

Figure 4.9 *Composition of gold, silver and copper in sampled gold grains.*

Copper content is below detection limits for most gold grains in samples GLD206-G1 and GLD207-G1. GLD205-G1 and GLD205-G2 have a relatively large range in copper content, between 0.02 and 0.13%, and a few outliers in GLD205-G1 having approximately 0.25-0.3% Cu.

Chapman et al. (2011) used previously established gold alloy compositions from lode gold sources (Townley et al., 2003) to differentiate between epithermal, gold-rich porphyry and gold-rich porphyry copper deposits. Using this method (Figure 4.10), we find that epithermal mineralization is the dominant source of gold grains containing <10% Ag, with lesser amounts derived from gold-rich porphyry mineralization. Gold grains from GLD206 are not entirely classified (Figure 4.10) due to high Ag content (>10%) in more than half of the analyzed grains. Multiple grains contain more than 50% Ag. One grain in GLD205-G2 was predominantly composed of Pb and S, suggesting galena is present from at least one of the sources.

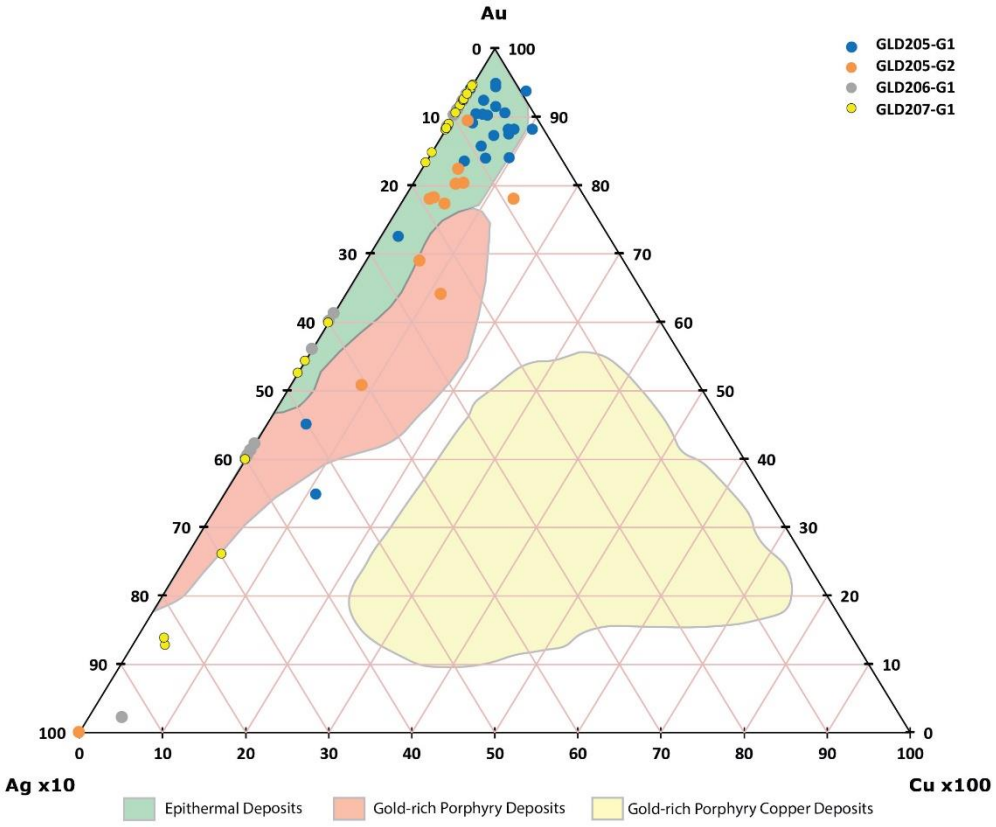

Figure 4.10 Au, Ag, and Cu plotted against composition ranges of epithermal, gold-rich porphyry, gold-rich copper porphyry deposits from Townley et al. (2003). Epithermal mineralization appears to be the dominant contributor to placer gold within Gladstone Creek, with minor contributions from gold-rich porphyry; however, many gold grains do not fit on this diagram due to >10% Ag content.

4.7. Discussion

4.7.1. Source Mineralization

Most placer mines in the Ruby Range are underlain by Kluane schist, making it the most prospective source of placer gold. Many of the gold grains having <10% Ag appear to be derived from epithermal or gold-rich porphyry mineralization (Figure 4.10), although this requires further confirmation. The gold grains having >10% Ag do not appear on this diagram and make up more than 50% of sampled gold grains, are likely orogenic gold from the Kluane schist. Stream sediment geochemistry in tributaries on the south side of lower Gladstone Creek have gold anomalies as high as 1315.5 ppb, with Swanson Creek having the highest values (Berdahl, 2013). These tributaries are therefore likely contributors to placer gold in Gladstone Creek.

Identifying gold particles derived from orogenic mineralization is commonly not possible based on Au, Ag, and Cu alone. Chapman et al. (2018) suggested that analysis of mineral inclusions may allow for differentiation, based on the presence of Bi-Pb-Te-S in the inclusions. Analysis of the geochemical signatures of inclusions is a logical next step for further work to confirm the suspected contribution of orogenic gold from Kluane schist.

Gold from porphyry and related epithermal systems is typically above 800 fineness (Sillitoe, 2000). Native gold particles coarse enough to be sorted into placer deposits are rare in the main porphyry, therefore, placer gold is typically sourced from later-stage epithermal mineralization (Chapman et al., 2018). This epithermal mineralization may be related to Cu-Mo-Au porphyries (Yukon MINFILE 115G 070, 115G 071) in the drainages north of Gladstone Creek. One active placer mine on Bliss Creek, 10 km north of Gladstone Creek, overlies Ruby Range batholith (Bond and van Loon, 2018), supporting the possibility of the batholith hosting other gold deposits.

4.7.2. Placer in a Glaciated Landscape

The stratigraphy exposed on Gladstone Creek records at least three glacial advances, represented by units of till and associated glaciofluvial and glaciolacustrine deposits, and intervening non-glacial stages. The three tills in section likely correlate to MIS 2, 4 and 6. Radiocarbon ages and tephra constrain the MIS 2 and 4 tills. The lowest

till, GLD205 Unit 1, has no lower age constraint. This till is suspected to be MIS 6 because pre-Reid Glaciation in southwestern Yukon was much less extensive than MIS 6 and has only been observed in sections on the west side of the Shakwak Trench, much closer to source areas (Turner et al., 2016). If this interpretation of the stratigraphy is correct, the GLD205-G2 placer deposit would have accumulated during the MIS 5 interglacial or during deglaciation at the end of MIS 6. GLD205 Unit 4 is a till not bracketed by glaciolacustrine sediment, diagnostic of up-valley ice from the St. Elias lobe, suggesting down-valley ice from the Ruby Range preceded arrival of the CIS. GLD205-G1 accumulated during MIS 3, an interstadial period, and GLD206-G1 accumulated during the Holocene (MIS 1). GLD207-G1 is suspected to have accumulated on an erosion-resistive glacial-stage floodplain surface.

Economic placer deposits typically occur when erosion and downcutting is dominant for long periods of time (Tuck, 1968). Glacial sediments rarely contain economic concentrations of gold (Boyle, 1979) unless they have reworked paleo-placers. The placer deposits examined in this study all appear to have accumulated during interglacial periods, or during later phases of deglaciation when valleys are ice-free, providing lower base levels and allowing incision through glacial sediments. Each of the glaciations in the area would have effectively reset the fluvial system, possibly causing subsequent periods of placer formation to occur in different portions of the Gladstone valley. Similarly, Madsen (2001) found that gold in Gladstone Creek had accumulated in interglacial and glaciofluvial gravel units in section as well as a minute amount of gold in a basal till unit, which likely reworked an older placer deposit.

It is possible that pre-glacial placer deposits exist in paleochannels somewhere under the thick stratigraphy of Gladstone Creek, but have not yet been uncovered. This is more likely if initial glacial advances were up-valley and depositional, rather than down-valley and erosional (cf. Levson 1992). Bedrock crops out at one location on lower Gladstone Creek, approximately 400 m above GLD205. It is likely that most of the pre-glacial placer accumulation would have occurred on this bedrock surface.

Placers sampled at GLD205 and GLD207 accumulated on clay-rich glacial sediment (GLD205 Unit 1 and Unit 4) and paleosurfaces (GLD207 Unit 2), which can act as false bedrock (Madsen, 2001; Slingerland and Smith, 1986). Clay-rich glaciolacustrine

units found elsewhere in Gladstone Creek may also limit downcutting (*cf.* Levson and Blyth, 1994) and should be explored for placer accumulation.

Gold grain populations defined by fineness (Figure 4.9) have heterogeneous morphology (Figure 4.8). This morphology could be due to widespread mineralization in the vein systems in the Kluane schist resulting in wide-ranging transport distances. In Gladstone Creek, some of the gold would have been transported by ice and subsequently subject to fluvial transport, thus transport distance curves may not apply as morphological modification may occur at different rates during glacial transport. This is a possible explanation for the indistinct rounding signatures of the samples, despite large differences in chemical composition. Based on transport distances suggested by gold grain roundness, gold sourced from mineralization in the Ruby Range batholith must have been transported in part by down-valley ice.

4.8. Conclusion

Economic placer deposits accumulate where bedrock, or resistant false-bedrock materials such as till or other relatively impervious surfaces, limit downcutting. Regional studies of glacial history and ice flow directions suggest the possibility of distal-intrabasinal and extrabasinal gold sources; however, in Gladstone Creek the most likely sources of mineralization are local Kluane schist and the Ruby Range batholith. Geochemical analysis suggests three populations of gold are present in Gladstone Creek. A high fineness population may be derived from epithermal mineralization, the other appears to be derived from gold-rich porphyry mineralization, both of which are likely hosted by the Ruby Range batholith. More than half of the gold grains sampled are not well constrained by Au-Ag-Cu analysis and are suspected of being derived from orogenic mineralization within Kluane schist. Further analyses, including gold grain microchemistry and inclusion mineralogy, are required to confirm these results.

4.9. Acknowledgements

This project took place in the Traditional Territory of the Kluane First Nation. The authors would like to thank Alan Dendys and the TIC Exploration crew for their hospitality and for sharing their local knowledge and enthusiasm for placer mining with us. We thank Megan Simao for providing competent field assistance and never refusing a till fabric or

pebble lithology count. Carbon sample preparation was completed by Alice Telka of Paleotec Services. This study was supported by the Yukon Geological Survey and the Canadian Northern Economic Development Agency's Strategic Investments in Northern Economic Development (SINED).

Chapter 5. Summary and Conclusions

This chapter summarizes the key findings of this project, and how they have furthered our understanding of the Quaternary history of the central Ruby Range as well as the broader northern Cordilleran Ice Sheet. In trying to answer the research questions of this thesis many more questions have arisen, these are presented in a discussion of future research to build on the knowledge gained in this study.

5.1. Summary and Key Findings

This project examined the Quaternary history of the central Ruby Range in southwest Yukon. A map of surficial geology and glacial limits (Cronmiller et al., 2018) was produced for the study area at 1:50,000 scale and extensive stratigraphic analysis was conducted at Gladstone Creek and select sites throughout the central Ruby Range. Stratigraphic studies also included collection of gold grains for analysis of placer gold geochemistry and sedimentology.

Field and desktop mapping found surficial evidence of two advances of the St. Elias lobe. The older advance, which may be a composite limit of MIS 4 and 6 glaciations, was more extensive than the younger MIS 2 glaciation. No limits are mapped for pre-Reid Glaciation, nor was definitive evidence of pre-Reid advances found in sections at Gladstone Creek. The MIS 2 ice sheet elevation was approximately 1700 m at the mouth of Gladstone Creek, decreasing to a terminus at 1150 m approximately 5 km east of the map area. The more extensive limit is approximately 500 m higher than the MIS 2 limit in the eastern portions of the map area, though its elevation is unclear around Kluane Lake. Local source areas contributed significant ice to the east margin of the St. Elias lobe, greatly increasing its apparent incursion into the Ruby Range. Plateau surfaces in the southeast of the map area appear to have hosted ice caps that contributed to CIS extent during MIS 2 and likely during earlier glaciations. Meltwater channels in lower Gladstone Creek suggest Ruby Range ice may have persisted after the retreat of the St Elias Lobe. A readvance or standstill of glaciers from Ruby Range from source areas occurred at 13.7 ± 0.9 ka, approximately 3.4 ka after the retreat of the St. Elias lobe from its maximum extent. This readvance was dated in Raft Creek but likely occurred in the cirques and tributary valleys above Gladstone Creek as well. This readvance correlates with a

widespread readvance documented by moraines in the Mackenzie and Cassiar mountains associated with short cooling events within the Bølling-Allerød cooling (Menounos et al., 2017) and ages obtained from boulders in Whitehorse dating the Chadburn readvance of the Cassiar Lobe (Bond, 2004). The Older Dryas cooling event, which was triggered by meltwater discharged by the collapse of the Cordilleran-Laurentide ice saddle at approximately 14.5 ka, weakening the Atlantic meridional overturning circulation leading to widespread hemispheric cooling may have caused the readvance (Ivanovic et al., 2017). Alternatively, the readvance may have been a response to the retreat of the St. Elias lobe when down-wasting in the source areas allowed for more moisture penetration into the Ruby Range, or increased precipitation resulting from eustatic sea-level rise and re-submergence of the Bering-Chukchi platform; the exposure of which was responsible in part for the aridity of much of Alaska and Yukon during MIS 2 (Briner et al., 2008).

Stratigraphic analysis found evidence of at least three advances from the Ruby Range, and two advances of the CIS from the St. Elias range. During glaciations, ice from Ruby Range source areas occupied Gladstone Creek prior to arrival of the St. Elias lobe, limiting the deposition of St. Elias lobe sediments. Glaciolacustrine sediments underlying Ruby Range tills indicate an elevated base level during the advance, likely associated with an advanced position of the St. Elias Lobe, and therefore suggesting advances from the St. Elias and Ruby ranges were roughly synchronous. The presence of CIS advance glaciolacustrine sediments and cirques which appear unoccupied during MIS 2 suggest Ruby Range ice may have been limited during the McConnell relative to previous glaciations.

Interglacial (MIS 5) and interstadial (MIS 3) sediments in Gladstone Creek contain bones, insect macrofossils, and tephra. These deposits indicate Gladstone Creek was ice-free in both MIS 5 and MIS 3. Dawson tephra in interstadial silt and supporting IRSL age (24.84 ± 1.13 ka) underlying McConnell till indicates lower Gladstone Creek remained ice free until sometime after 25,400 ± 140 ^{14}C yr.

Gold grain analysis at three sites on Gladstone Creek found gold is typically concentrated in fluvial gravels and possibly in Ruby Range retreat glaciofluvial gravels. The auriferous gravels erode down to bedrock or resistive, clay-rich, false-bedrock surfaces, such as till. These stratigraphic distribution is in general agreement with previous work by Madsen (2001). No correlation was found between gold grain morphology and

geochemistry, suggesting that typical fluvial transport distance rounding curves may not apply due to glacial transport, or that source mineralization may be widespread. Gold grain chemistry suggests both epithermal and gold-rich porphyry mineralization sources are present. Gold-rich porphyry mineralization may be present in the Ruby Range batholith, and epithermal gold is likely sourced from Kluane schist.

5.2. Applications

Exploration for pre-glacial channels under Gladstone Creek drift could discover considerable placer deposits. If the initial glaciations moved up-valley, burying the deposits in-situ rather than re-working them, pre-glacial gravels immediately overlying bedrock may contain most of the placer gold concentrated prior to the late Pleistocene glaciations. If down-valley ice from local Ruby Range cirques was the first glacial incursion in Gladstone Creek, the ice may have re-worked pre-glacial deposits. Future mining further up-valley should focus on gravel units overlying bedrock or false bedrock surfaces including tills or paleosurfaces in gravels. The elevated gold values observed in Swanson Creek (Berhdahl, 2013) indicate the most prospective source of placer gold in Gladstone Creek are the valleys above the south side of lower Gladstone Creek, and therefore warrant further exploration for both hard rock and placer potential.

The detailed surficial geology and glacial limits mapping produced for this thesis (Cronmiller et al., 2018) can be used to inform till and sediment sampling programs for mineral exploration. The type, age, and distribution of materials will allow for better-informed sampling and selection of proper analytical methods. The glacial limits mapping increases the understanding of sediment dispersal patterns and could be used to help trace geochemical anomalies to sources. Glacial limits and cirque mapping can be used for climate modelling studies aiming to understand drivers and boundary conditions of Quaternary glaciations.

5.3. Limitations

Glacial limits mapped in this study are based on interpolation of trim lines and rare moraines and meltwater channels. These are more common for the McConnell limit than Gladstone, resulting in greater uncertainty in the Gladstone limit. However, it is likely that cold-based ice occurred near the margins of the ice sheet during both glaciations, adding

further uncertainty to the exact extent of ice. The age of the McConnell limit is not well constrained within the study area; however,

Sections in Gladstone Creek suffer from lack of age constraint, particularly for units lower in section, where radiocarbon ages are non-finite. Lower in section only relative ages are known based on stratigraphic relationships with constrained units. Many ages in section were obtained using IRSL and the reliability of the results is currently uncertain for some samples.

5.4. Future Work

While this study has made some important advances in understanding the Quaternary history of southwestern Yukon, many questions remain, and new questions have been formulated. The extensive moraine complexes in Albert Creek appear to contain moraines of multiple ages deposited by alpine glaciers. Boulders on these moraines were sampled for ^{10}Be dating in July 2018. The results of this work will further illuminate the timing and extent of alpine glaciations in the Ruby Range. It is unknown how widespread this cirque glaciation was during pre-McConnell glaciations. A study of cirque morphologies as conducted by Nelson and Jackson (2003) paired with limits mapping in areas unaffected by the CIS would aid understanding of local ice development during older glaciations. Identifying trends in alpine glaciation may give insight into the lack of correlation in regional ice extent.

Southwest Yukon is the only area in the territory where an MIS 4 advance has been identified with an extent comparable to or more extensive than MIS 6. On top of this MIS 4 surface should be a paleosol formed during the Boutillier interstadial. This paleosol has not yet been identified and characterized but would likely be much less developed than the Wounded Moose and less developed than Diversion Creek paleosols. Study of stratigraphy in southwest Yukon, or elsewhere, containing an MIS 4 glaciation may reveal this paleosol, is the MIS 3 surface was stable and located in an environment conducive to soil development.

Extensive ice from local sources may add considerably to the perceived extent of ice from distal source areas, such as the St. Elias Mountains. Research aiming to understand the drivers resulting in variability in ice sheet extents should account for

contributions from multiple source areas. This is especially important in areas where sheets move up-valley into ice-producing ranges. The extensive ice produced in the Ruby Range stands in stark contrast to the ranges in central Yukon, such as Glenlyon Range in the Pelly Mountains, where minor or no ice was produced during the McConnell Glaciation (Ward and Jackson, 1992). Because the northern CIS is precipitation-limited (Ward et al., 2007), this difference in ice production may be explained by changes in moisture gradient during glaciations, which requires further study to resolve and explain.

Evidence for ice cap formation on the plateaus and highlands of eastern portion of the study area is scant, though the ice would likely be cold-based, leaving surfaces relatively unmodified. Evidence consists primarily of U-shaped valleys draining the uplands and rare moraines and meltwater channels of unknown origin. Exposure dating on tors using paired ^{10}Be and ^{36}Al cosmogenic nuclides (Knudsen and Egholm, 2018) may show these features were buried under ice for prolonged periods. Other high plateau surfaces away from main source areas of the northern CIS may have hosted significant ice caps that contributed to ice sheet extent. Using this technique may be a way to confirm ice cover in the absence of diagnostic landforms and sediments.

Photo: Clouds lifting in the Ruby Range

References

Alexander, C.S., Price, L.W., 1980. Radiocarbon Dating of the Rate of Movement of Two Solifluction Lobes in the Ruby Range, Yukon Territory. Quaternary Research 13, 365-379.

Ball, G.E., and Currie, D.C. 1997. Ground Beetles (Coleoptera: Trachypachidae and Carabidae) of the Yukon: Geographical Distribution, Ecological Aspects, and Origin of the Extant Fauna. In Danks, H.V. and Downes, J.A. (Eds.), Insects of the Yukon. Biological Survey of Canada (Terrestrial Arthropods), Ottawa. 1034 pp

Barendregt, R. W., Enkin, R. J., Duk-Rodkin, A. & Baker, J. 2010: Paleomagnetic evidence for multiple late Cenozoic glaciations in the Tintina Trench, west-central Yukon, Canada. Canadian Journal of Earth Science 47, 987–1002.

Berdhal, S. 2013. Geochemical Assessment Report for Work Performed on the Gladstone Property. Yukon Energy, Mines and Resources Assessment Report 096163 46 p.

Berger, G.W., Pewe, T.L., Westgate, J.A., and Preece, S.J. (1996). Age of Sheep Creek tephra (Pleistocene) in central Alaska from thermoluminescence dating of bracketing loess. Quaternary Research 45, 263–270.

Brahney, J., Clague, J.J., Menounos, B., Edwards, T.W.D., 2008. Timing and cause of water level fluctuations in Kluane Lake, Yukon Territory, over the past 5000 years. Quaternary Research: 70, 213-227.

Bond, J., 2004. Late Wisconsinan McConnell glaciation of the Whitehorse map area (105D), Yukon. In: Yukon Exploration and Geology 2003, D.S. Emond and L.L. Lewis (eds.), Yukon Geological Survey, p. 73-88.

Bond, J.D. and Lipovsky, P.S., 2009A. Surficial geology of Kiyera Lake (115G/15), Yukon (1: 50 000 scale). Yukon Geological Survey, Open File 2009-46.

Bond, J.D., Lipovsky, P.S., 2009B. Surficial Geology of Talbot Creek (NTS 115G/09) Yukon (1:50 000 scale). Yukon Geological Survey, Energy, Mines and Resources, Yukon Government, Open File 2009-48.

Bond, J.D. and Lipovsky, P.S., 2009C. Surficial geology of Toshingermann Lakes (115G/14), Yukon (1: 50 000 scale). Yukon Geological Survey, Open File 2009-45.

Bond, J.D., Lipovsky, P.S., von Gaza, P., 2008. Surficial geology investigations in Wellesley Basin and Nisling Range, southwest Yukon. In D.S. Emond, L.R. Blackburn, R.P. Hill, L.H. Weston (Eds.), Yukon Exploration and Geology 2007 (pp. 125-138). Yukon Geological Survey.

Bond, J.D. and van Loon, S. 2018. Yukon Placer Mining Industry 2015-2017. Yukon Geological Survey, 284 p.

Bonnaventure, P. P., Lewkowicz, A. G., Kremer, M., and Sawada M. C., 2012. A permafrost probability model for the southern Yukon and northern British Columbia, Canada, Permafrost Periglacial. Proc., 23, 52–68

Bostock, H.S., 1966: Notes on glaciation in central Yukon Territory; Geol. Surv. Can., Paper 65-36.

Bostock, H. S., 1969, Kluane Lake, Yukon Territory, Its Drainage and Allied Problems (1150, and 115E): Geological Survey of Canada, Paper 69-28, 19 pp.

Boyle, R. W., 1979. The geochemistry of gold and its deposits. Geological Survey of Canada, Bulletin 280, 584pp.

Briner, J.P., Kaufman, D.S., Manley, W.F., Finkel, R.C., Caffee, M.W., 2005. Cosmogenic exposure dating of late Pleistocene moraine stabilization in Alaska. Geological Society of America Bulletin 117, 1108–1120.

Briner, J. P. and Kaufman, D. S. 2008. Late Pleistocene mountain glaciation in Alaska: key chronologies. J. Quaternary Sci., Vol. 23 pp. 659–670

Cairnes, D.D. 1915. Exploration in southwestern Yukon. Summary Report of the Geological. Survey Department of Mines for the calendar year 1914.

Chapman, R.J., Allan, M.M., Mortensen, J.K., Wrighton, T.M., Grimshaw, M.R. 2018. A new indicator mineral methodology based on a generic Bi-Pb-Te-S mineral inclusion signature in detrital gold from porphyry and low/intermediate sulfidation epithermal environments in Yukon Territory, Canada. Mineralium Deposita: 53, 815-834.

Chapman R.J., Mortensen J.K., LeBarge W.P. 2011. Styles of lode gold mineralization contributing to the placers of the Indian River and Black Hills Creek, Yukon Territory, Canada as deduced from microchemical characterization of placer gold grains. Mineral Deposita 46(8):881-903.

Church, M. and Ryder, J. M. 1972. Paraglacial sedimentation; a consideration of fluvial processes conditioned by glaciation. Geological Society of America Bulletin, 83: 3059-3072.

Clague, J.J., 1989. Cordilleran Ice Sheet. In: Fulton, R.J. (Ed.), Chapter 1 of Quaternary Geology of Canada and Greenland. Geological Survey of Canada, Ottawa, ON, pp. 40–43. 17

Clague, J.J., Evans, S.G., Rampton, V.N., Woodsworth, G.J., 1995. Improved age estimates for the White River and Bridge River tephras, western Canada. Canadian Journal of Earth Sciences 32, 1172–1179.

Clague, J. J., Luckman, B. H., Van Dorp, R. D., Gilbert, R., Froese, D., Jensen, B. J., and Reyes, A. V. 2006. Rapid changes in the level of Kluane Lake in Yukon Territory over the last millennium, Quaternary Research: 66, 342–355

Clark, P.U., Clague, J.J., Curry, B.B., Dreimanis, A., Hicock, S.R., Miller, G.H., Berger, G.W., Eyles, N., Lamothe, M., Miller, B.B., Mott, R.J., Oldale, R.N., Stea, R.R., Szabo, J.P., Thorleifson, L.H., Vicent, J.-S., 1993. Initiation and development of the Laurentide and Cordilleran Ice Sheets following the last interglaciation. Quaternary Science Reviews 12, 79–114.

Cockburn, H. A. P., & Summerfield, M. A. 2004. Geomorphological applications of cosmogenic isotope analysis. Progress in Physical Geography: Earth and Environment, 28(1), 1–42.

Cronmiller, D.C., Ward, B.C., Bond, J.D. and Layton-Matthews, D., 2019. Constraints on the evolution of placer deposits at Gladstone Creek, Yukon (NTS 115G/7, 8). In: Yukon Exploration and Geology 2018, K.E. MacFarlane (ed.), Yukon Geological Survey, p. 61–74.

Cronmiller, D.C., Ward, B.C., Bond, J.D., 2018, Surficial Geology of Gladstone Creek (115G/08 and part of 115G/07), Yukon (1:50,000 scale). Yukon Geological Survey, Energy, Mines, and Resources, Yukon Government, Open File 2018-20

Dawson, G. M., 1889. Report on an exploration in the Yukon District, N.W.T., and adjacent portion of British Columbia. Geological Survey of Canada.

Day, S.J., and Fletcher, W.K., 1991. Concentration of magnetite and gold at bar and reach scales in a gravel-bed stream, British Columbia, Canada. Journal of Sedimentary Petrology 61, 871– 882.

Denton, G. H. & Stuiver, M. 1967: Late Pleistocene glacial stratigraphy and chronology, northeastern St. Elias Mountains, Canada. American Journal of Science 264, 577–599.

Demuro, M., Froese, D.G., Arnold, L.J., Roberts, R.G., 2012. Single-grain OSL dating of glaciofluvial quartz constrains Reid Glaciation in NW Canada to MIS 6. Quat. Res. 77, 305-316.

Dreimanis, A. and Schlüchter, C. 1985. Field criteria for the recognition of till or tillite. Palaeogeography, Palaeoclimatology, Palaeoecology, 51(1), 7-14.

Duk-Rodkin, A., 1999. Glacial limits map of Yukon Territory; Geological Survey of Canada, Open File 3694, Indian and Northern Affairs Canada Geoscience Map 1999-2, scale 1:1 000 000.

Duller, G. A. T .2008. Luminescence Dating: guidelines on using luminescence dating in archaeology. Swindon: English Heritage

Eamer, J., Shugar, D., Walker, I., Lian, O., Neudorf, C., & Telka, A. (2017). A glacial readvance during retreat of the Cordilleran Ice Sheet, British Columbia central coast. Quaternary Research, 87(3), 468-481. doi:10.1017/qua.2017.16

Eyles, N., 1995. Characteristics and origin of coarse gold in Late Pleistocene sediments of the Cariboo placer mining district, British Columbia, Canada. Sedimentary Geology. Vol. 95. pp 69-95.

Forget Brisson, L., Lamothe, M., Hardy, F. et Graf, K.E. Submitted. Exploring the use of a low temperature preheat in IRSL dating of feldspar in Beringian archaeological contexts, Quaternary Geochronology.

Foscolos, A.E., Rutter, N.W., Hughes, O.L., 1977. The Use of Pedological Studies in Interpreting the Quaternary History of Central Yukon Territory. Bulletin 271. Geological Survey of Canada, Ottawa, Canada

Froese, D.G., Barendregt, R.W., Enkin, R.J., Baker, J., 2000. Paleomagnetic evidence for multiple Late Pliocene – Early Pleistocene glaciations in the Klondike area, Yukon Territory. Canadian Journal of Earth Science, 37, 863-877.

Froese, D.G., Westgate, J.A., Preece, S.J., Storer, J., 2002. Age and significance of the late Pleistocene Dawson tephra in eastern Beringia. Quaternary Science Reviews 21, 2137–2142.

Froese, D.G., Zazula, G., Reyes. A., 2006. Seasonality of the late Pleistocene Dawson tephra and exceptional preservation of a buried riparian surface in central Yukon Territory, Canada. Quaternary Science Reviews. 25. 1542-1551.

Fulton, R. (1991). A Conceptual Model for Growth and Decay of the Cordilleran Ice Sheet. *Géographie physique et Quaternaire*, *45*(3), 281–286.

Gosse, J.C. and Phillips, F.M. 2001: Terrestrial in situ cosmogenic nuclides: theory and application. Quaternary Science Reviews 20, 1475–560.

Hattestrand, C., Stroeven, A.P. 2002. A relict landscape in the centre of Fennoscandian glaciation: Geomorphological evidence of minimal Quaternary glacial erosion. Geomorphology 44, 127-143.

Heyman, J., Stroeven, A.P., Harbor, J.M., Caffee, M.W. 2011. Too young or too old: Evaluating cosmogenic exposure dating based on an analysis of compiled boulder exposure ages. Earth and Planetary Science Letters, 302(1-2), 71-80

Hicock, S. R., Goff, J. R., Lian, O. B., and Little, E. C. 1996. On the interpretation of subglacial till fabric. Journal of Sedimentary Research, 66: 928-934.

Hidy, A.J., Gosse, J.C., Froese, D.G., Bond, J.D., Rood, D.H., 2013. A latest Pliocene age for the earliest and most extensive Cordilleran Ice Sheet in northwestern Canada. Quaternary Science Reviews 61, 77-84.

Howes, D. E. and Kenk, E. 1997. Terrain classification system for British Columbia. Version 2. British Columbia Ministry of Environment, Lands and Parks, Victoria, B.C.

Hughes, O.L., 1990. Surficial geology and geomorphology, Aishihik Lake, Yukon Territory. Geological Survey of Canada, Paper 87-29. 23 p. + maps.

Hughes, O.L., Campbell, R.B., Muller, J., Wheeler, J.D., 1969. Glacial limits and flow patterns, Yukon Territory south of 65o N latitude. Geological Survey of Canada Paper 68-34

Huscroft, C.A., Ward B.C., Barendregt, R.W., Jackson L.E., Opdyke, N.D. 2004. Pleistocene Volcanic Damming of Yukon River and the Maximum Age of the Reid Glaciation, West-central Yukon. Canadian Journal of Earth Sciences 41: 151-64.

Israel, S., Murphy, D., Bennett, V., Mortensen, J. and Crowley, J., 2011A. New insights into the geology and mineral potential of the Coast Belt in southwestern Yukon. *In:* Yukon Exploration and Geology 2010, K.E. MacFarlane, L.H. Weston and C. Relf (eds.), Yukon Geological Survey, p. 101-123.

Israel, S., Cobbett, R., Westberg, E., Stanley, B., and Hayward, N. 2011B, Preliminary bedrock geology of the Ruby Ranges, southwest Yukon, (Parts of NTS 115G, 115H, 115A and 115B) (1:150 000 scale)

Ivanovic, R. F., L. J. Gregoire, A. D. Wickert, P. J. Valdes, and A. Burke (2017), Collapse of the North American ice saddle 14,500 years ago caused widespread cooling and reduced ocean overturning circulation, Geophysical Research Letters, 44, 383–392

Jackson Jr., L.E., Barendregt, R.W., Baker, J., Irving, E., 1996. Early Pleistocene volcanism and glaciation in central Yukon; a new chronology from field studies and paleomagnetism. Canadian Journal of Earth Sciences 33, 904–916.

Jackson, L. & Harington, C. 1991. Middle Wisconsinan Mammals, Stratigraphy, and Sedimentology at the Ketza River Site, Yukon Territory. Géographie physique et Quaternaire, 45 (1), 69–77.

Jackson, L.E., Jr., Ward, B.C., Duk-Rodkin, A., Hughes, O.L., 1991. The latest Cordilleran Ice Sheet in Yukon Territory. Geographie Physique et Quaternaire, 45-3, 341-354.

Jensen, B.J.L., Reyes, A.V., Froese, D.G., 2013. Marine tephrostratigraphy in the Gulf of Alaska and comparison to terrestrial records from eastern Beringia. In: Program and Abstracts, CANQUA-CGRG Biannual Meeting, August 18-21, 2013. University of Alberta, Edmonton.

Kennedy, K.E., 2018. Evidence for limited glaciation in northern Kluane Range, southwestern Yukon, with implications for surficial geochemical exploration. In: Yukon Exploration and Geology 2017, K.E. MacFarlane (ed.), Yukon Geological Survey, p. 89-102.

Kleman, J., Stroeven, A.P., 1997. Preglacial surface remnants and Quatemary glacial regimes in northwestern Sweden. Geomorphology 19, 35-54.

Knight, J.B.; Morrison, S.R.; Mortensen; J.K. 1999. The Relationship between Placer Gold Particle Shape Rimming and Distance of Fluvial Transport as Exemplified by Gold from the Klondike District Yukon Territory, Canada. Economic Geology: 94, 635-648

Knudsen, M.F., Egholm, D.L., 2018. Constraining Quaternary ice covers and erosion rates using cosmogenic 26Al/10Be nuclide concentrations. Quaternary Science Reviews, Vol: 181, Page: 65-75

Levson, V., 1992. The sedimentology of Pleistocene deposits associated with placer gold bearing gravels in the Livingstone Creek area, Yukon Territory. In: Yukon Geology, vol. 3; Exploration and Geological Services Division, Yukon, Indian and Northern Affairs Canada, p. 99-132.

Levson, V.M., Blyth, H. 1994. Applications of Quaternary geology to placer deposit investigations in glaciated areas; a case study, Atlin, British Columbia. Quaternary International, 20: 93-105

Linton, D., 1955. The Problem of Tors. The Geographical Journal, 121(4), 470-487.

Madsen, J., 2001. The Quaternary History and Placer Deposits of Gladstone Creek, Southwest Yukon. B.Sc. Honours Thesis, University of Victoria.

Matthews, J., Schweger, C. & Hughes, O. 1990. Plant and Insect Fossils from the Mayo Indian Village Section (Central Yukon): New Data on Middle Wisconsinan Environments and Glaciation. Géographie physique et Quaternaire, 44(1), 15–26.

Menounos, B. M. Goehring, G. Osborn, M. Margold, B. Ward, J. Bond, G. K. C. Clarke, J. J. Clague, T. Lakeman, J. Koch, M. W. Caffee, J. Gosse, A. P. Stroeven, J. Seguinot, J. Heyman. 2017. Cordilleran Ice Sheet mass loss preceded climate reversals near the Pleistocene Termination. Science, 358, 781-784.

Montgomery, D.R., 2002. Valley formation by fluvial and glacial erosion. Geology; 30 (11): 1047–1050

Muller, J.E., 1967, Kluane Lake map area, Yukon Territory, Geological Survey of Canada Memoir 340, 137pp.

Murphy, D.C., Mortensen, J.K. and van Staal, C.R., 2009. 'Windy-McKinley' terrane, western Yukon: new data bearing on its composition, age, correlation and paleotectonic settings. In: Yukon Exploration and Geology, L.H. Weston, L.R. Blackburn and L.L. Lewis (eds.), Yukon Geological Survey, p. 195-209.

Nelson, F.E.N. and Jackson, L.E., Jr., 2003. Cirque forms and alpine glaciation during the Pleistocene, west-central Yukon. In: Yukon Exploration and Geology 2002, D.S. Emond and L.L. Lewis (eds.), Exploration and Geological Services Division, Yukon Region, Indian and Northern Affairs Canada, p. 183-198.

Porter, C., Morin, P,Howat, I., Noh, M.,Bates, B., Peterman, K., Keesey, S. Schlenk, M., Gardiner, J., Tomko, K., Willis, M., Cloutier, M., Husby, E., Foga, S., Nakamura, H., Platson, M., Wethington, M., .;Williamson, C., Bauer, G., Enos, J., Arnold, G., Kramer, W., Becker, P., ;Doshi, A., D'Souza, C., Cummens, P., Laurier, F., Bojesen, M., 2018. ArcticDEM. Harvard Dataverse, V1

Preece, S. J., Westgate, J. A., Froese, D. G. Pearce, N. J. G., Perkins, W. T., 2001. A catalogue of late Cenozoic tephra beds in the Klondike goldfields and adjacent areas, Yukon Territory. Canadian Journal of Earth Sciences, 48(10), 1386-1418.

Putkonen, J., Swanson, T., 2003. Accuracy of cosmogenic ages for moraines. Quaternary Research 59, 255–261.

Rampton, V.N., 1971. Late Pleistocene glaciations of the Snag-Klutlan area, Yukon Territory. Arctic, vol. 24, p. 277-300.

Rampton, V. N., 1978. Surficial geology and geomorphology, Burwash Creek, Yukon Territory. Geological Survey of Canada, Preliminary map 6-1978.

Reger, R.D., and Pewe, T.L., 1976. Cryoplanation Terraces: Indicators of a Permafrost Environment. Quaternary Research, 6, 99-109.

Rust, B.R. 1977. Mass flow deposits in a Quaternary succession near Ottawa, Canada: diagnostic criteria for subaqueous outwash. Canadian Journal of Earth Sciences, 14: 175–184

Schweger, C.E., Janssens, J.A.P., 1980. Paleoecology of the Boutellier nonglacial interval, St. Elias Mountains, Yukon Territory, Canada. Arctic and Alpine Research 12, 309–317.

Shugar, D., Clague, J., Best, J., Schoof, C., Willis, M., Copland, L., & Roe, G. (2017). River piracy and drainage basin reorganization led by climate-driven glacier retreat. *Nature Geoscience, 10*(5), 370-375.

Sillitoe, R.H. 2000. Gold-rich porphyry deposits: descriptive and genetic models and their role in exploration and discovery. Reviews in Economic Geology 13:315–345.

Slingerland, R., and Smith, N. 1986. Occurrence and Formation of Water-Laid Placers. Annual Review of Earth and Planetary Sciences, 14(1), 113-147.

Smith, C.A.S., Meikle, J.C., and Roots, C.F. (eds.) 2004. Ecoregions of the Yukon Territory: Biophysical properties of Yukon landscapes. Agriculture and Agri-Food Canada, Technical Bulletin 04-01. 313 pp.

Smith, C., Tarnocai, C., Hughes, O., 1986. Pedological investigations of Pleistocene glacial drift surfaces in the central Yukon. Géog. Phys. Quat. 40, 29-37.

Stroeven, A.P., Fabel, D., Codilean, A.T., Kleman, J., Clague,J.J., Miguens-Rodriguez, M., Xu, S. 2010 Investigating the glacial history of the northern sector of the Cordilleran Ice Sheet with cosmogenic 10Be concentrations in quartz, Quaternary Science Reviews, Volume 29, Issues 25–26, 3630-3643.

Stroeven, A.P., Fabel, D., Hättestrand, C., Harbor, J. 2002. A relict landscape in the centre of Fennoscandian glaciation: Cosmogenic radionuclide evidence of tors preserved through multiple glacial cycles. *Geomorphology, 44*(1), 145-154.

Stroeven, A.P., Fabel, D., Margold, M., Clague, J.J., Xu, S. 2014. Investigating absolute chronologies of glacial advances in the NW sector of the Cordilleran Ice Sheet with terrestrial in situ cosmogenic nuclides, Quaternary Science Reviews, Volume 92, 429-443.

Tempelman-Kluit, D.J., 1980. Evolution of physiography and drainage in southern Yukon. Canadian Journal of Earth Sciences 17, 1189 – 1203.

Tempelman-Kluit, D.J., 1974. Reconnaissance geology of Aishihik Lake, Snag and part of Stewart River map areas, west central Yukon. Geological Survey of Canada Paper 73-41, 97 pp.

Townley, B.K., Herail, G., Maksaev, V., Palacios, C., de Parseval, P., Sepuldeva, F., Orellana, R., Rivas P, Ulloa C. 2003. Gold grain morphology and composition as an exploration tool: application to gold exploration in covered areas. Geochemistry: Exploration, Environment, Analysis 3:29–38

Tuck, R., 1968. Origin of the Bedrock Values of Placer Deposits, Economic Geology, 63, 191-193.

Turner, D.G., Ward, B.C., Bond, J.D., Jensen, B.J., Froese, D.G., Telka, A.M., Zazula, G.D., Bigelow, N.H., 2013. Middle to Late Pleistocene ice extents, tephrochronology and paleoenvironments of the White River area, southwest Yukon. Quat. Sci. Rev. 75, 59-77.

Turner, D. G., Ward, B. C., Froese, D. G., Lamothe, M., Bond, J. D. & Bigelow, N. H. 2016. Stratigraphy of Pleistocene glaciations in the St. Elias Mountains, southwest Yukon, Canada. Boreas, Vol. 45, pp. 521–536.

Turner, D.G., Froese, D.G., Ward, B.C., Jensen, B.J., Bond, J., In Preparation. The timing, extent and controls on Plio-Pleistocene glacial limits in Yukon Territory, Canada.

Ward, B.C., Bond, J.D., Gosse, J.C., 2007. Evidence for a 55-50 ka (early Wisconsin) glaciation of the Cordilleran Ice Sheet, Yukon Territory, Canada. Quaternary Research, 68, 141-150.

Ward, B.C., Bond, J.D., Froese, D., Jensen, B., 2008. Old Crow tephra (140 ± 10 ka) constrains penultimate Reid Glaciation in central Yukon Territory. Quaternary Science Reviews, 27, 1909-1915

Ward, B.C. and Jackson, L.E., 1992. Late Wisconsinan glaciation of the Glenlyon Range, Pelly Mountains, Yukon Territory, Canada. Canadian Journal of Earth Sciences, 29, pp.2007–2012.

Wentworth, C. 1922. A scale of grade and class for clastic sediments. Journal of Geology, 30: 377-392.

Westgate, J.A., Preece, S.J., Kotler, E., Hall, S., 2000. Dawson tephra: a prominent stratigraphic marker of Late Wisconsin age in west-central Yukon. Canadian Journal of Earth Sciences 37,621–627.

Westgate, J.A., Preece, S.J., Froese, D.G., Walter, R.C., Sandhu, A.S., Schweger, C.E., 2001. Dating early and middle (Reid) Pleistocene glaciations in central Yukon by tephrochronology. Quat. Res. 56, 335-348. J.,

White, S.E. 1976. Rock glaciers and block fields, review and new data. Quaternary Research 6, 77-97.

Yukon MINFILE, 2009. Yukon MINFILE – A database of mineral occurrences. Yukon Geological Survey, <http://www.geology.gov.yk.ca/databases_gis.html>.

Appendix A.

Map: Surficial geology of Gladstone Creek

Description:

This file contains 1:50,000 scale surficial geology and glacial limits mapping for the study area. This map is published as:

> Cronmiller, D., Ward, B.C. and Bond, J.D., 2018. Surficial geology of Gladstone Creek (115G/08 and part of 115G/07), Yukon (scale 1: 50 000). Yukon Geological Survey, Energy, Mines and Resources, Government of Yukon, Open File 2018-20.

File name:

Gladstone_Creek_50k.pdf

Appendix B.

Stratigraphy and sedimentology

File names:

Gladstone_Creek_Stratigraphy.pdf

Gladstone_Creek_Composite_Section.pdf

Description:

These supplementary files contain stratigraphic logs for sections examined in the study area and an idealized composite stratigraphic section for Gladstone Creek.

Appendix C.

Gold grain morphology and geochemistry data

Supplementary Data Files

File name: gold_grain_geochemistry.xlsx

Description: Gold grain geochemistry data collected by Queens University's geochemistry lab using laser ablation ICP-MS.

File name: gold_grain_images.pdf

Description: Gold grain images collected with by Queens University's geochemistry lab using a Scanning Electron Microscope.

File name: gold_grain_morphology.xlsx

Description: Gold grain morphology data collected from SEM images using SPIP™ image recognition software.

Appendix D.

Infrared Stimulated Luminescence Data

Supplementary Data Files

File name: Luminescence_Data.pdf

Description: Technical note presenting IRSL ages and methodologies from University of Quebec at Montreal.

Appendix E.

Cosmogenic Nuclide Dating (^{10}Be) Data

Supplementary Data Files

File name: Cosmo_Data.xls

Description: Technical note presenting field observations and cosmogenic nuclide dating ages and calculations from Dalhousie University.